2015

General Vector Explicit - Impact Time and Angle Control Guidance

Loren Robinson
University of Central Florida

GENERAL VECTOR EXPLICIT - IMPACT TIME AND ANGLE CONTROL GUIDANCE

by

LOREN ROBINSON
B.S. University of Central Florida, 2012

A thesis submitted in partial fulfilment of the requirements
for the degree of Master of Science
in the Department of Electrical Engineering and Computer Science
in the College of Engineering and Computer Science
at the University of Central Florida
Orlando, Florida

Summer Term
2015

Major Professor: Zhihua Qu

ABSTRACT

This thesis proposes and evaluates a new cooperative guidance law called General Vector Explicit - Impact Time and Angle Control Guidance (GENEX-ITACG). The motivation for GENEX-ITACG came from an explicit trajectory shaping guidance law called General Vector Explicit Guidance (GENEX). GENEX simultaneously achieves design specifications on miss distance and terminal missile approach angle while also providing a design parameter that adjusts the aggressiveness of this approach angle. Encouraged by the applicability of this user parameter, GENEX-ITACG is an extension that allows a salvo of missiles to cooperatively achieve the same objectives of GENEX against a stationary target through the incorporation of a cooperative trajectory shaping guidance law called Impact Time and Angle Control Guidance (ITACG).

ITACG allows a salvo of missile to simultaneously hit a stationary target at a prescribed impact angle and impact time. This predetermined impact time is what allows each missile involved in the salvo attack to simultaneously arrived at the target with unique approach angles, which greatly increases the probability of success against well defended targets. GENEX-ITACG further increases this probability of kill by allowing each missile to approach the target with a unique approach angle rate through the use of a user design parameter.

The incorporation of ITACG into GENEX is accomplished through the use of linear optimal control by casting the cost function of GENEX into the formulation of ITACG. The feasibility GENEX-ITACG is demonstrated across three scenarios that demonstrate the ITACG portion of the guidance law, the GENEX portion of the guidance law, and finally the entirety of the guidance law. The results indicate that GENEX-ITACG is able to successfully guide a salvo of missiles to simultaneously hit a stationary target at a predefined terminal impact angle and impact time, while also allowing the user to adjust the aggressiveness of approach.

Dedicated to my beautiful wife and son.

ACKNOWLEDGMENTS

I would like to thank Dr.Qu for his continuous support and guidance throughout my graduate research studies and completing this thesis. I would like to thank my wife, Kelly, for her unwavering support through this challenging process and believing in all of my grandiose aspirations. I would like to thank my parents, Kimberle and Mark, for their dedication in providing me with a solid academic foundation.

TABLE OF CONTENTS

LIST OF FIGURES ix

LIST OF TABLES xi

CHAPTER 1: INTRODUCTION 1

CHAPTER 2: LITERATURE REVIEW 9

2.1 Introduction 9

2.2 Equations of Motion 12

2.2.1 Polar Equations of Motion 16

2.2.2 Cartesian Equations of Motion 20

2.3 Classical Guidance Laws 23

2.3.1 True Proportional Navigation Guidance (TPN) 23

2.3.2 Pure Proportional Navigation Guidance (PPN) 25

2.3.3 Augmented Proportional Navigation Guidance (APN) 28

2.4 Advanced Guidance Laws 30

2.4.1 Advanced Guidance Law (AGL) 31

2.4.2 Advanced Augmented Guidance Law 32

2.4.3 Advanced Optimal Guidance Law (OGL) 33

2.5 Explicit Guidance Laws 34

2.5.1 Trajectory Shaping Guidance 35

2.5.2 General Vector Explicit Guidance (GENEX) 36

2.6 Cooperative Guidance Laws 38

2.6.1 Impact Time Control Guidance (ITCG) 40

2.6.2 Impact Time and Angle Control Guidance Control Guidance (ITACG) . . . 42

CHAPTER 3: METHODOLOGY 45

3.1 Introduction 45

3.2 Linear Optimal Control 46

3.3 GENEX-ITACG 50

CHAPTER 4: RESULTS 57

4.1 Introduction 57

4.2 Case 1: Impact Angle Control Guidance (IACG) 60

4.3 Case 2: General Vector Explicit Guidance (GENEX) 64

4.4 Case 3: Impact Time Control Guidance (ITCG) 68

4.5 Case 4: GENEX-ITACG Single Missile Flyout 73

4.6 Case 5: GENEX-ITACG Salvo Attack Flyout 78

CHAPTER 5: CONCLUSION 80

APPENDIX A: DETAILED DERIVATION OF GENEX-ITACG 81

A.1 Equations of Motion 82

A.2 Linear Quadratic Control Problem 85

A.3 Additional Impact Time Correction Command 96

A.4 GENEX-ITACG With Dimensional State Variables 102

APPENDIX B: SIMULINK MODEL 104

APPENDIX C: FIGURE REPRODUCTION PERMISSIONS 109

REFERENCES 114

LIST OF FIGURES

1.1 Phases of Flight:©The Johns Hopkins University Applied Physics Laboratory 3

1.2 GNC Structure:©The Johns Hopkins University Applied Physics Laboratory . 4

2.1 Geometries of Three Different Forms of Proportional Navigation 13

2.2 Advanced Guidance Law Cartesian Geometry 15

2.3 Stationary Target Homing Geometry 39

4.1 Results: IACG Trajectory 60

4.2 Results: IACG Flight Path Angle 61

4.3 Results: IACG Guidance Command 62

4.4 Results: IACG Acceleration 63

4.5 Results: GENEX Trajectory 64

4.6 Results: GENEX Flight Path Angle 65

4.7 Results: GENEX Guidance Command 66

4.8 Results: GENEX Acceleration 67

4.9 Results: ITCG Trajectory 68

4.10 Results: ITCG Time to Go 69

4.11 Results: ITCG Flight Path Angle 70

4.12 Results: ITCG Guidance Command 71

4.13 Results: ITCG Acceleration 72

4.14 Results: GENEX-ITACG Trajectory 73

4.15 Results: GENEX-ITACG Time to Go 74

4.16 Results: GENEX-ITACG Flight Path Angle 75

4.17 Results: GENEX-ITACG Guidance Command 76

4.18 Results: GENEX-ITACG Acceleration 77

4.19 Results: GENEX-ITACG Salvo Trajectory 78

4.20 Results: GENEX-ITACG Salvo Flight Path Angle 79

B.1 Simulink Model: Time Control 105

B.2 Simulink Model: Nonlinear Dynamic Equations 107

B.3 Simulink Model: Stop Conditions 108

LIST OF TABLES

4.1 Initial Conditions: Single Missile Flyout 57

4.2 Test Parameters: Single Missile Flyout 58

4.3 Initial Conditions: 3 Missile Salvo Attack Flyout 59

4.4 Test Parameters: 3 Missile Salvo Attack Flyout 59

CHAPTER 1: INTRODUCTION

Guided missile technology is a challenging, multi-discipline subject that has provided war fighters with innovative weapons since their introduction in World War II. The guidance law that is the subject of this thesis, General Vector Explicit - Impact Time and Angle Control guidance (GENEX-ITACG), represents only a portion of many subsystems that must be integrated together to accurately guide a missile to a target. It may be beneficial to provide readers who are unfamiliar with guided missile background information before the discussion of missile guidance laws. Therefore, the history of guided missiles, the three phases of guided flight and the traditional guidance, navigation and control (GNC) architecture for guided missiles are discussed in this section.

Guided missiles were introduced by the Germans in 1939. Warheads were previously delivered through the use of unguided rockets, which were essentially projectile weapons that flew ballistic trajectories. These unguided rockets were notoriously inaccurate due to their inability to alter their flight path once launched. Errors from target position uncertainty, wind gust and other disturbances to the missile flight path cannot be reduced without the ability to alter flight path. Guided missiles improved accuracy by altering the missiles flight path through the use of aerodynamic surfaces, thrust vectoring or side thrusters.

The first guided missile developed by the Germans was the Fritz X (FX1400), which was an unpowered, air-to-ground missile that glided to its target. During the same time period, the Germans also produced the HS293 missile. Unlike the FX1400, the HS293 was powered by a liquid fuel rocket motor and had a maximum range of about 8km. Several variants of the HS293 were produced, one being the larger HS294 which had two solid fuel rocket motors. Several ground-to-air missiles were also being developed by the end of WWII.

Two long range missiles produced by the Germans during WWII were the V1 and V2 missiles, which were used extensively against the British. The V1 missile was a catapult launched missile with a pulse jet motor that flew at 300mph before entering a preprogrammed dive. The V2 missile was larger and had a one minute rocket motor burn time that allowed it to reach cruising altitudes of Mach 5.

In 1946, the British began experimenting with guided weapons through the use of test vehicles. The first test vehicle was the short range, air-to-air, CTV1 test vehicle. This test vehicle incorporated three boost stages and had a maximum range of about 20,000 feet. Guidance and control techniques such as staging, roll stabilization, beam rider guidance and command link guidance were experimented with on this vehicle. The next test vehicle developed was the two stage RTV1 which had an increased range of about 46,000 feet. The second version of the RTV1 test vehicle, RTV2, also known as the GPV, had 8 solid fuel motors. An elaborate recovery system that included three first stage parachutes, a 20 foot second stage parachute and flotation gear was experimented with on this vehicle. Then a number of high altitude, high mach experiments were down with the CTV5 series of test vehicles. A few of these experiments were on kinetic heating, heat transfer at high Mach, and high altitude tracking. These experiments by Britain on test vehicles lasted until 1958 [14].

The phases of flight for a guided missile are shown in Fig. 1.1 to better understand the aforementioned boost stages. The purpose of the boost phase is to boost the missile up to flight speed while establishing a flight path to intercept the target. The purpose of the mid-course phase of flight is to guide the missile relatively close to the target at some desired orientation to aid in acquisition of the target. It is typically for this phase of flight to incorporate other objectives such as minimizing time of flight or conservation of energy. Conservation of energy is important because high maneuverability is typically needed during the terminal phase of flight, whose purpose is to minimize miss distance by eliminating all of the accumulated errors from the previous stages of flight.

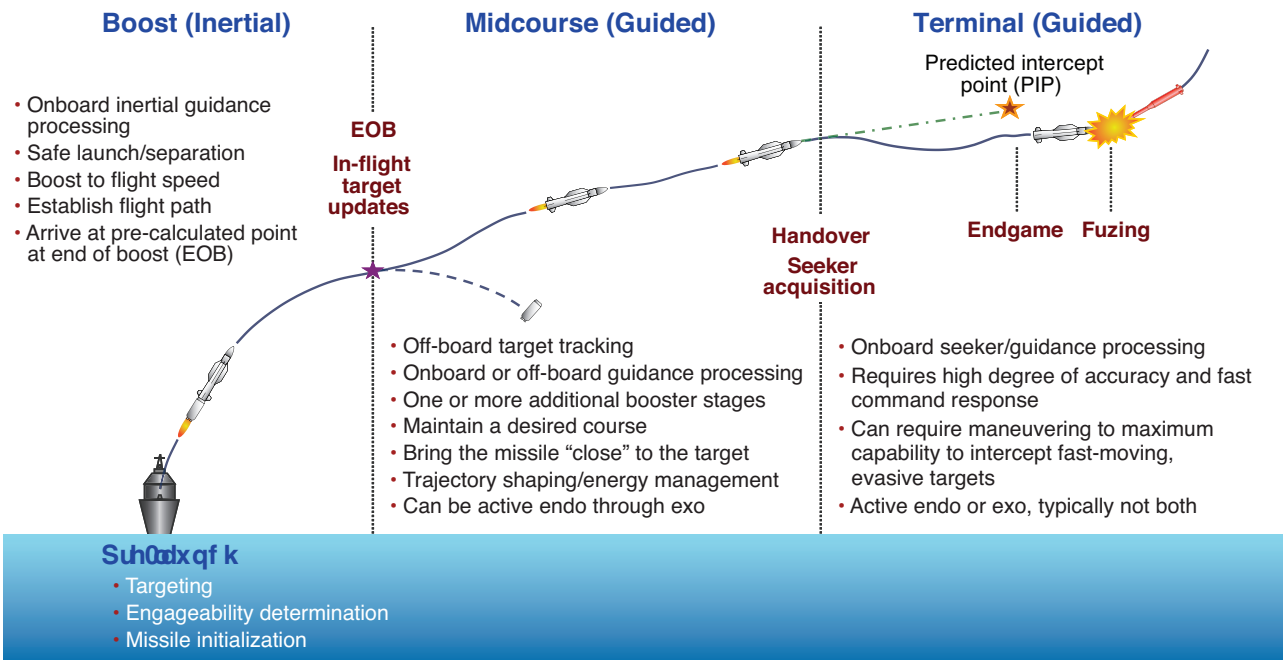

Figure 1.1: Phases of Flight:©The Johns Hopkins University Applied Physics Laboratory

The latter part of the terminal phase is known as the endgame. During the endgame the missile may be required to maneuver at maximum capability. The target is destroyed by guiding the missile to some lethal radius and using blast fragmentation, or by directly hitting the target. Not all missiles incorporate every phase of flight, but those that do are known as multi-stage missiles [12].

The traditional architecture of a missile's GNC system is shown in Fig. 1.2. There are three methods for target sensing: passive, semi-active, and active. Passive sensing is accomplished through the use of sensors that detects stray signals emitted from the target, such as the heat signature or radio frequency signals. This method of sensing directly provides the angular direction of the target, but does not directly provide range or range-rate information. Range and range-rate is typically needed by advanced guidance laws.

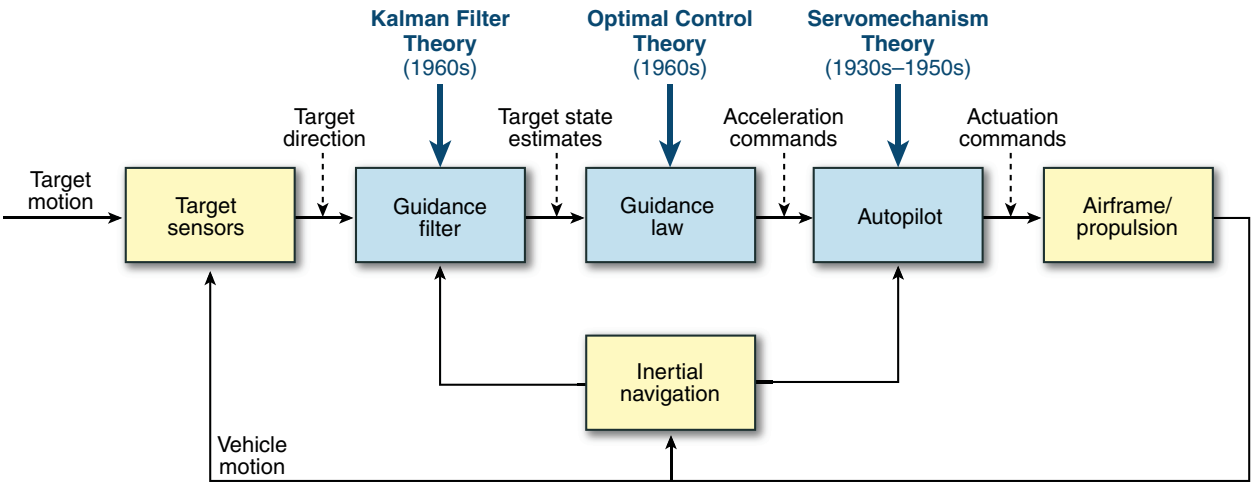

Figure 1.2: GNC Structure:©The Johns Hopkins University Applied Physics Laboratory

Semi-active homing is accomplished through the use of an off-board designator that illuminates the target and a onboard sensors that detects reflected signals emitted by the designator. Not only may range, range-rate, the angular direction of the target be provided by this method, but a significant increase in signal power may also be introduced without a increasing the size or weight of the missile.

Conversely, active sensing is accomplished through the use of an onboard designator. This method adds additional cost and weight to the missile. But, active sensing is self-sufficient after launch (fire and forget). Semi-active sensing is typically used during the mid-course phase of flight, while active sensing is typically restricted to the terminal phase of flight [12].

The role of the guidance filter is to remove noise from the states measured by the sensors and provide estimates on any states needed by the guidance law not directly provided by the sensors. This is typically accomplished through the use of linear or extended Kalman filters.

The guidance law uses the states provided by the guidance filter and generates commands that minimize the final miss distance between missile and target. The first method of guidance was for a person to compute commands based off observations and alter the flight path of the missile through a command link. Although relatively cheap, this method of guidance suffered from human errors and loss of slight in unfavorable conditions.

Eventually, the human was replaced with a radar set. The radar set eliminated many of these errors, but was more expensive and noisy. With the use of telemetry, semi-automatic systems came into use that used the radar to track the target and person to keep the target in the field of view. Then the first method of homing guidance called beam riding was introduced. Beam rider guidance was accomplished by following the target with a beam and keeping the missile within this beam until the missile reached the target. The beam is emitted from an off-board eliminator and a onboard sensor tracks the beam.

Contrary to homing guidance, with inertial guidance the missile is commanded to a predetermined position. The guidance commanded are based off the error between the missile's position and the predetermined position. The missile's position is calculated from measured accelerations. Obviously, this type of guidance is not suitable against highly maneuvering targets [14].

The autopilot forces the missile to follow guidance commands while maintaining stable flight by issuing commands to actuators. This can be accomplished through three different control techniques:

1. Roll stabilized - the missile is rolled so that lateral surfaces aligned with inertial axes.
2. Twist and steer - the missile is rolled so that lateral surfaces are normal to the direction of motion.
3. Non-roll position controlled - no attempt is made to control the missile's roll position.

Cartesian guidance commands can be fed directly into the actuator of a roll stabilized missile since the surfaces are aligned with the inertial axis. Whereas in twist and steer controlled missiles, cartesian guidance commands need to be converted to polar form before being used. In non-roll position controlled missile the roll rate must be kept lower than than the lateral command rates or else lateral commands cannot be followed [14].

Early guided missiles were built like airplanes with the use of rudders, canards and elevators to control motion in three planes. Then a symmetric cruciform design, which allowed maneuvering in all directions came, into use. Actuators force physical surfaces on the missile to follow control input from the autopilot. In early design and analysis actuators are typically modeled as a second order transfer function. For endoatmospheric flight several different aerodynamic control surfaces may be used such as moving wings, moving tailfins, and canards. Several non-aerodynamic means of control are also used such as thrust vectoring, jet vanes, and side thrustors [14].

The inertial navigation system provides several missile parameters used by the guidance law and autopilot through the use of accelerators which measure acceleration and gyroscopes which measure angular velocity. Similar to actuators, during early design and analysis the INS is typically modeled as a second order transfer function. Care must be in the flight control design to ensure that the dynamic range of the INS and the dynamic range of the actuator are not exceeded. The former leads to loss of inertial reference and the later may lead to significant performance degradation. Typically dynamic parameters evaluated are actuator position limit, actuator rate limit and INS measured acceleration limit [14].

This thesis concentrates on the guidance law component of the GNC system. The guidance law developed in this thesis, GENEX-ITACG, allows for a salvo homing missiles to simultaneously hit a stationary target at a prescribed impact time and impact angle, while also providing a user design parameter to alter the aggressiveness approach. Two guidance laws, general vector explicit guidance (GENEX) and impact time and angle control guidance (ITACG), motivated the creation GENEX-ITACG.

GENEX is an explicit guidance law that provides the user with a design parameter to adjust the aggressiveness of approach at a prescribed impact angle. However, GENEX does not allow for a simultaneous attack. This is accomplished through the integration of ITACG, which allows a salvo of missiles to simulatively hit a stationary target at a prescribed impact angle and impact time.

Chapter 2 provides the reader with an overview of several existing guidance laws. First the engagement geometry is presented to develop the dynamic equations of motion. Then proportional navigation (ProNav) is presented along with its several variations. Then concept of developing guidance laws through linear optimal control is presented. Then trajectory shaping guidance laws that specifies impact angles are presented. Finally, cooperative guidance laws that allow for several missiles to simulatively hit a target are presented.

Chapter 3 present the methods used to formulate GENEX-ITACG and applies these methods to develop the guidance law. An overview of linear optimal control, which establishes a flight objective while satisfying the constraints of the equations of motion, is presented. Then the derivation of GENEX-ITACG using the equations of motion and linear optimal control is presented.

Chapter 4 presents the simulation results of the cooperative guidance law. First, the effects of adjusting the prescribed impact angle of GENEX-ITACG is presented. Then the effects of adjusting the user design parameter of GENEX-ITACG on flight aggressiveness is presented. Then the effects of adjusting the prescribed impact time of GENEX-ITACG is presented. Lastly, a three missile salvo attack using GENEX-ITACG is presented.

Chapter 5 concludes this document with comments and areas of future development. One of these areas include removing the need to specify a predetermined impact time. Regardless, GENEX-ITACG is a power guidance law in itself. Let the journey begin.

CHAPTER 2: LITERATURE REVIEW

2.1 Introduction

In this chapter, several guidance laws are presented. The first guidance law presented is the well proven proportional navigation (Pro-Nav) guidance law. Pro-Nav essentially guides the missile by commanding accelerations directly proportional to the line of sight rate until impact. Many fielded missiles today use this guidance law or some variant of it due to its ease of implementation and proven robustness.

Two common forms presented are true proportional navigation (TPN) and pure proportional navigation (PPN). These two forms of Pro-Nav differ in the direction of commanded acceleration as shown in Fig. 2.1. TPN commands accelerations normal to the line of sight (LOS) vector while PPN commands accelerations normal to the missile's velocity. Simply put, the LOS vector is the line that connects the center of gravity of the missile to the center of gravity of the target.

A closed-form solution is obtainable for TPN because the components of acceleration along the LOS and transverse to the LOS to can be completely separated. In [5] Guelman provides a closed-form solution for using TPN against a nonmaneuvering target, alongwith the set of initial conditions that guarantees interception. These conditions that gurantee intercept are known as capture conditions. In [2], Ghose extends these results by performing a qualitative analysis for using TPN against a maneuvering target, alongwith analogous capture conditions.

Contrary to TPN, a general closed-form solution for PPN is unobtainable. However, in [4] Guelman performs a qualitative study that provides capture conditions for using PPN against a non maneuvering. In [4], Guelman extends these results by providing the capture conditions against a maneuvering target. These capture conditions for TPN and PPN are presented.

Then a commonly used variant of Pro-Nav called augmented proportional navigation (APN) is presented. APN directly accounts for target maneuvering in its derivation, whereas the previously mentioned Pro-Nav guidance laws do not. This additional information makes APN significantly more effective against highly maneuvering targets. In [16] and [17], APN is derived by recasting the polar dynamic equations into cartesian form. Several concepts such as time-to-go and zero effort miss are introduced. The derivation of APN alongwith these associated concepts are presented next.

Next, the formulation of guidance laws through what is known as linear optimal control is presented. Linear optimal control is accomplished by making reasonable assumptions about the nonlinear dynamic equations that govern the intercept scenario. With these assumptions, linear optimal control allows for the development of power guidance laws that take in additional information to achieve flight objectives such as minimum time trajectories, minimum energy trajectories and terminal impact angles. In [13] Palumbo, Jackson and Blauwkamp present the equations of motion in cartesian form alongwith the representation of this nonlinear equations in state space format through linearization. This derivation of the linear equations of motion in state space format are presented next.

In [17], Zipfel presents the linear optimal control equivalent to Pro-Nav called advanced guidance law (AGL). In [7], Lukacs extends AGL by taking target maneuvering into account to formulate the linear optimal control equivalent to APN called augmented advanced guidance law (AAGL). In [13], Palumbo, Jackson and Blaukamp extend AAGL by taking system lags into account to formulate advanced optimal guidance law (OGL). Each of these guidance laws are presented next.

Next, two trajectory shaping guidance laws designed to achieve a desired terminal impact angle are presented. The ability to control impact angle is crucial in penetrating the defense of well guarded or well armored targets. In [9], Kim and Grinder present a trajectory shaping guidance law that controls the terminal impact angle. In [11], Ohlmeyer presents a trajectory shaping guidance law that controls the terminal impact angle while also providing the user with a design parameter to shape the aggressiveness of the trajectory called general vector explicit guidance (GENEX). Each of these trajectory shaping guidance laws are presented next.

Finally, two cooperative guidance laws that allow for several missiles to simultaneously hit a target are presented. In [6], Jeon and Lee present a cooperative guidance law called impact time control guidance (ITCG) that allows multiple missiles to simultaneously hit a target at a prescribed impact time. In [10], Jeon and Lee extend ITCG by adding the ability to simultaneously hit a target at a prescribed impact time and impact angle. These two cooperative guidance laws are the last guidance laws presented before attention is turned to GENEX-ITACG.

2.2 Equations of Motion

The engagement geometry that is used to derive the polar equations of motion that governs the analysis of PPN and TPN is illustrated in Fig. 2.1. The reference coordinate system is aligned with the i-axis pointing towards the initial velocity vector of the target, $\mathbf{V}_{T0}$, the j-axis normal to the x-axis, and the k-axis completing the RHS by pointing out of the page. It is assumed that the velocities of the missile and shooter, denoted by $\mathbf{V}_M$ and $\mathbf{V}_T$, are constant.

The flight path angle, defined as the angle from the i-axis to the respective velocity vectors, is denoted as γ for the missile and β for the target. The LOS vector is denoted by $\mathbf{r}$ and its magnitude is denoted as R. The LOS angle, defined as the angle from the i-axis to the LOS vector, is denoted as θ. The angle of attack (AOA), defined as the angle from the line of sight vector to the missile's velocity vector, is denoted as α.

The closing velocity between the missile and the target has two polar components, V_r and V_θ. V_r is defined as the component along the LOS in the direction of the unit vector $\mathbf{e}_r$. V_r only reduces the time until intercept, but does not contribute to miss distance. V_θ is the component transverse to the LOS and directly contributes to miss distance.

The achieved acceleration of the target, a_T, is assumed to be normal to its velocity vectors. The direction of the commanded acceleration for the missile depends on which form of proportional navigation is used as described below:

TPN Acceleration is commanded normal to LOS vector, $\mathbf{r}$, in the direction of the unit vector $\mathbf{e}_\theta$

PPN Acceleration is commanded normal to missile velocity vector, $\mathbf{V}_M$, in the direction of the unit vector $\mathbf{e}_\gamma$

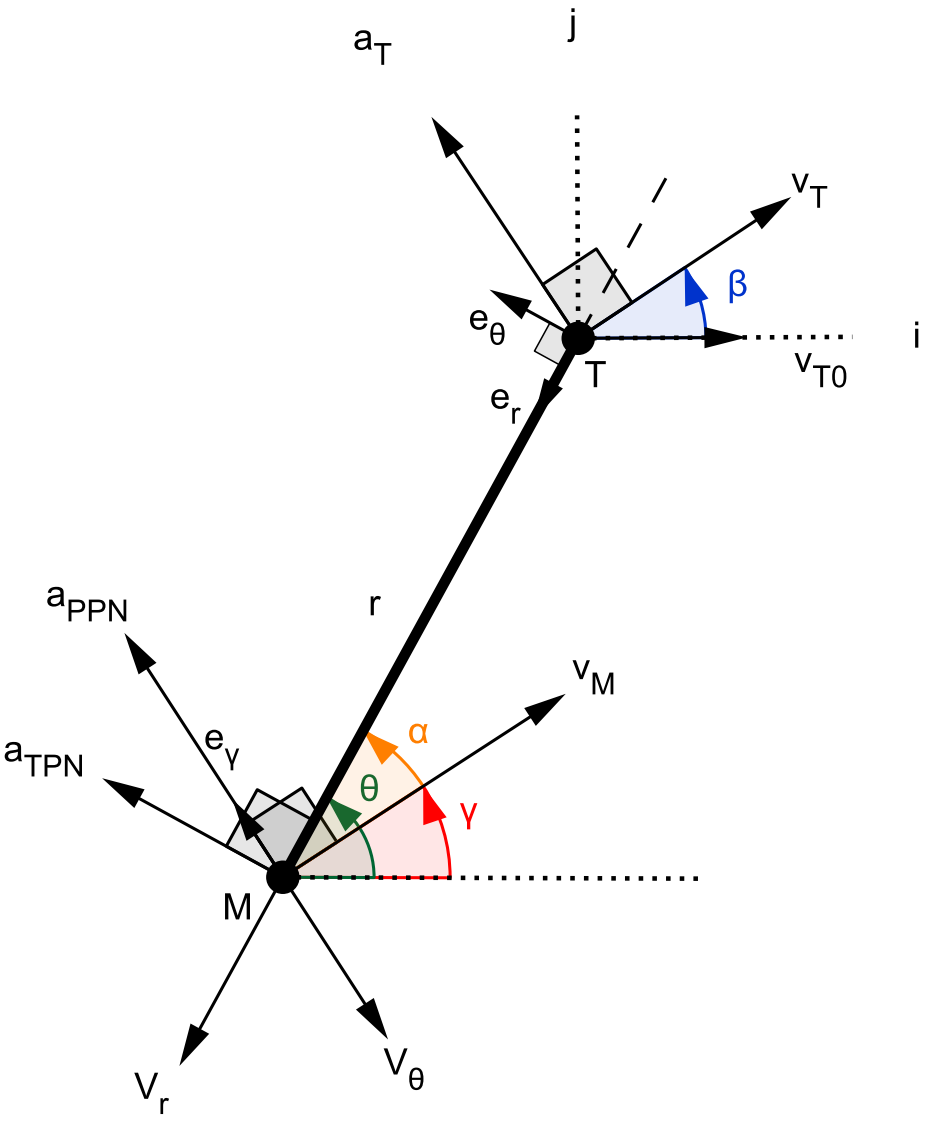

Figure 2.1: Geometries of Three Different Forms of Proportional Navigation

The engagement geometry that is used to derive the cartesian equations of motion which governs the analysis of APN and the advanced guidance laws is illustrated in Fig. 2.1. The LOS vector, $\bar{r}$, is defined as $\bar{r} = \bar{r}_T - \bar{r}_M$. The relative velocity vector, $\bar{v}$, and the relative acceleration vector, $\bar{a}$, are defined in a similar manner such that $\bar{v} = \bar{v}_T - \bar{v}_M$ and $\bar{a} = \bar{a}_T - \bar{a}_M$. The cartesian components of each of these vectors along the x-axis and y-axis are denoted by a x and y subscript. The acceleration of the missile and target is assumed to be normal to the respective velocity vector.

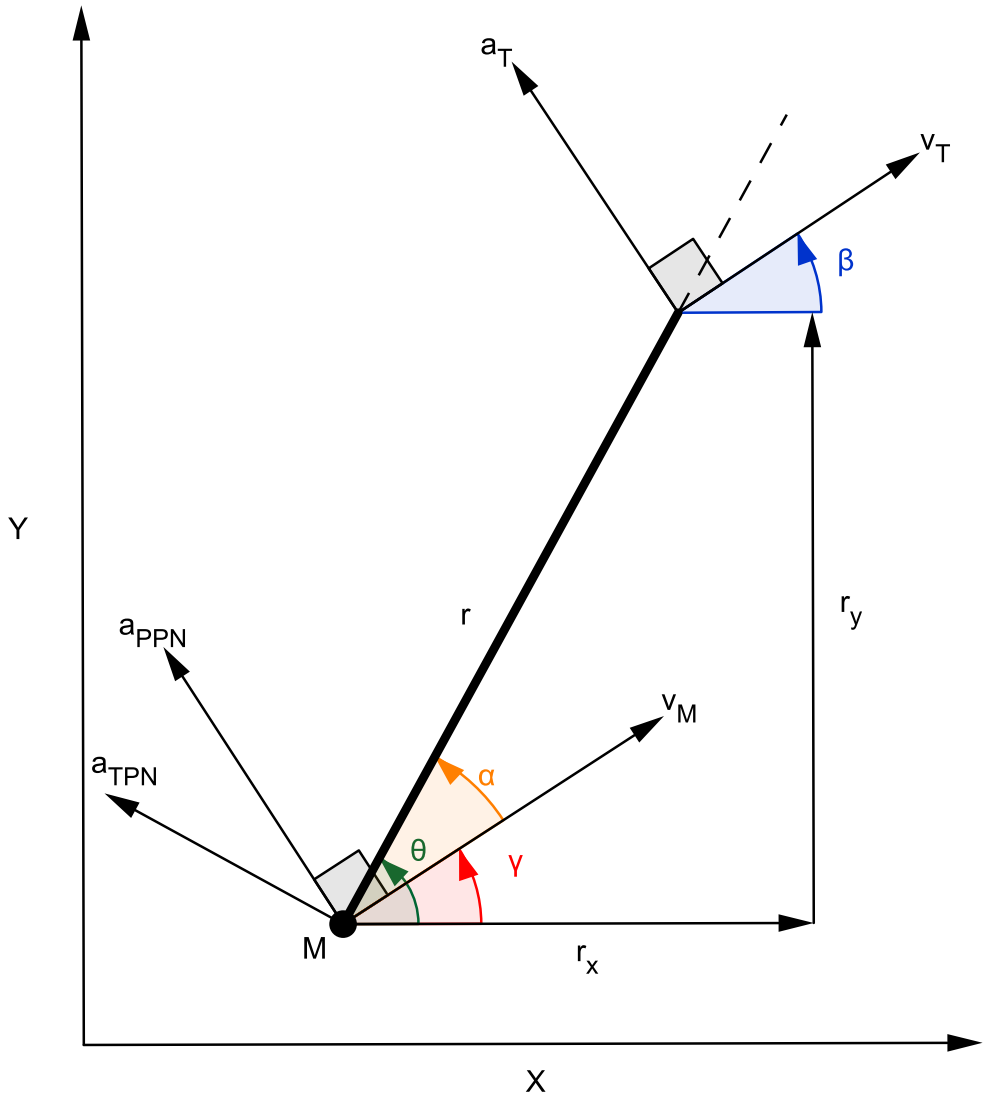

Figure 2.2: Advanced Guidance Law Cartesian Geometry

2.2.1 Polar Equations of Motion

In this section, the polar equations of motion that govern the engagement geometry depicted in Fig. 2.1 are derived in the same manner done by Shukla and Mahapatra in [15]. Without loss of generality, it may be assumed that both the missile and target have the same mass, m. Through the use of Newton's second law the relative motion between the missile and target can be expressed in vector form as

$$F = F_T - F_M = m(\frac{d^2\mathbf{r}_T}{dt^2} - \frac{d^2\mathbf{r}_M}{dt^2}) \tag{2.1}$$

The rotation of the unit triad (e_r,e_θ,e_k) about the e_k vector can be expressed as

$$\omega = \dot{\theta}\mathbf{e}_k \tag{2.2}$$

The LOS vector from the missile to the target can be expressed as

$$\mathbf{r} = \mathbf{r}_T - \mathbf{r}_M = R\mathbf{e}_r \tag{2.3}$$

where R is the range.

Taking the derivative of Eq. 2.3, the LOS rate can be expressed as

$$\begin{aligned} \frac{d\mathbf{r}}{dt} &= \dot{R}\mathbf{e}_r + \omega \times \mathbf{r} \\ &= \dot{R}\mathbf{e}_r + R\dot{\theta}\mathbf{e}_\theta \end{aligned} \tag{2.4}$$

where ω represents the angular velocity cause by missile maneuvering.

Furthermore, by taking the derivative of Eq. 2.4 the LOS acceleration can be expressed as

$$\begin{aligned}\frac{d^2\mathbf{r}}{dt^2} &= \ddot{R}\mathbf{e}_r + \omega \times \mathbf{r} + \omega \times (\omega \times \mathbf{r}) + 2\omega \times \mathbf{r} \\ &= (\ddot{R} - R\dot{\theta}^2)\mathbf{e}_r - (R\ddot{\theta} + 2\dot{R}\dot{\theta})\mathbf{e}_\theta\end{aligned} \tag{2.5}$$

Recall that the principle of Pro-Nav is to guide the missile by commanding accelerations directly proportional to the LOS rate, $\dot{\theta}$. An intelligent target would counter a missile guided by Pro-Nav by commanding accelerations indirectly proportional $\dot{\theta}$ [2]. Dividing both sides of Eq. 2.1 by m and applying these principles of guidance to the left hand side of the equation results in

$$a = a_T - a_M = \frac{F_T - F_M}{m_T} = (\Lambda_{\theta T}\frac{1}{\dot{\theta}} - \Lambda_{\theta M}\dot{\theta})\mathbf{e}_\theta + (\Lambda_{rT} - \Lambda_{rM})\dot{\theta}\mathbf{e}_r \tag{2.6}$$

where Λ_θ and Λ_r are proportionality constants.

Using TPN, these constants can be expressed as

$$\Lambda_{rT} = \Lambda_{rM} = 0 \qquad \Lambda_{\theta T} = b \qquad \Lambda_{\theta M} = c = -\lambda V_R \tag{2.7}$$

where V_R is the initial closing velocity.

Through the use of Eq. 2.1, by equating the RHS of Eq. 2.5 to the RHS Eq. 2.6 and using the constants defined in Eq. 2.7 the equations of motion for TPN can be expressed as

$$\begin{aligned}\ddot{R} - R\ddot{\theta}^2 &= 0 \\ R\ddot{\theta} + (2\dot{R} + c)\dot{\theta} &= \frac{b}{\dot{\theta}}\end{aligned} \tag{2.8}$$

With PPN acceleration is commanded normal to the missile's velocity vector such that

$$a_M = \frac{\mathbf{F}}{m} = V_M \dot{\gamma} \mathbf{e}_\gamma \tag{2.9}$$

and by using PPN the following relations can be made

$$\begin{aligned} \dot{\gamma} &= N\dot{\theta} \\ a_M &= N V_M \dot{\theta} \mathbf{e}_\gamma \end{aligned} \tag{2.10}$$

where N is the proportionality constant.

The components of relative velocity along the LOS in the direction of e_r and normal to the LOS in the direction of e_θ can be expressed as

$$\begin{aligned} V_r &= \dot{R} = V_T \cos(\theta - \beta) - V_M \cos(\theta - \gamma) \\ V_\theta &= R\dot{\theta} = -V_T \sin(\theta - \beta) + V_M \sin(\theta - \gamma) \\ \beta &= \frac{a_T}{V_T} t \end{aligned} \tag{2.11}$$

where β is the flight path angle of the target.

These components of relative velocity may be expressed strictly in terms of time and the LOS angle by integrating Eq. 2.10 such that

$$\theta - \gamma = b\theta - c \tag{2.12}$$

where $b = 1 - N$,$c = \gamma_i - N\theta_i$, γ_i is the initial missile flight path angle and θ_i is the initial LOS angle.

Substituting Eq. 2.12 into Eq. 2.11 results in

$$\begin{aligned} V_r(\theta, t) &= V_T \cos(\theta - \beta) - V_M \cos(b\theta - c) \\ V_\theta(\theta, t) &= -V_T \sin(\theta - \beta) + V_M \sin(b\theta - c) \end{aligned} \tag{2.13}$$

Furthermore, when the target velocity is assumed constant, i.e $\beta = 0$, the components of velocity are no longer time dependent and Eq. 2.13 reduces to

$$\begin{aligned} V_r(\theta) &= V_T \cos(\theta) - V_M \cos(b\theta - c) \\ V_\theta(\theta) &= -V_T \sin(\theta) + V_M \sin(b\theta - c) \end{aligned} \tag{2.14}$$

2.2.2 Cartesian Equations of Motion

In this section, the cartesian equations of motion that govern the engagement geometry depicted in Fig. 2.2 are derived in the same manner done by Palumbo Jackson and Blauwkamp in [13]. The relative position between the missile and target can be expressed as

$$\bar{r} = r_x\bar{1}_x + r_y\bar{1}_y = R\cos(\theta)\bar{1}_x + R\sin(\theta)\bar{1}_y \tag{2.15}$$

The relative velocity between the missile and target can be expressed as

$$\begin{aligned}\bar{v} = v_x\bar{1}_x + v_y\bar{1}_y = [v_T\cos(\beta) - v_M\cos(\gamma)]\bar{1}_x \\ + [v_T\sin(\beta) - v_M\sin(\gamma)]\bar{1}_y\end{aligned} \tag{2.16}$$

The relative acceleration between the missile and target can be expressed as

$$\begin{aligned}\bar{a} = a_x\bar{1}_x + a_y\bar{1}_y = [a_T\sin(\beta) - a_M\sin(\gamma)]\bar{1}_x \\ + [a_T\cos(\beta) - a_M\cos(\gamma)]\bar{1}_y\end{aligned} \tag{2.17}$$

$$\gamma = \frac{a_M}{v_M} \tag{2.18}$$

$$\beta = \frac{a_T}{v_T} \tag{2.19}$$

where $\bar{1}_x$ and $\bar{1}_y$ are unit vectors along the reference x-axis and y-axis.

These equations are clearly nonlinear and are not suitable for linear optimal control. By assuming small missile and target flight path angles the equations can be linearized such that

$$\bar{r} = r_x\bar{1}_x + r_y\bar{1}_y = R\cos(\theta)\bar{1}_x + R\sin(\theta)\bar{1}_y \tag{2.20}$$

$$\begin{aligned}\bar{v} = v_x\bar{1}_x + v_y\bar{1}_y = [v_T\cos(\beta) - v_M\cos(\gamma)]\bar{1}_x \\ + [v_T\sin(\beta) - v_M\sin(\gamma)]\bar{1}_y\end{aligned} \tag{2.21}$$

$$\begin{aligned}\bar{a} = a_x\bar{1}_x + a_y\bar{1}_y = [a_T\sin(\beta) - a_M\sin(\gamma)]\bar{1}_x \\ + [a_T\cos(\beta) - a_M\cos(\gamma)]\bar{1}_y\end{aligned} \tag{2.22}$$

When the missile is close to colliding with the target the line of sight angle is very small. If the targets flight path angle is also very small, then the following approximation can be made:

$$r_y \simeq R\lambda$$

$$a_y \simeq a_T - a_M$$

Furthermore, if the closing velocity between the missile and target is less than or equal to zero throughout the entirety of the flight, then only the y-axis component of acceleration needs to be controlled to intercept the target.

The nonlinear equations of motion expressed in Eq. 2.22 can be linearized in expressed in state space format as

$$\begin{aligned}
\dot{\bar{x}}(t) =& \mathbf{A}\bar{x}(t) + \mathbf{B}\bar{u}(t) \\
\bar{y}(t) =& \mathbf{C}\bar{x}(t) \\
\mathbf{A} =& \begin{bmatrix} 0 & 1 \\ 0 & 0 \end{bmatrix} \qquad \mathbf{B} = \begin{bmatrix} 0 \\ -1 \end{bmatrix} \qquad \mathbf{C} = \begin{bmatrix} 1 & 0 \end{bmatrix}
\end{aligned} \tag{2.23}$$

These linearized cartesian equations form the basis for developing the advanced guidance laws.

2.3 Classical Guidance Laws

2.3.1 True Proportional Navigation Guidance (TPN)

In [5], Guelman obtained a closed-form solution for TPN against a nonmaneuvering target through the manipulation of Eq. 2.8 with $b = 0$. Although the full results are not presented here, the capture conditions are. This analysis was conducted through the definitions of three concentric circle, C_c, C_s, and C_d, defined by the initial conditions of V_{r0} and $V_{\theta 0}$.

These three concentric circles in order of decreasing radius are defined as:

$$C_c : (V_{r0} + c)^2 + V_{\theta 0}^2 = c^2 \tag{2.24}$$

$$C_s : (V_{r0} + c)^2 + V_{\theta 0}^2 = (c/2)^2 \tag{2.25}$$

$$C_d : (V_{r0} + c)^2 + V_{\theta 0}^2 = (2c/3)^2 \tag{2.26}$$

In terms of the missile's ability to capture the target, Guelman proves that a missile starting its course outside of C_c with initial closing velocity $V_{r0} > -2c$ will not reach the target. The capture region is proved to be the initial conditions that are inside of C_c. Thus the capture region is strictly a function of the initial conditions and their relation with the navigation constant, c. Furthermore, if a missile begins within this capture region it reaches the target in a finite time, closing velocity and LOS angle, all defined in [5].

However, nothing has been said about the boundness of the LOS rate yet. This boundness is critical in the design of the missile because it directly effects the required maximum maneuver capability of the missile. Guelman assesses the boundness of the LOS rate by acknowledging five zones within the capture region, C_c, as follows:

1. For a missile starting its course outside of C_d, but inside of C_c with initial closing velocity $V_{r0} > -2c$, $\theta(\dot{t}_f) = 0$ and $\theta(\ddot{t}_f) = 0$.

2. For a missile starting its course inside of C_d and C_c with initial closing velocity $V_{r0} > -2c$, $\theta(\dot{t}_f) = 0$ and $\theta(\ddot{t}_f) = -[sign(\dot{\theta}_0]\infty$.

3. For a missile starting its course inside of C_s and C_d, $\theta(\dot{t}_f) = \infty$ and $\theta(\ddot{t}_f) = [sign(\dot{\theta}_0]\infty$.

4. For a missile starting its course outside of C_s, but inside of C_d and C_c with initial closing velocity $V_{r0} < -2c$, $\theta(\dot{t}_f) = 0$ and $\theta(\ddot{t}_f) = -[sign(\dot{\theta}_0]\infty$.

5. For a missile starting its course inside of C_d and C_c with initial closing velocity $V_{r0} < -2c$, $\theta(\dot{t}_f) = 0$ and $\theta(\ddot{t}_f) = 0$.

In summary, the commanded acceleration of a missile guided by TPN starting its course within the circle C_c, but outside of C_s (zones 1,2,4,5) is bounded throughout flight. Otherwise, the commanded acceleration of a missile starting its course within C_s (zone 3) becomes unbounded at pursuit end.

In [2], Ghose extended these results to define a new capture region against a target that intelligently maneuvers by commanding acceleration indirectly proportional to the LOS rate in a direction that is normal to the LOS vector. Altough a closed-form solution is not available for Eq. 2.8, Ghose performed a qualitative analysis. Through this analysis Ghose proved that for a missile pursing a target, with maneuvers defined in Eqs. 2.8-2.7, a capture region exist if $br_0 < (2c/3)^3$ and the capture region satisfies the following two conditions:

1. $k \leq 0$, where k is a circle defined as $k = V_{r0}^2 + V_{\theta 0}^2 + 2cV_{r0}$.

2. $k^2 \geq 4br_0(V_{r0} + 2c)$

2.3.2 Pure Proportional Navigation Guidance (PPN)

In [3], Guelman performed a qualitative analysis for PPN against a nonmaneuvering target through the manipulation of Eq. 2.14. Once again, the full results are not presented here, but the capture conditions are.

This analysis was conducted through the definitions of two sectors of the polar $V_r - V_\theta$ plane: σ^- with negative closing velocity and σ^+ with positive closing velocity. Each of these sectors contain a single straight line trajectory, i.e $V_\theta = 0$ and $V_r \neq 0$. In addition, the range from the missile to target is monotonic within these sectors.

Guelman proved that if $v > 1$ and $bv > 1$, where $v = \frac{V_T}{V_M}$, then

- any trajectory starting in σ^+ will leave σ^+ for increasing time and
- any trajectory starting in σ^- will stay within σ^- for increasing time while approaching the target along a straight line trajectory.

Therefore, any trajectory that starts within sector σ^+ will exit this sector and enter sector σ^-. Once in sector σ^- the trajectory will approach the target along a straight line trajectory. The only time the trajectory will not reach the target is if it begins in sector σ^+ and $V_\theta = 0$.

Furthermore, regarding the boundness of the LOS rate, Guelman proves that if:

1. $\frac{dV_\theta}{d\theta} < V_r$, then the LOS rate is a decreasing function of time
2. $\frac{N-2}{2} v_M > v_T$, the LOS rate at the final phase of flight is a decreasing function of time.

In [4], Guelman extended these results for the case against a maneuvering target through the manipulation of Eq. 2.14. The analysis was conducted through the definition of two sector S_θ and S_r defined as:

$$\begin{aligned} \theta_{n0} - \frac{1}{b}\arcsin(\frac{1}{v}) \leq \theta_\theta &\qquad \leq \theta_{n0} + \frac{1}{b}\arcsin(\frac{1}{v}) \\ \theta_{n0} + \frac{\pi}{2b} - \frac{1}{b}\arcsin(\frac{1}{v}) \leq \theta_r &\qquad \leq \theta_{n0} + \frac{\pi}{2b} + \frac{1}{k}\arcsin(\frac{1}{v}) \end{aligned}$$

where

$$\theta_{n0} = \theta_0 - \frac{\gamma_0}{b} - \frac{n\pi}{b}$$

If $V_M > \sqrt{2}V_T$, these sectors do not intercept and an additional eight sectors can be defined as

$$\begin{aligned} S_\theta^+ &= \{\theta\colon \text{given any real} t, V_\theta(\theta,t) = 0, V_r(\theta,t) > 0\} \\ S_\theta^- &= \{\theta\colon \text{given any real} t, V_\theta(\theta,t) = 0, V_r(\theta,t) < 0\} \\ S_r^+ &= \{\theta\colon \text{given any real} t, V_r(\theta,t) = 0, V_\theta(\theta,t) > 0\} \\ S_r^- &= \{\theta\colon \text{given any real} t, V_r(\theta,t) = 0, V_\theta(\theta,t) < 0\} \end{aligned}$$

$$\begin{aligned} \sigma\theta^+ &= \{\theta\colon V_\theta(\theta,t) > 0, \text{for all t}\} \\ \sigma\theta^- &= \{\theta\colon V_\theta(\theta,t) < 0, \text{for all t}\} \\ \sigma\theta^+ &= \{\theta\colon V_r(\theta,t) > 0, \text{for all t}\} \\ \sigma r^- &= \{\theta\colon V_r(\theta,t) < 0, \text{for all t}\} \end{aligned}$$

Guelman proved that if $V_M > \sqrt{2}V_t$ and $N > 1 + \frac{V_T}{V_M}$, then the missile reaches the target for any initial state exterior to S_θ^+ along a straight line trajectory of sector S_θ^-. Even if the missile begins its course away from the target, $\sigma_r^+ \cap \sigma_\theta^-$ or $\sigma_r^+ \cap \sigma_\theta^+$, the missile eventually enters segment S_θ^- after entering σ_r^-. The condition $V_M > \sqrt{2}V_t$ guarantees that the missile enters σ_r^-. Once in S_θ^-, the missile remains in this section until it reaches the target.

In addition, Guelman proved that the missile reaches the target when the initial conditions lay within S_θ^+ only if:

1. $V_M > \sqrt{2}V_T$
2. $N > 2 + \left(\frac{2V_T}{\sqrt{V_M^2 - V_T^2}} \right) > 1 + \frac{V_T}{V_M}$
3. $\left| \dot{\theta}_0 \right| > \frac{|a_T|}{(N-2)\sqrt{V_M^2 - V_T^2} - 2V_T}$

In [15], Shukla argues that PPN is the better implementation of PPN for several reasons. For one, PPN does not require the missile to accelerate and decelerate because acceleration commands are issued normal to the velocity vector. Whereas, TPN requires significant accelerations and decelerations, especially for large collision course deviations. These large accelerations and deceleration are impossible to achieve with aerodynamically controlled missile and leads to excessive control efforts when compared to PPN.

In addition, the capture regions for TPN are more restrictive than PPN. Even for the cases where interception is possible, the LOS rate does not uniformly decrease for all navigation constants. Contrarily, the LOS rate for PPN uniformly decreases for all navigation constants.

2.3.3 Augmented Proportional Navigation Guidance (APN)

A popular variation of Pro-Nav that tries to accommodate for the target's acceleration is augmented Pro-Nav (APN). The derivation of APN guidance is derived following the lead of Zarchan and Zipfel while referring to Fig 2.2[16][17][13]. If the line of sight angle between the missile is small, then using the small angle approximation the line of sight angle can be expressed as

$$\theta = \frac{r_y}{R} \tag{2.27}$$

where r_y lateral relative position and R is the range to the target.

The approximate closing velocity between the missile and target in a head-on scenario or tail-chase scenario may be expressed as $V_c = V_M + V_T$ or $V_c = V_M - V_T$. Moreover, since the closing velocity is defined as the negative rate of range,R, and the range must go to zero at the end of flight, R can be expressed as

$$R = V_c(t_f - t) \tag{2.28}$$

where the quantity $t_f - t$ is the time until intercept known as time-to-go, t_{go}.

Substituting Eq. 2.28 into Eq. 2.27 and taking the derivative of the result yields

$$\dot{\theta} = \frac{r_y + \dot{r}_y t_{go}}{V_c t_{go}^2}. \tag{2.29}$$

Moreover, substituting Eq. 2.29 into the true PN guidance law of Eq. 2.7 yields

$$a_M = NV_c\dot{\theta} = \frac{N(r_y + \dot{r}_y t_{go})}{t_{go}^2} = \frac{N(ZEM)}{t_{go}^2}. \tag{2.30}$$

The expression in parentheses is the miss distance that would occur if the missile made no further corrective actions and target did not maneuver. This expression is commonly known as the zero effort miss distance (ZEM). If the target does maneuver, then the ZEM must be augmented by an additional term to account for this acceleration such that

$$ZEM = r_y + \dot{r}_y t_{go} + \frac{1}{2} a_T t_{go}^2. \tag{2.31}$$

Substituting Eq. 2.31 into Eq. 2.30 yields

$$a_M = N V_c \dot{\theta} = \frac{N(ZEM)}{t_{go}^2} = N V_c \dot{\theta} + \frac{N a_T}{2} \tag{2.32}$$

which is the augmented proportional navigation law.

It may be shown that for a constant acceleration target maneuver that augmented proportional navigation requires half the acceleration of proportional navigation with a proportionality constant of 3. Moreover, augmented proportional navigation requires much less total acceleration than proportional navigation because it makes use of more detailed information to operate in a more efficient manner [16].

2.4 Advanced Guidance Laws

Linear optimal control theory requires the equations to be in linear state space form such that

$$\begin{aligned} \dot{\bar{x}} &= A(t)\bar{x}(t) + B(t)\bar{u}(t) \\ \bar{y} &= C(t)\bar{x}(t) \end{aligned} \tag{2.33}$$

where $\bar{x} \in \Re^n$ is the state vector, $\bar{y} \in \Re^m$ is the output vector, $\bar{u} \in \Re^r$ is the control vector, $A \in \Re^{n\times n}$ is the state matrix, $B \in \Re^{n\times r}$ is the input matrix, and $C \in \Re^{m\times n}$ is the output matrix. Representing these equations in linear state space form may be accomplished by making the following assumptions [13]: V_c is positive such that only the kinematics in the y/z plane need to be actively controlled to achieve an intercept; λ is very small such that $r_y \approx R\lambda$, and γ_T is very small such that $a_y \approx a_T - a_M$.

With these assumptions the state vector may be defined as $\bar{x} \equiv [x_1 \;\; x_2]^T = [r_y \;\; v_y]^T$, the input may be defined as $\bar{u} \equiv a_M$, and the matrices of Eq. 2.33 can be expressed as

$$A = \begin{bmatrix} 0 & 1 \\ 0 & 0 \end{bmatrix}, \;\; B = \begin{bmatrix} 0 \\ -1 \end{bmatrix} \;\; C = \begin{bmatrix} 1 & 0 \end{bmatrix} \tag{2.34}$$

Now the linear optimal control problem with a quadratic PI may be formulated as

$$\begin{aligned} &\underset{u(t)}{\text{minimize}} \;\; J = \frac{1}{2}\bar{x}(t_f)^T Q_f \bar{x}(t_f) + \frac{1}{2}\int_{t_0}^{t_f} u(t)Ru(t)dt \\ &\text{subject to} \;\; \dot{\bar{x}} = A\bar{x}(t) + Bu(t) \end{aligned}$$

The meaning of this problem statement and the methodology to solve it is presented in the next chapter. The structure is presented here for reference.

2.4.1 Advanced Guidance Law (AGL)

According to Zipfel [17], when goal is to minimize miss distance and limit control power without considering target maneuvering the linear optimal control problem can be formulated as

$$\begin{aligned} &\underset{u(t)}{\text{minimize}} \;\; J = \frac{1}{2}\bar{x}(t_f)^T Q_f \bar{x}(t_f) + \frac{1}{2}\int_{t_0}^{t_f} u(t) R u(t) dt \\ &\text{subject to} \;\; \dot{\bar{x}} = \begin{bmatrix} 0 & 1 \\ 0 & 0 \end{bmatrix} \bar{x}(t) + \begin{bmatrix} 0 \\ -1 \end{bmatrix} \end{aligned}$$

The solution to this linear optimal control problem yields

$$\begin{aligned} a &= \frac{3t_{go}}{3\|R\| + t_{go}^3} ZEM \\ ZEM &= x_T - x_M + (v_T - v_M) t_{go} \end{aligned} \tag{2.35}$$

Assuming the missile is on a near collision course with the target if the control input is not limited, i.e $\|R\| = 0$, then the result is called the advanced guidance law (AGL). AGL is simply PN guidance in cartesian form with an proportionality constant equal to 3 expressed as

$$a = \frac{3}{t_{go}^2} ZEM \tag{2.36}$$

2.4.2 Advanced Augmented Guidance Law

According to Lukacs [7], target acceleration may be taken back into account by redefining the state vector such that $\bar{x} \equiv [x_1 \;\; x_2 \;\; x_3]^T = [r_y \;\; v_y \;\; a_T]^T$. The linear optimal control problem with target acceleration included and no control effort limit, $\|R\| = I$ can be formulated as

$$\begin{aligned} \underset{u(t)}{\text{minimize}} \;\; & J = \frac{1}{2}\bar{x}(t_f)^T Q_f \bar{x}(t_f) + \frac{1}{2}\int_{t_0}^{t_f} u^2(t)dt \\ \text{subject to} \;\; & \dot{\bar{x}} = \begin{bmatrix} 0 & 1 & 0 \\ 0 & 0 & 1 \\ 0 & 0 & 0 \end{bmatrix} \bar{x}(t) + \begin{bmatrix} 0 \\ -1 \\ 0 \end{bmatrix} u(t) \end{aligned}$$

The solution to this linear optimal control problem yields

$$\begin{aligned} a &= \frac{3}{t_{go}^2} ZEM \\ ZEM &= x_T - x_M + (v_T - v_M)t_{go} + \frac{1}{2} + a_T t_{go}^2 \end{aligned} \tag{2.37}$$

This guidance law is simply augmented PN guidance with an proportionality constant equal to 3. It is now clear how advanced guidance laws make use of more detailed information to derive more efficient guidance laws. Even high maneuvering targets can be taken into account by considering jerk. In addition, inceptor dynamics such as first, second, and higher order lags in the guidance law may be taken into account.

2.4.3 Advanced Optimal Guidance Law (OGL)

The aforemention guidance laws all assume perfect command response. According to Palumbo, Blaukamp and Lloyd [13], a more realistic assumption would be to have the missile acceleration, a_M, respond to an acceleration command, a_c, via the first order transfer function

$$\frac{a_M}{a_c} = \frac{1}{1+\tau s} \tag{2.38}$$

The first order lag may be taken into account by redefining the state vector such that $\bar{x} \equiv [x_1 \ x_2 \ x_3 \ x_4]^T = [r_y \ v_y \ a_T \ a_M]^T$ and redefining the input to be the commanded acceleration, a_c. This linear optimal control problem can be formulated as

$$\begin{aligned}
&\underset{u(t)}{\text{minimize}} \ \ J = \frac{1}{2}\bar{x}(t_f)^T Q_f \bar{x}(t_f) + \frac{1}{2}\int_{t_0}^{t_f} u^2(t)dt \\
&\text{subject to} \ \ \dot{\bar{x}} = \begin{bmatrix} 0 & 1 & 0 & 0 \\ 0 & 0 & 1 & -1 \\ 0 & 0 & 0 & -1 \\ 0 & 0 & 0 & -\frac{1}{\tau} \end{bmatrix} \bar{x}(t) + \begin{bmatrix} 0 \\ 0 \\ 0 \\ \frac{1}{\tau} \end{bmatrix} u(t)
\end{aligned}$$

The solution to this linear optimal control problem yields

$$\begin{aligned}
a_c &= \frac{6\tilde{N}}{t_{go}^2} ZEM \\
ZEM &= x_T - x_M + (v_T - v_M)t_{go} + \frac{1}{2} + a_T t_{go}^2 - \tau^2\left(\frac{t_{go}}{\tau} + e^{-\frac{t_{go}}{\tau}} - 1\right)a_M \\
\tilde{N} &= \frac{6\left(\frac{t_{go}}{\tau}\right)^2\left(\frac{t_{go}}{\tau} + e^{-\frac{t_{go}}{\tau}} - 1\right)}{3 + 6\frac{t_{go}}{\tau} - 6\frac{t_{go}^2}{\tau^2} + 2\frac{t_{go}^3}{\tau^3} - 12\frac{t_{go}}{\tau}e^{-\frac{t_{go}}{\tau}} - 3e^{-2\frac{t_{go}}{\tau}}}.
\end{aligned} \tag{2.39}$$

This guidance law is called "optimal" guidance law (OGL).

2.5 Explicit Guidance Laws

A class of modern missile guidance called explicit guidance laws that allows a missile to hit the target with specified relative velocity and/or position constraints have also become an interesting subject of research. These terminal constraints cause the trajectory of the missiles to deviate from the straight line trajectory during the terminal phase of flight. Therefore, these explicit guidance laws are all trajectory shaping guidance laws. Similar to the advanced terminal guidance laws the state vector may be defined as $\bar{x} \equiv [x_1 \;\; x_2]^T = [r_y \;\; v_y]^T$ and the input may be defined as $\bar{u} \equiv u = a_M$. The linear optimal control problem for explicit guidance laws can be formulated as

$$\begin{aligned} &\underset{u(t)}{\text{minimize}} \;\; J = \frac{1}{2}[\bar{x}(t_f) - x_f]^T Q_f [\bar{x}(t_f) - x_f] + \frac{1}{2}\int_{t_0}^{t_f} u(t) R u(t) dt \\ &\text{subject to} \;\; \dot{\bar{x}} = A\bar{x}(t) + Bu(t) \end{aligned}$$

or equivalently

$$\begin{aligned} &\underset{u(t)}{\text{minimize}} \;\; J = \frac{1}{2}\int_{t_0}^{t_f} u(t) R u(t) dt \\ &\text{subject to} \;\; \dot{\bar{x}} = A\bar{x}(t) + Bu(t) \\ &\bar{x}(t_f) = D\bar{x}_f \end{aligned}$$

Both forms may be solved through linear optimal control. The former penalizes the system for terminal state errors. The later includes the terminal states as constraints. Both are equivalent when as the terminal weight matrix, Q_f, approaches infinity.

2.5.1 Trajectory Shaping Guidance

According to Zarchan [16], target acceleration may be taken back into account by redefining the state vector such that $\bar{x} \equiv [x_1 \;\; x_2 \;\; x_3]^T = [r_y \;\; v_y \;\; a_T]^T$. The linear optimal control problem with target acceleration included and control effort limit, can be formulated as

$$\begin{aligned}
&\underset{u(t)}{\text{minimize}} \;\; J = \int_{t_0}^{t_f} u^2(t)dt \\
&\text{subject to} \;\; \dot{\bar{x}} = \begin{bmatrix} 0 & 1 & 0 \\ 0 & 0 & 1 \\ 0 & 0 & 0 \end{bmatrix} \bar{x}(t) + \begin{bmatrix} 0 \\ -1 \\ 0 \end{bmatrix} u(t) \\
&\bar{x}(t_f) = \begin{bmatrix} 0 \\ \\ v_f \end{bmatrix}
\end{aligned}$$

The solution to this linear optimal control problem yields

$$a = \frac{4(r_y + v_y t_{go})}{t_{go}^2} + \frac{2(r_y + v_f t_{go})}{t_{go}^2} + a_T \tag{2.40}$$

According to Lukacs [7] this guidance law is simply augmented PN guidance with an proportionality constant equal to 4, double the target acceleration, and an additional term proportional to the difference between the true LOS and desired LOS.

2.5.2 General Vector Explicit Guidance (GENEX)

Lukacs [7], also states that Kim, Lee and Han [8] proved the constant gains of 2.40 are not optimal because the commanded acceleration may be excessive at terminal phase of flight. Instead, time-varying gains that allow aggressive maneuvering during the mid-course phase of flight while limiting control action during the terminal phase of flight should be used. Kim, Lee and Han suggested making these time-varying gains a function of range to target and closing velocity.

A relatively new trajectory guidance law proposed by Ohlmeyer [11] that does this is general vector explicit guidance law (GENEX). GENEX restricts control action at the terminal phase of flight by applying a control weighting term that is indirectly proportional to the time until impact (time-to-go) into the cost function.

Ohlmeyer takes a different approach by neglecting target movement and defining the states as $\bar{x} \equiv [x_1 \;\; x_2]^T = [ZEM \;\; v_y]^T$ and the input may be defined as $\bar{u} \equiv u = a_M$ such that

$$ZEM = x_T - x_M - v_M t_{go} \tag{2.41}$$

Then the linear optimal control problem is formulated as

$$\begin{aligned}
&\underset{u(t)}{\text{minimize}} \;\; J = \frac{1}{2}\int_{t_0}^{t_f} \frac{u^2}{t_{go}^n} dt \\
&\text{subject to} \;\; \dot{\bar{x}} = \begin{bmatrix} 0 & 0 \\ 0 & 0 \end{bmatrix} \bar{x}(t) + \begin{bmatrix} t_{go} \\ -1 \end{bmatrix} u(t) \\
&\bar{x}(t_f) = \begin{bmatrix} 0 \\ v_f \end{bmatrix}
\end{aligned}$$

The solution to this linear optimal control problem yields

$$\begin{aligned} a &= \frac{1}{t_{go}^2}[K_1(x_T - x_M - v_M t_{go}) + K_2(v_T - V_M)t_{go}] \\ k_1 &= (n+2)(n+3) \\ k_2 &= -(n+1)(n+2) \end{aligned} \tag{2.42}$$

where k_1 and k_2 are guidance gains, v_f is the desired terminal relative velocity and n is a user design parameter.

The user design parameter allows the user to adjust the curvature of the flight trajectory, while enforcing a specified final position and velocity orientation. The first term of this guidance law drives the miss distance to zero while the second term of drives the error in velocity orientation to zero. The successful implementation of this guidance law is highly dependent of the accurate calculation of time-to-go. Nonetheless, GENEX offers an attractive trajectory shaping guidance law by offering a user design parameter to meet the needs of various mission objectives.

2.6 Cooperative Guidance Laws

In this section, two cooperative laws that allow a salvo of missile to simulateously hit a stationary target are presented. The first guidance law obtained in [6] is called impact time control guidance (ITCG) and allows multiple missiles to hit a stationary target at a predetermined impact time. It accomplished this by augmenting Pro-Nav with an additional command which adjust the trajectory to achieve this desired impact time. The second guidance law impact time and angle control guidance (ITACG) obtained in [10] is an extension of ITCG that also allows the missile's to hit the target at a specified impact angle.

The simplified geometry that govern the derivation of these two guidance laws is shown below in Fig. 2.3. Similar to PPN, the missile's acceleration command is issued normal to the missile's velocity vector. As mentioned earlier, this removes the requirement of having a missile that can accelerate and decelerate. In addition, the missile is able to reach the target for every set of initial conditions as opposed to issuing commands normal to the LOS with a uniformly decreasing LOS angle rate.

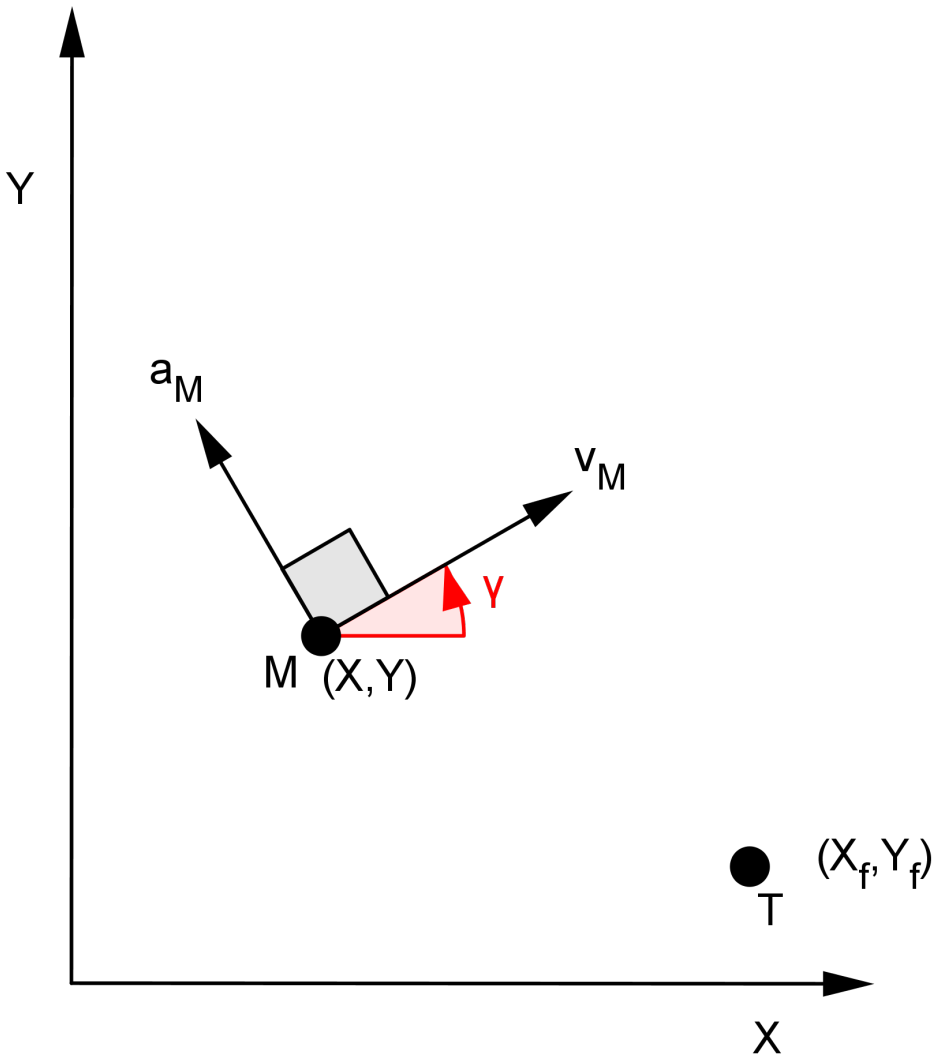

Figure 2.3: Stationary Target Homing Geometry

2.6.1 Impact Time Control Guidance (ITCG)

The equations of motion that govern ITCG are

$$\begin{aligned} \dot{X}(t) &= V\ \cos(\gamma(t)) \\ \dot{Y}(t) &= V\ \sin(\gamma(t)) \\ \dot{\gamma}(t) &= \frac{A(t)}{V} == \frac{a_B(t) + a_F(t)}{V} \end{aligned} \tag{2.43}$$

where $X(t)$ is the missile's downrange position, $Y(t)$ is the missile's crossrange position, $V(t)$ is the missile's velocity, $A(t)$ is the missile's acceleration which is applied normal to the velocity vector, and $\gamma(t)$ is the missile's flight path angle.

The acceleration command has two components, a_B and a_F. The first component is a PPN like component that minimizes miss distance and the second component is a trajectory correcting component that enables the missile to hit the target at a predetermined impact time. By nondiscriminating these equations as a function of downrange, these equations can be expressed in state space format as

$$\begin{bmatrix} \frac{dy}{dx} \\ \\ \frac{d\theta}{dx} \end{bmatrix} = \begin{bmatrix} 0 & 1 \\ \\ 0 & 0 \end{bmatrix} \begin{bmatrix} y \\ \\ \theta \end{bmatrix} + \begin{bmatrix} 0 \\ \\ 1 \end{bmatrix} u_B(t) + u_F(t) \tag{2.44}$$

The linear optimal control problem may be formulated as

$$\begin{aligned} &\underset{u(t)}{\text{minimize}}\ \ J = \frac{1}{2}\int_{x_0}^{x_f} u_B^2 dx \\ &\text{subject to}\ \ \dot{\bar{x}} = \begin{bmatrix} 0 & 1 \\ \\ 0 & 0 \end{bmatrix} \bar{x}(t) + \begin{bmatrix} 0 \\ \\ 1 \end{bmatrix} (u_B + u_F) \end{aligned}$$

The solution to this linear optimal control problem is

$$\begin{aligned} u_B &= \frac{3\left(y_{go} - \gamma\, x_{go}\right)}{x_{go}^2} - \frac{3}{2}u_F \\ &= UPN - \frac{3}{2}u_F \end{aligned} \tag{2.45}$$

The first term, u_P is a linear approximation of PPN with a navigation constant of 3. Therefore, Eq. 2.45 has a similar structure to APN where instead of augmenting the command with a term to account for target maneuvering, the command is augmented with a term to correct the trajectory.

The constraint on impact time is expressed as a path constraint wrt downrange such that

$$\int_{x_0}^{x_f} \sqrt{1+\gamma^2(x)}dx = \bar{\tau}_{go} \tag{2.46}$$

where $\bar{\tau}_{go}$ is the difference between the designated impact time and the current time. The evaluation of this integral yields

$$\bar{\tau}_{go} = \frac{x_{go}^3}{240}\left(u_F^2 + 2u_P u_F + 16u_P^2 + \frac{80\theta u_P}{x_{go}} + \frac{240\left(1+\frac{\theta^2}{2}\right)}{x_{go}^2}\right)$$

The estimation of time to go without the use of the trajectory correcting command, u_F, is expressed as

$$\hat{\tau}_{go} = \frac{1}{15}u_P^2 x_{go}^3 + \frac{1}{3}u_P\theta x_{go}^2 + \left(1+\frac{\theta^2}{2}\right)x_{go}$$

Solving for u_F yields

$$u_F = -u_P\left(1 - \sqrt{1+\frac{240}{u_P^2 x_{go}^3}\epsilon_t}\right)$$

where ϵ_t is the impact time error defined as

$$\epsilon_t = \bar{\tau}_{go} - \hat{\tau}_{go}$$

2.6.2 *Impact Time and Angle Control Guidance Control Guidance (ITACG)*

The equations of motion that govern ITACG are

$$\begin{aligned}
\dot{X}(t) &= V\ \cos(\gamma(t)) \\
\dot{Y}(t) &= V\ \sin(\gamma(t)) \\
\dot{\gamma}(t) &= \frac{A(t)}{V} \\
\dot{A}(t) &= g(t) = g_B(t) + g_F(t)
\end{aligned} \tag{2.47}$$

To add an additional degree of freedom the control variable is jerk not acceleration. The jerk commmand has two components, g_B and g_F. By nondiscriminating these equations as a function of downrange, these equations can be expressed in state space format as

$$\begin{bmatrix} \frac{dy}{dx} \\ \frac{d\theta}{dx} \\ \frac{da}{dx} \end{bmatrix} = \begin{bmatrix} 0 & 1 & 0 \\ 0 & 1 & 0 \\ 0 & 0 & 0 \end{bmatrix} \begin{bmatrix} y \\ \theta \\ a \end{bmatrix} + \begin{bmatrix} 0 \\ 0 \\ 1 \end{bmatrix} u_B(t) + u_F(t) \tag{2.48}$$

The linear optimal control problem may be formulated as

$$\begin{aligned}
\underset{u_B(x)}{\text{minimize}}\ \ J &= \frac{1}{2}\int_{x_0}^{x_f} u_B^2(x)dx \\
\text{subject to}\ \ \dot{\bar{X}} &= A\bar{X}(x) + B(u_B(x) + u_F) \\
E &= D\bar{X}(x_f)
\end{aligned}$$

D is the terminal weighting cost matrix defined as

$$D = \begin{pmatrix} 1 & 0 & 0 \\ 0 & 1 & 0 \\ 0 & 0 & 0 \end{pmatrix}$$

that places constraints on terminal crossrange and terminal flight path angle, but places no constraint on terminal acceleration.

The solution to this linear optimal control problem is

$$u_B = K^\top z - \frac{2}{3} u_F$$

The constraint on impact time is expressed as a path constraint wrt downrange such that

$$\int_{x_0}^{x_f} \sqrt{1 + \gamma^2(x)} dx = \bar{\tau}_{go} \tag{2.49}$$

where $\bar{\tau}_{go}$ is the difference between the designated impact time and the current time. The evaluation of this integral yields

$$\bar{\tau}_{go} = \alpha u_F^2 + \beta u_F + \hat{\tau}_{go}$$

where $\hat{\tau}_{go}$ is the estimation of time to go without the use of the trajectory correcting command, u_F, expressed as

$$\hat{\tau}_{go} = C + L^\top z + z^\top Q z$$

Solving for u_F yields

$$\begin{aligned} u_F = &-\frac{1}{2}\eta_L \pm \frac{1}{2}\sqrt{\eta_L^2 + \eta_E} \\ &-\frac{1}{2}\eta_L \pm \frac{1}{2}\eta_L\sqrt{1 + \frac{\eta_E}{\eta_L^2}} \end{aligned} \tag{2.50}$$

where ϵ_t is the impact time error defined as

$$\epsilon_t = \bar{\tau}_{go} - \hat{\tau}_{go}$$

The values of $z, K, C, L, Q, \eta_L, and \eta_L$ may all be obtained by setting $n = 0$ in Appendix A, which contains the detailed derivation of GENEX-ITACG. This detailed derivation uses the same methodology found in [10]. GENEX-ITACG reduces to ITACG when the user defined parameter is set to zero.

CHAPTER 3: METHODOLOGY

3.1 Introduction

In this chapter, the derivation of GENEX-ITACG is presented. GENEX-ITACG allows a salvo of missiles to simultaneously hit a stationary target at a prescribed impact time with a specified terminal impact angle while providing a user design parameter to shape the aggressiveness of the trajectories. The simultaneous attack by a salvo of missiles at a specified time and impact angle with the user design parameter are of great interest to the military for the following reasons:

1. Saturation attacks at specified impact angles allows well defended targets to be defeated by creating one on many scenarios.

2. Saturation attacks at specified impact times creates the element of surprise which disallows the target to warn other systems.

3. Saturation attacks allow the use of smaller and less expensive munitions

4. The user design parameter allows the user to tailor the trajectory of the munitions in a manner that best fits their systems.

First, as done in [13], an overview of the linear optimal control for linear time-varying systems with a quadratic performance index is presented. Then the abbreviated derivation of GENEX-ITACG through the use of linear optimal control is presented. The full derivation is included in Appendix A.

3.2 Linear Optimal Control

In this section, the linear optimal control problem for linear time-varying systems with a quadratic performance index is presented. Consider a linear time-varying systems represented in state space form as

$$\begin{aligned} \dot{\bar{x}} &= \mathbf{A}(t)\bar{x}(t) + \mathbf{B}(t)\bar{u}(t) \\ \bar{y} &= \mathbf{C}(t)\bar{x}(t) \end{aligned} \tag{3.1}$$

where $\bar{x}(t) \in \Re^n$ is the state vector, $\bar{y}(t) \in \Re^m$ is the output vector, $\bar{u}(t) \in \Re^r$ is the control vector, $\mathbf{A}(t) \in \Re^{n \times n}$ is the state matrix, $\mathbf{B}(t) \in \Re^{n \times r}$ is the input matrix, and $\mathbf{C}(t) \in \Re^{m \times n}$ is the output matrix, $0 < m \leq r \leq n$ and $\bar{u}(t)$ is unconstrained.

The objective is to control the system in 3.1 in a manner that drives the states along a desired trajectory with terminal state constraints

$$\mathbf{E}(t_f) = \mathbf{D}\bar{x}(t_f) \tag{3.2}$$

where $\mathbf{E}(t_f)$ is the terminal state matrix, $\mathbf{D}$ is the terminal weighting cost matrix, and $\bar{x}(t_f)$ are the desired terminal state.

However, excessive control effort may be commanded while trying to achieve this objective because $\bar{u}(t)$ is unconstrained. A more desirable behavior would be to keep the states of the system close to a desired trajectory without using unnecessary large control effort [1].

This objective can be accomplished by minimizing a quadratic performance index defined as

$$J = \frac{1}{2}\int_{t_0}^{t_f} [\bar{x}^\top(t)\mathbf{Q}(t)\bar{x}(t) + \bar{u}^\top(t)\mathbf{R}(t)\bar{u}(t)]dt \tag{3.3}$$

where $\mathbf{Q}(t) \in \Re^{n\times n}$ is a positive semi-definite state weighting matrix and $\mathbf{R}(t) \in \Re^{r\times r}$ is a positive definite control weighting matrix.

The overall objective of this linear optimal control problem can be formally stated as

$$\begin{aligned}
\underset{\bar{u}(t)}{\text{minimize}}\ \ & J = \frac{1}{2}\int_{t_0}^{t_f} [\bar{x}^\top(t)\mathbf{Q}(t)\bar{x}(t)\bar{u}(t) + \bar{u}^\top(t)\mathbf{R}(t)\bar{u}(t)\bar{u}(t)]dt \\
\text{subject to}\ \ & \dot{\bar{x}} = \mathbf{A}(t)\bar{x}(t) + \mathbf{B}(t)\bar{u}(t) \\
& \bar{y} = \mathbf{C}(t)\bar{x}(t) \\
& \mathbf{E}(t_f) = \mathbf{D}\bar{x}(t_f)
\end{aligned}$$

where control term $\bar{u}^\top(t)\mathbf{R}(t)\bar{u}(t)$ is a positive weighting term that penalizes the system for large control values and the terminal term $\mathbf{D}\bar{x}(t_f)$ that forces the system to reach the desired terminal states.

The Euler-Lagrange approach can be used to solve this problem by adjoining the state equations to the performance index with lagrangian multipliers, $\bar{\lambda}(t)$. This approach yields an augmented performance index defined as

$$J = \int_{t_0}^{t_f} \frac{1}{2}[\bar{x}^\top(t)\mathbf{Q}(t)\bar{x}(t) + \bar{u}^\top(t)\mathbf{R}(t)\bar{u}(t)] + \bar{\lambda}^\top(t)\left[\mathbf{A}(t)\bar{x}(t) + \mathbf{B}(t)\bar{u}(t) - \dot{\bar{x}}(t)\right] dt \tag{3.4}$$

A function called the Hamiltonian function that penalizes the system for large control values is defined as

$$H(t) = \frac{1}{2}[\bar{x}^\top(t)\mathbf{Q}(t)\bar{x}(t)\bar{u}(t) + \bar{u}^\top(t)\mathbf{R}(t)\bar{u}(t)\bar{u}(t)] + \bar{\lambda}^\top(t)[\mathbf{A}(t)\bar{x}(t) + \mathbf{B}(t)\bar{u}(t)] \tag{3.5}$$

A function called the terminal function that penalizes the system for large terminal errors is defined as

$$\phi(t_f) = \bar{v}^\top[\mathbf{D}\bar{x}(t_f)] \tag{3.6}$$

From the principles of calculus of variation, the following four conditions must be satisfied to minimize the augmented performance index subject to the terminal constraints:

1. State Equation: $\partial H(t)/\partial\bar{\lambda}(t) = \dot{\bar{x}}(t)$, for $t \geq 0$
2. Costate Equation: $\partial H(t)/\partial\bar{x}(t) = -\dot{\bar{\lambda}}(t)$, for $t \leq t_f$
3. Stationarity: $\partial H(t)/\partial\bar{u}(t) = 0$, for $t \geq 0$
4. Boundary: $\partial\phi(t_f)/\partial\bar{x}(t_f) = \bar{\lambda}(t_f)$, $\bar{x}(t_0)$ given

Condition 3 is known as the minimum principle of Pontryagin. Through its use the optimal control can be expressed as

$$\bar{u}^*(t) = -\mathbf{R}^{-1}(t)\mathbf{B}^\top(t)\bar{\lambda}(t) \tag{3.7}$$

Under the assumption that $\mathbf{R}(t)$ is positive definite the inverse $\mathbf{R}^{-1}(t)$ exists. Condition 3 only guarantees $\bar{u}^*(t)$ minimizes or maximizes the Hamiltonian function. The fact that $\partial H^2(t)/\partial\bar{u}^2(t) = \mathbf{R}(t)$ guarantees that $\bar{u}^*(t)$ minimizes the Hamiltonian function, which minimizes the augmented performance index [1].

Substituting (3.7) into the condition 1 yields

$$\begin{aligned}\dot{\bar{x}} &= \mathbf{A}(t)\bar{x}(t) - \mathbf{B}(t)\mathbf{R}^{-1}(t)\mathbf{B}^{\top}(t)\bar{\lambda}(t) \\ \dot{\bar{x}} &= \mathbf{A}(t)\bar{x}(t) - \mathbf{S}(t)\bar{\lambda}(t)\end{aligned} \tag{3.8}$$

Furthermore, applying condition 2 yields

$$\dot{\bar{\lambda}}(t) = -\mathbf{A}^{\top}(t)\bar{\lambda}(t) \tag{3.9}$$

The canonical equations of 3.8 and 3.9 can be combined in the state-space form

$$\begin{bmatrix}\dot{\bar{x}}(t) \\ \dot{\bar{\lambda}}(t)\end{bmatrix} = \begin{bmatrix}\mathbf{A}(t) & -\mathbf{S}(t) \\ \mathbf{0} & -\mathbf{A}^{\top}(t)\end{bmatrix}\begin{bmatrix}\bar{x}(t) \\ \bar{\lambda}(t)\end{bmatrix} \tag{3.10}$$

This is a two point boundary problem with $2n$ time-varying homogenous differential equations that must be solved. A total of $2n$ boundary conditions are needed to obtain a unique solution to these equations. The first n boundary conditions come from the initial states, $\bar{x}(t_0)$. The final n boundary conditions come from condition 4.

Applying condition 4 yields

$$\bar{\lambda}(t_f) = \mathbf{D}\bar{v} \tag{3.11}$$

The state equations must be solved forward in time from the initial conditions. The costate equations must be solved backwards in time from the boundary conditions. The state equation and costate equation are both linear time-varying equations.

3.3 GENEX-ITACG

In this section, GENEX-ITACG is formulated and solved through the use of linear optimal control. Let N missile participate in the salvo attack. The goal of GENEX-ITACG is to simultaneously hit a stationary target at a prescribed impact time with a specified terminal impact angle while providing a user design parameter to shape the aggressiveness of the trajectories. It is assumed that each missile has a perfect command response.

The equations of motion that govern the flight of each missile are

$$\begin{aligned} \dot{X}(t) &= V\ \cos(\gamma(t)) \\ \dot{Y}(t) &= V\ \sin(\gamma(t)) \\ \dot{\gamma}(t) &= \frac{A(t)}{V} \\ \dot{A}(t) &= g(t) = g_B(t) + g_F(t) \end{aligned} \tag{3.12}$$

where $X(t)$ is the missile's downrange position, $Y(t)$ is the missile's crossrange position, V is the missile's velocity, $A(t)$ is the missile's acceleration which is applied normal to the velocity vector, and $\gamma(t)$ is the missile's flight path angle.

The missile acceleration rate, jerk, is included to provide an additional degree of freedom for impact time control. The first jerk term, $g_B(t)$, is the command to eliminate the miss distance and the impact angle error. The second jerk term, g_F, is the additional command that corrects the trajectory to achieve impact at the desired impact time.

These equations are nondimensionalized to simplify the derivation of GENEX-ITACG by introducing the following nondimensional variables

$$x(t) = \frac{X(t)}{V\,t_f}, y(t) = \frac{Y(t)}{V\,t_f},\;\; a = \frac{A(t)\,t_f}{V},\;\; \tau = \frac{t}{t_f},\;\; u(t) = \frac{{t_F}^2\,g(t)}{V} \tag{3.13}$$

These equations are represented in state space format by making downrange the independent variable as

$$\dot{\bar{X}} = A\,\bar{X} + B\,u = \begin{pmatrix} 0 & 1 & 0 \\ 0 & 0 & 1 \\ 0 & 0 & 0 \end{pmatrix} \bar{X} + \begin{pmatrix} 0 \\ 0 \\ 1 \end{pmatrix} (u_B + u_F) \tag{3.14}$$

where $\bar{X}(x) = [y(x)\;\; \gamma(x)\;\; a(x)]^T$.

Now the formal problem definition of GENEX-ITACG may be stated as

$$\begin{aligned} \underset{u_B(x)}{\text{minimize}}\;\; J &= \frac{1}{2}\int_{x_0}^{x_f} u_B^2(x) R(x) dx \\ \text{subject to}\;\; \dot{\bar{X}} &= A\bar{X}(x) + B(u_B(x) + u_F) \\ E &= D\bar{X}(x_f) \end{aligned}$$

where $R(x)$ is the control weighting function defined as

$$R(x) = \frac{1}{(x_f - x)^n} \tag{3.15}$$

that penalizes the control effort more severely as the missile approaches its final destination, the target. This penalization not only limits excessive commanded maneuvering during the terminal phases of flights, but also allows the missile to command additional acceleration at handover. Handover is the transition between the midcourse phase of flight and the terminal phase of flight. At handover additional acceleration may be needed to eliminate large heading errors.

D is the terminal weighting cost matrix defined as

$$D = \begin{pmatrix} 1 & 0 & 0 \\ 0 & 1 & 0 \\ 0 & 0 & 0 \end{pmatrix}$$

that places constraints on terminal crossrange and terminal flight path angle, but places no constraint on terminal acceleration. No constraint is placed on terminal because there is no way of knowing this value beforehand.

E is the terminal state matrix defined as

$$E = \begin{pmatrix} y(x_f) \\ \gamma(x_f) \\ 0 \end{pmatrix} \tag{3.16}$$

that consists of two user defined parameters: the missile's terminal crossrange position and terminal flight path angle. Intuitively, the desired terminal crossrange position would be the targets crossrange position or some position close to it.

The costate equations are obtained as follows

$$\frac{\partial H}{\partial x} = \begin{bmatrix} \frac{\partial H}{\partial y} \\ \frac{\partial H}{\partial \gamma} \\ \frac{\partial H}{\partial a} \end{bmatrix} = \begin{bmatrix} 0 \\ \lambda_y \\ \lambda_\gamma \end{bmatrix} = -\dot{\lambda} = - \begin{bmatrix} \dot{\lambda}_y \\ \dot{\lambda}_\gamma \\ \dot{\lambda}_a \end{bmatrix} \tag{3.17}$$

Using the boundary condition, the costate equations at terminal downrange are obtained as

$$\frac{\partial \phi(x_f)}{\partial x} = \begin{bmatrix} \frac{\partial \phi(x_f)}{\partial y} \\ \frac{\partial \phi(x_f)}{\partial \gamma} \\ \frac{\partial \phi(x_f)}{\partial a} \end{bmatrix} = \begin{bmatrix} v_y \\ v_\gamma \\ 0 \end{bmatrix} = \lambda(x_f) = \begin{bmatrix} \lambda_y(x_f) \\ \lambda_\gamma(x_f) \\ \lambda_a(x_f) \end{bmatrix} \tag{3.18}$$

Integrating Eq. 3.17 backwards from Eq. 3.18 yields

$$\begin{aligned} \lambda_y(x) &= v_y \\ \lambda_\gamma(x) &= v_\gamma + v_y\,(x_f - x) \\ \lambda_a(x) &= v_\gamma\,(x_f - x) + \frac{1}{2} v_y (x_f - x)^2 \end{aligned} \tag{3.19}$$

Furthermore, applying the stationarity condition yields

$$\begin{aligned} \frac{\partial H}{\partial u_B} &= \frac{u_B}{(x_f - x)^n} + \lambda_a(x) = 0 \\ u_B &= -(x_f - x)^n\,\lambda_a(x) = -v_\gamma\,(x_f - x)^{n+1} - \frac{1}{2} v_y\,(x_f - x)^{n+2} \end{aligned} \tag{3.20}$$

where

$$\begin{bmatrix} v_y \\ v_\gamma \end{bmatrix} = \begin{bmatrix} -\frac{4\,\mathrm{UPN}\,(n+4)^2\,(n+5)}{{x_{\mathrm{go}}}^{n+3}\,(n+3)} & \frac{2\,\gamma_{\mathrm{go}}\,(n+3)\,(n+4)\,(n+5)}{{x_{\mathrm{go}}}^{n+4}} & \frac{2\,a\,(n+4)\,(n+5)}{{x_{\mathrm{go}}}^{n+3}} \\ \frac{2\,\mathrm{UPN}\,(n+4)\,(n+5)}{{x_{\mathrm{go}}}^{n+2}} & -\frac{\gamma_{\mathrm{go}}\,(n+3)\,(n+4)^2}{{x_{\mathrm{go}}}^{n+3}} & -\frac{a\,(n+3)\,(n+4)}{{x_{\mathrm{go}}}^{n+2}} \end{bmatrix} z + \begin{bmatrix} -\frac{u_F\,(n+1)\,(n+4)\,(n+5)}{3\,{x_{\mathrm{go}}}^{n+2}} \\ \frac{u_F\,(n+3)\left(n^2+6\,n+8\right)}{6\,{x_{\mathrm{go}}}^{n+1}} \end{bmatrix} u_F$$

and

$$z = \begin{bmatrix} UPN \\ \gamma_{go} \\ a \end{bmatrix} \qquad UPN = \frac{\mathrm{y_{go}}\,(n+3)}{\mathrm{xgo}^2} - \frac{\gamma\,(n+3)}{\mathrm{xgo}} \qquad \gamma_{go} = \gamma_f - \gamma$$

Eq. 3.20 is written in a compact form as

$$u_B = K^\top z + \frac{(n-1)(n+4)}{6} u_F$$

where

$$K = \begin{pmatrix} \frac{2\,(n+4)\,(n+5)}{x_{\rm go}\,(n+3)} \\ -\frac{(n+3)\,(n+4)}{{x_{\rm go}}^2} \\ -\frac{2\,(n+4)}{x_{\rm go}} \end{pmatrix}$$

Now total control term, u, is expressed as

$$u = u_B + u_F = K^\top z + \frac{(n+1)(n+2)}{6} u_F$$

Next, the additional command, u_F, is solved for. This command corrects the trajectory to ensure the missile impacts the target at the designated impact time. The time to go until the missile impacts the target is expressed as

$$\begin{aligned} \bar{\tau}_{go} &= \int_x^{x_f} \sqrt{1+\gamma^2(s,u_F)ds} \\ &= \int_0^{x_f - x} \sqrt{1+\gamma^2(\zeta,u_F)ds} \end{aligned} \tag{3.21}$$

where $\zeta = x_f - s$ and

$$\begin{aligned} \gamma(\zeta,u_F) = \gamma_f - a_x\zeta + \left(\frac{1}{2}\zeta^2 - (x_f - x)\,\zeta\right) u_F \\ \left(\frac{1}{(n+2)}(x_f-x)^{n+2}\zeta - \frac{1}{(n+2)\;(n+3)}\zeta^{n+3}\right) v_\gamma \\ \left(\frac{1}{2\,(n+3)}(x_f-x)^{n+3}\zeta - \frac{1}{2\;(n+3)\;(n+4)}\zeta^{n+4}\right) v_y \end{aligned} \tag{3.22}$$

If the additional control command is not applied, an estimation of time to go is expressed as

$$\hat{\tau}_{go} = \int_0^{x_f - x} \sqrt{1 + \gamma^2(\zeta, u_F = 0)ds} \tag{3.23}$$

Evaluating the integral yields

$$\hat{\tau}_{go} = C + L^\top z + z^\top Q z \tag{3.24}$$

where

$$C = x_{\mathrm{go}} \left(\frac{{\gamma_{\mathrm{f}}}^2}{2} + 1 \right)$$

$$L = \begin{pmatrix} \frac{\gamma_{\mathrm{f}} {x_{\mathrm{go}}}^2}{n+3} \\ -\gamma_{\mathrm{f}} x_{\mathrm{go}} \\ 0 \end{pmatrix}$$

$$Q = \begin{pmatrix} \frac{2 {x_{\mathrm{go}}}^3 (4n+19)(n+4)(n+5)}{3(2n+7)(2n+9)(n+3)^2(n+6)} & -\frac{x_{\mathrm{go}}^2 \left(16n^3+206n^2+880n+1245\right)}{6(2n+7)(2n+9)(n+3)(n+6)} & -\frac{x_{\mathrm{go}}^3 (4n+19)}{6(2n+7)(2n+9)(n+3)(n+6)} \\ -\frac{x_{\mathrm{go}}^2 \left(16n^3+206n^2+880n+1245\right)}{6(2n+7)(2n+9)(n+3)(n+6)} & -\frac{x_{\mathrm{go}} \left(\frac{17n^3}{6}+\frac{71n^2}{2}+147n+201\right)}{(2n+7)(2n+9)(n+5)(n+6)} + \frac{2x_{\mathrm{go}}}{3} & -\frac{x_{\mathrm{go}}^2 (4n+19)(n+3)}{12(2n+7)(2n+9)(n+5)(n+6)} \\ -\frac{x_{\mathrm{go}}^3 (4n+19)}{6(2n+7)(2n+9)(n+3)(n+6)} & -\frac{x_{\mathrm{go}}^2 (4n+19)(n+3)}{12(2n+7)(2n+9)(n+5)(n+6)} & \frac{x_{\mathrm{go}}^3 (3n+13)}{6(2n+7)(2n+9)(n+5)(n+6)} \end{pmatrix}$$

Notice, that the time to go of Eq. 3.21 is a $2(n+4)$ order function of γ, and second order function if u_F. Therefore, u_F is solved for by using the quadratic formula. Evaluating the integral of Eq. 3.21 yields

$$\begin{aligned} \bar{\tau}_{go} &= \int_x^{x_f} \sqrt{1 + \gamma^2(s, u_F)ds} \\ &= \alpha u_F^2 + \beta u_F + \hat{\tau}_{go} \\ 0 &= u_F^2 + \frac{\beta}{\alpha} u_F - \frac{\epsilon_t}{\alpha} \end{aligned}$$

where the time to go estimation error is defined as

$$\epsilon_t = \bar{\tau}_{go} - \hat{\tau}_{go}$$

By making the following definitions

$$\eta_L = \frac{\alpha}{\beta} = M^\top z$$
$$M = \begin{pmatrix} \frac{(n+5)\left(4\,n^2+20\,n+7\right)30}{x_{\rm go}\,(8\,n+35)\,(n+1)\,(n+2)\,(n+3)} \\ -\frac{(n+3)\left(4\,n^2+38\,n+91\right)30}{x_{\rm go}^2\,(8\,n+35)\,(n+1)\,(n+2)} \\ \frac{30}{x_{\rm go}\,(n+1)\,(n+2)} \end{pmatrix}$$

$$\eta_E = \frac{4}{\alpha}\epsilon_t = N\epsilon_t$$
$$N = \frac{4320\ (2\,n+7)\ (2\,n+9)\ (n+5)\ (n+6)\ (n+7)}{x_{\rm go}^5\ (8\,n+35)\ (n+1)^2\,(n+2)^2}$$

the additional control command, u_F is solved for as

$$\begin{aligned} u_F = &-\frac{1}{2}\eta_L \pm \frac{1}{2}\sqrt{\eta_L^2+\eta_E} \\ &-\frac{1}{2}\eta_L \pm \frac{1}{2}\eta_L\sqrt{1+\frac{\eta_E}{\eta_L^2}} \end{aligned} \tag{3.25}$$

When the time to go estimation error equals zero the additional control command should equal zero. Therefore, the positive sign solution of Eq. 3.25 should be used. Furthermore, $\frac{\eta_E}{\eta_L^2} << 1$ and approaches zero as $\epsilon_t \to 0$.

Therefore, Eq. 3.25 can be approximated as

$$u_F \simeq -\frac{1}{2}\eta_L + \frac{1}{2}\eta_L\left(1+\frac{\eta_E}{2\eta_L^2}\right) \simeq \frac{\eta_E}{4\eta_L}$$

CHAPTER 4: RESULTS

4.1 Introduction

In this chapter simulation, results that demonstrate the capabilities of GENEX-ITACG are presented. The simulation model was constructed in Simulink as shown in App. B. There are three conditions that stop the simulation based on the states of the system. If the missile flies past the target, if the missile flies into the ground, or if the time of flight is relative close to the terminal time the simulation is halted.

The inner layer of the model contains the nonlinear dynamic equations that govern flight. The middle layer forces the missile to hit the target at a specified terminal impact angle and has the ability to alter the aggressiveness of this terminal impact with the user design parameter, n. The outer layer forces the system to impact the target at a specified impact time.

The capabilities of GENEX-ITACG are demonstrated by first conducting single missile flyouts that isolate the three different components of GENEX-ITACG. The baseline initial conditions for each of these single missile flyouts are shown in Table 4.1.

Table 4.1: Initial Conditions: Single Missile Flyout

IC	Missile	Target
$x_0(m)$	0	10,000
$y_0(m)$	500	0
$\gamma_0(deg)$	30	0
$a_0(m/s^2)$	0	0
$V(m/s)$	250	0

To begin, the capabilities of the impact angle control guidance portion of GENEX-ITACG are presented by setting $n = 0$, cutting off the outer loop, and adjusting the desired impact angle, γ_f. Then the capabilities of the GENEX portion of GENEX-ITACG are presented by keeping the outer loop off, setting the desired impact angle to zero, and adjusting the user design parameter. Next, the capabilities of the impact time control portion of GENEX-ITACG are presented by cutting the outer loop on, setting the desired impact angle and user design parameter to zero, and adjusting the desired impact time, t_d.

At last, the full capabilities of GENEX-ITACG are presented for a single missile flyout by turning the outer loop on, setting the desired impact angle to -30 degrees, setting the desired impact time to 50, and adjusting the user design parameter. The test parameters of these cases are summarized in Table 4.2.

Table 4.2: Test Parameters: Single Missile Flyout

Case	Subcase	Guidance Law	$\gamma_f(deg)$	n	$t_d(s)$
1	1	IACG	0	0	n/a
1	2	IACG	-30	0	n/a
1	3	IACG	-60	0	n/a
2	1	GENEX	-30	0	n/a
2	2	GENEX	-30	1	n/a
2	3	GENEX	-30	2	n/a
3	1	ITCG	-30	0	45
3	2	ITCG	-30	0	50
3	3	ITCG	-30	0	55
4	1	GENEX-ITACG	-30	0	50
4	1	GENEX-ITACG	-30	0.1	50
4	2	GENEX-ITACG	-30	0.2	50

Finally, the full capabilities of GENEX-ITACG are demonstrated once again, but this time through a coordinated 3 missile salvo attack. The initial conditions for each missile participating the the salvo attack is shown in Table 4.3.

Table 4.3: Initial Conditions: 3 Missile Salvo Attack Flyout

IC	Missile 1	Missile 2	Missile 3	Target
$x_0(m)$	-10,000	-6,000	-3,000	0
$y_0(m)$	500	6,000	10,000	0
γ_0(deg)	30	50	-20	0
$a_0(m/s^2)$	0	0	0	0
$V(m/s)$	250	250	250	0

To demonstrate the full capabilities of GENEX-ITACG three different values of n and three different terminal impact angles are used. To simultaneously hit the target each missile is given the same desired impact time. These flight parameters are shown for each missile in Table 4.2.

Table 4.4: Test Parameters: 3 Missile Salvo Attack Flyout

Missile	$\gamma_f(deg)$	n	$t_d(s)$
1	0	0	50
1	0	0.1	50
1	0	0.2	50
2	-30	0	50
2	-30	0.1	50
2	-30	0.2	50
3	-60	0	50
3	-60	0.1	50
3	-60	0.2	50

4.2 Case 1: Impact Angle Control Guidance (IACG)

Case 1 demonstrates the ability of IACG to hit a stationary target at three different desired impact angles. The trajectories for each subcase in shown below in Fig. 4.1. The blue, green and red traces represent desired terminal impact angles of 0, -30, and 60 degrees, respectively.

As the desired impact angle is decreased, the shaping of the trajectory becomes more pronounces. This illustrates the meaning of a trajectory shaping guidance law.

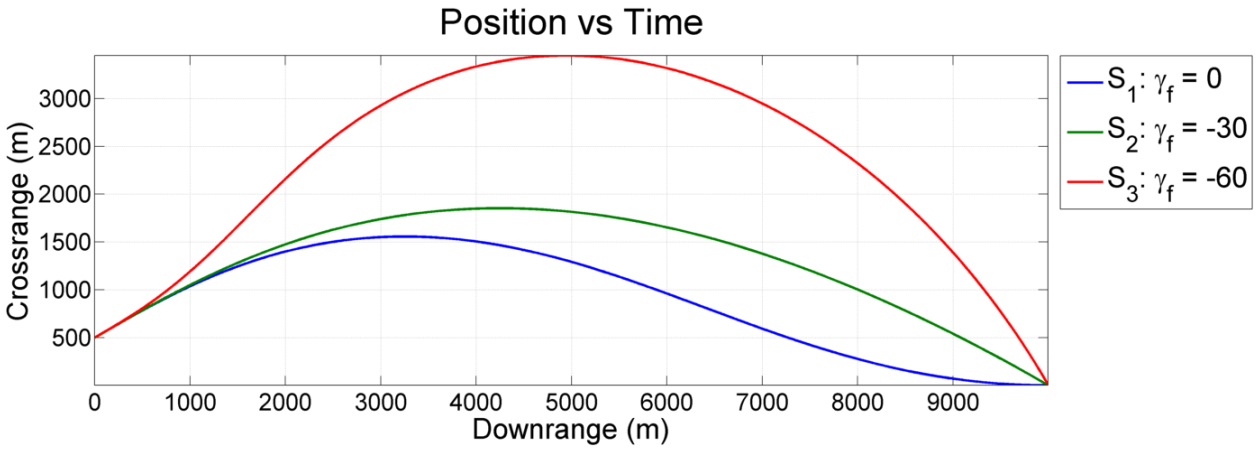

Figure 4.1: Results: IACG Trajectory

As shown in Fig. 4.2 in each case the missile successfully achieved the desired impact angle. The lower the terminal impact angle the longer the time of flight. This difference in time occurs because the additional command to adjust the trajectory for impact time was zeroed out.

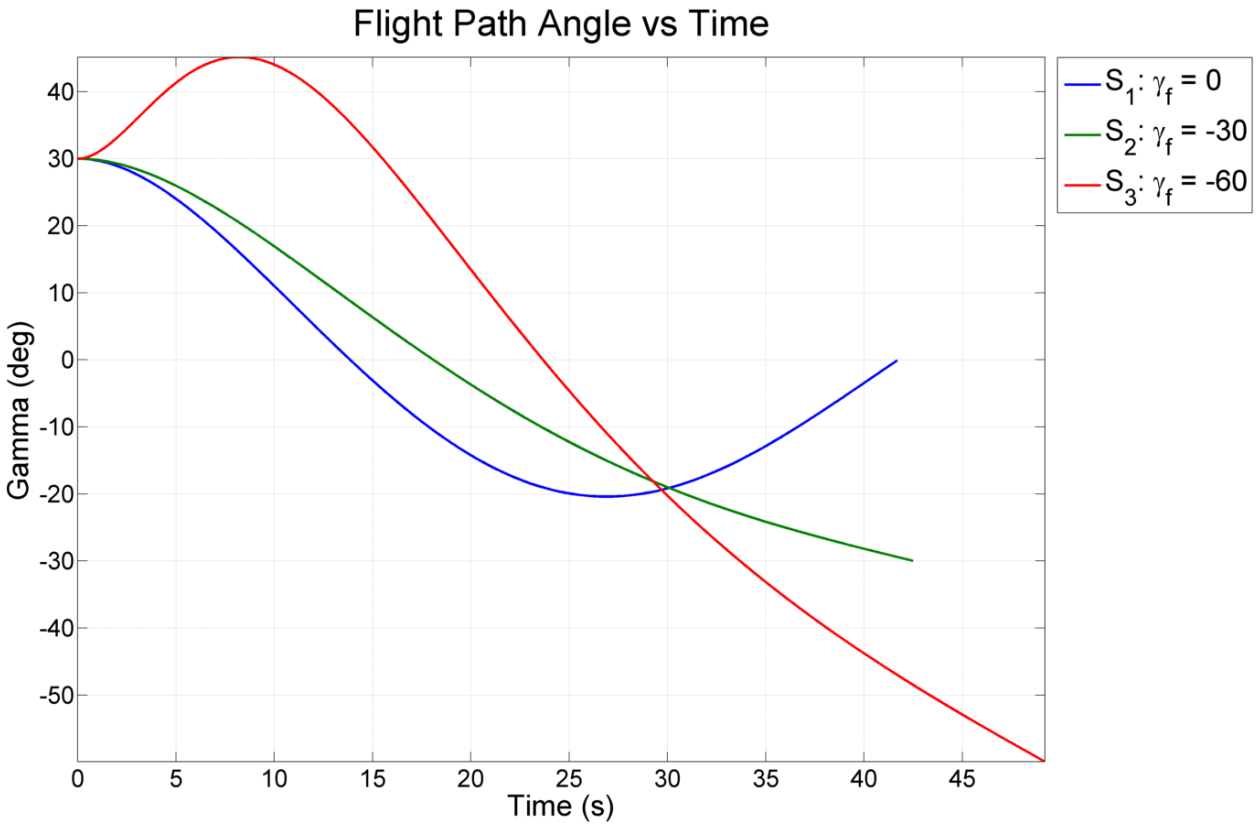

Figure 4.2: Results: IACG Flight Path Angle

The IACG command and acceleration is shown below in Fig. 4.3 and Fig. 4.4. The term to control impact time is zero throughout the entire, which causes discrepancies in impact time. It is apparent that more acceleration is needed as the desired impact angle is decreased.

This observation is valid because to achieve a lower impact angle the missile must divert further from a straight-line trajectory, thus expending more energy.

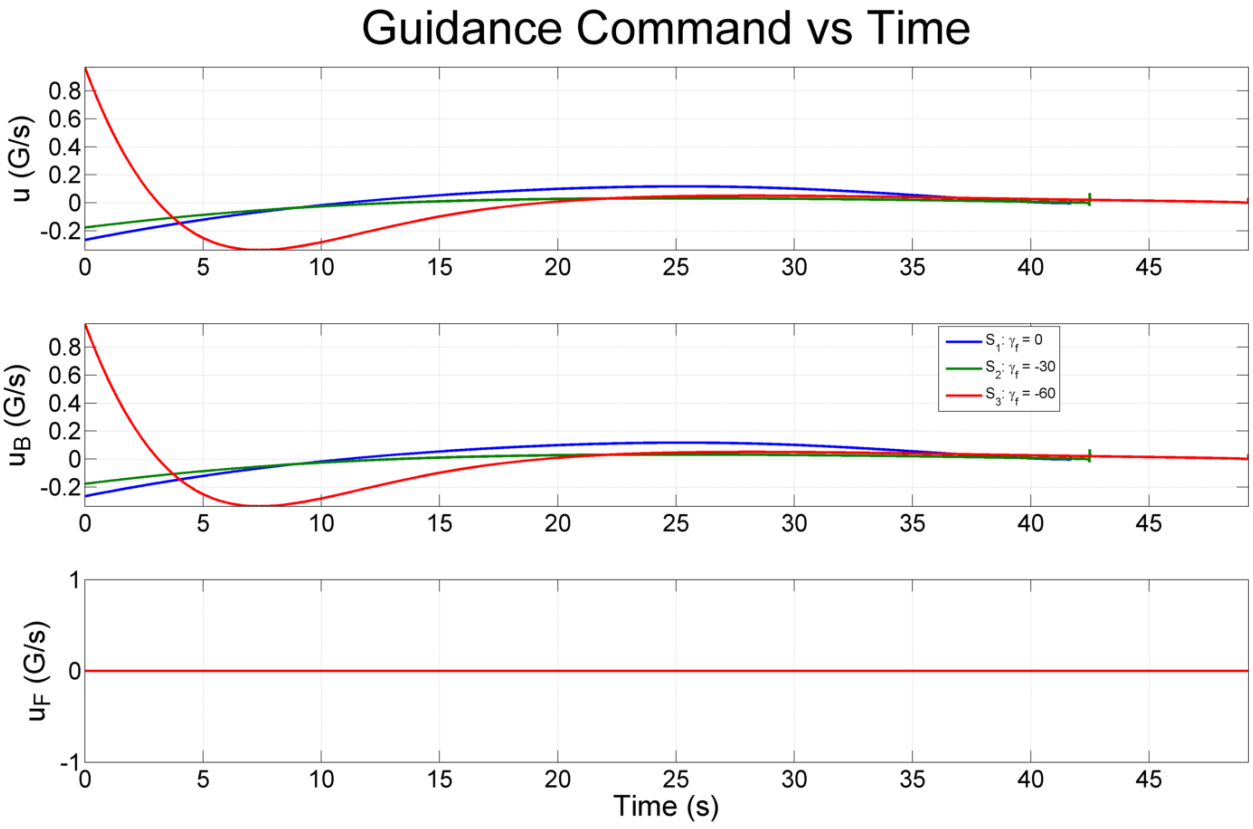

Figure 4.3: Results: IACG Guidance Command

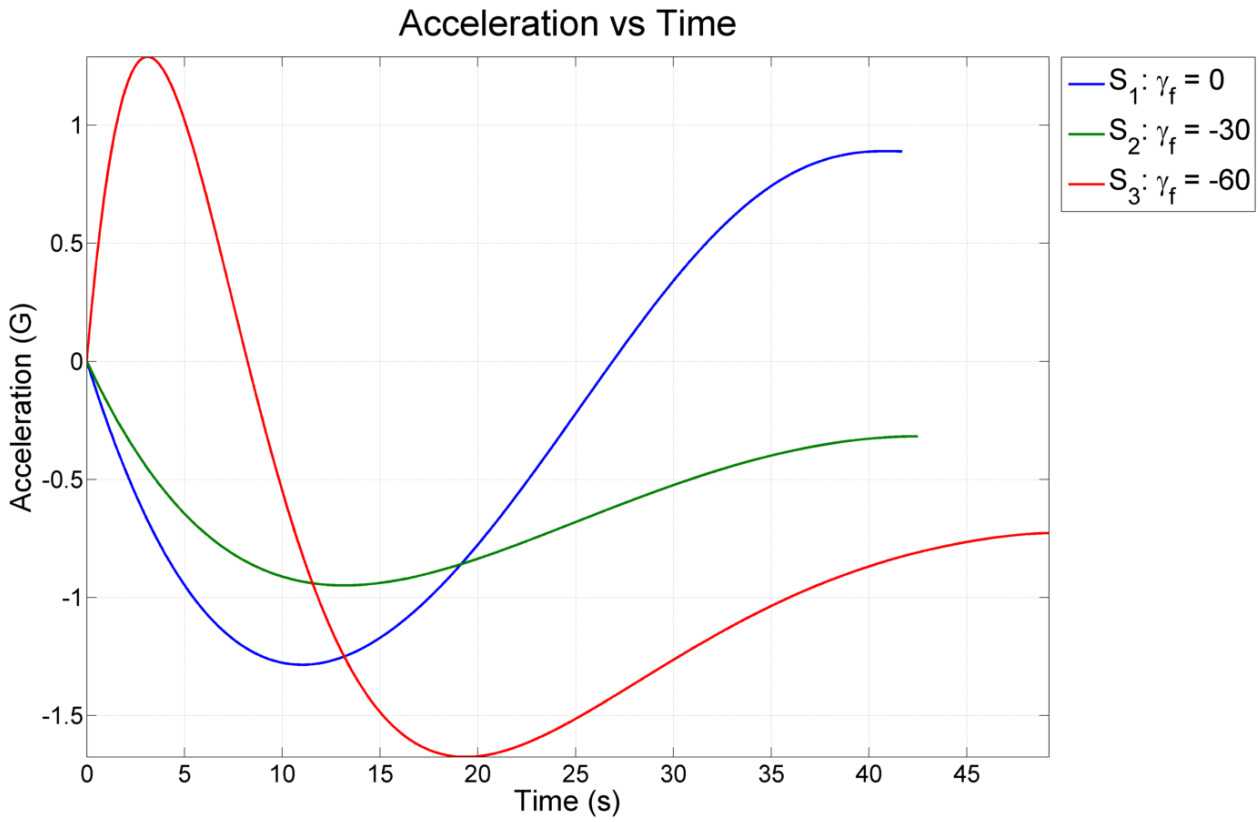

Figure 4.4: Results: IACG Acceleration

4.3 Case 2: General Vector Explicit Guidance (GENEX)

Case 2 demonstrates the ability of GENEX to hit a stationary target using three different values of n. The trajectories for each subcase are shown below in Fig. 4.5. The blue, green and red traces represent n values of 0,1, and 2, respectively.

During the initial phase of flight, the trajectory of the missile changes more rapidly as n is increased. Whereas, during the terminal phases of flight the trajectory of the missile changes more slowly as n is increased.

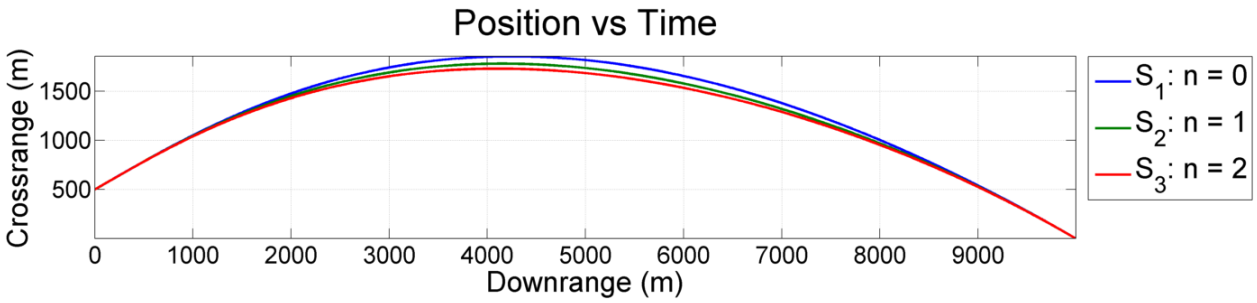

Figure 4.5: Results: GENEX Trajectory

As shown in Fig. 4.6 in each case the missile successfully achieved the desired impact angle. However, the lower the value of n the longer the time of flight. Once again, this difference in time occurs because the impact time control portion of the guidance was not implemented.

By comparing the slopes of the lines it is apparent that as n is increased the flight path angle is changing more rapidly during the initial phase of flight. By observing the slopes of the flight path angles during the terminal phase of flight it is clear that the missile approaches the desired impact angle more aggressively with increasing n.

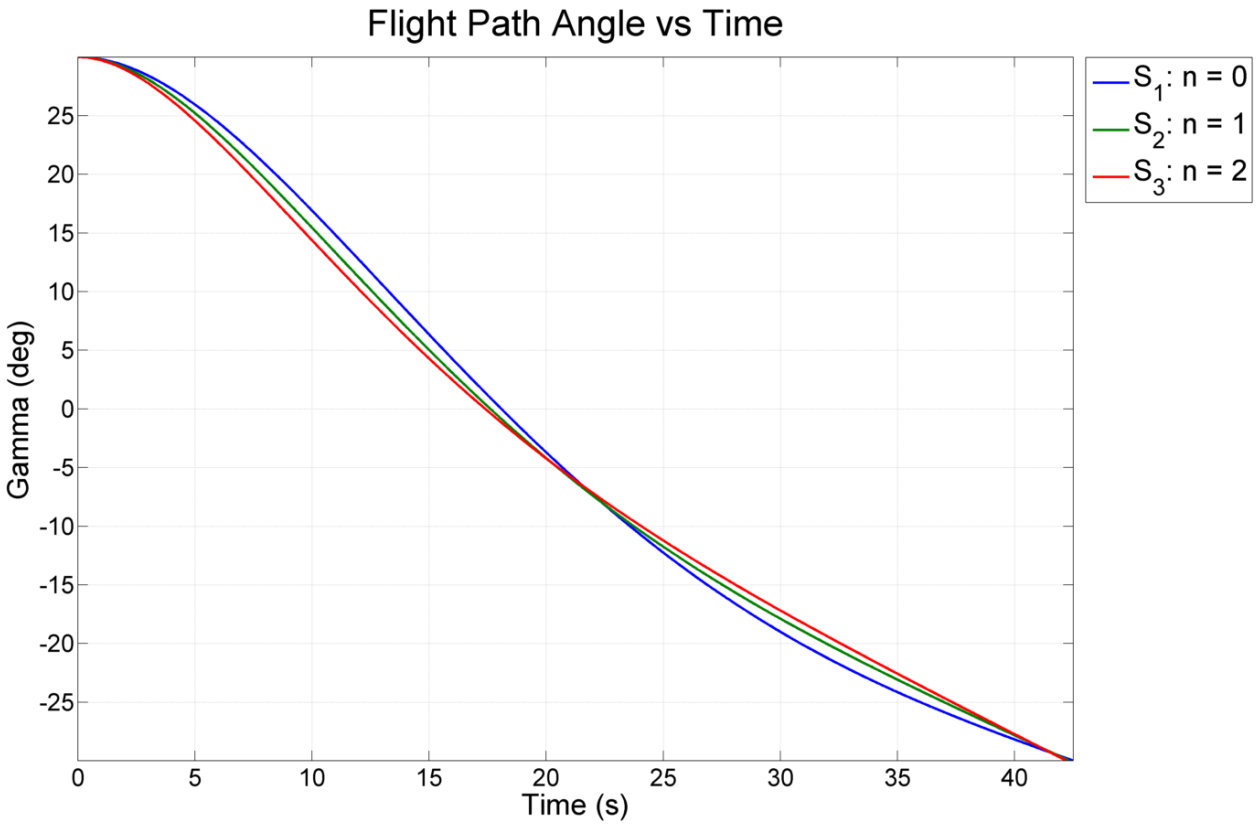

Figure 4.6: Results: GENEX Flight Path Angle

The GENEX command and acceleration is shown below in Fig. 4.7 and Fig. 4.8. Once again, the term to control impact time is zero throughout the entire, which causes discrepancies in impact time. It is apparent that with increasing value of n more acceleration is being commanded during the initial phase of flight and less acceleration is being commanded during the terminal phase of flight.

This behavior agrees with cost function of GENEX which increasing the weight on the control input as downrange to go approaches zero. The less acceleration commanded during the terminal phase of flight, the steeper the approach angle to the desired impact angle.

Figure 4.7: Results: GENEX Guidance Command

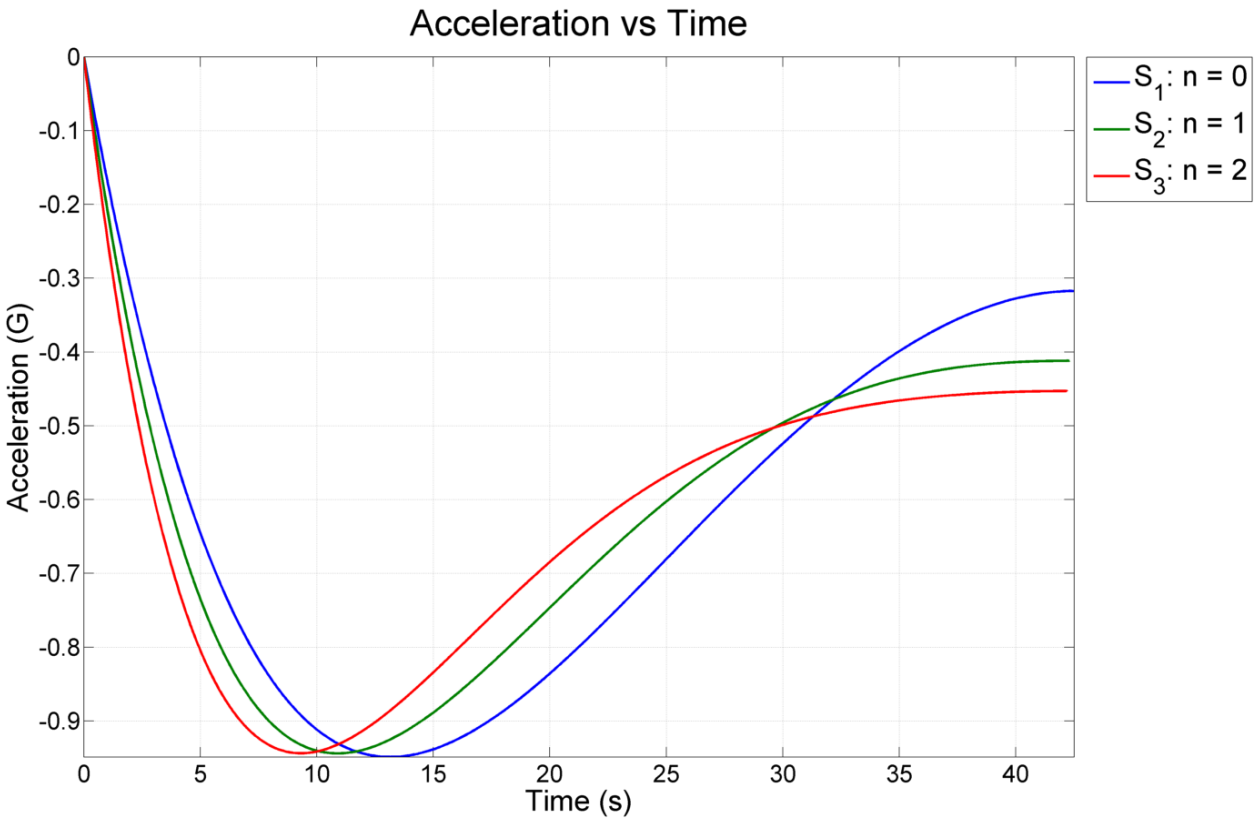

Figure 4.8: Results: GENEX Acceleration

4.4 Case 3: Impact Time Control Guidance (ITCG)

Case 3 demonstrates the ability of ITCG to hit a stationary target at three different desired impact times. The trajectories for each subcase in shown below in Fig. 4.9. The blue, green and red traces represent desired terminal impact times of 45,50, and 55 seconds, respectively.

As the desired impact time is increased the trajectory of the missile is altered to fly a longer flight path which ensures the missile arrives at the target at the specified time.

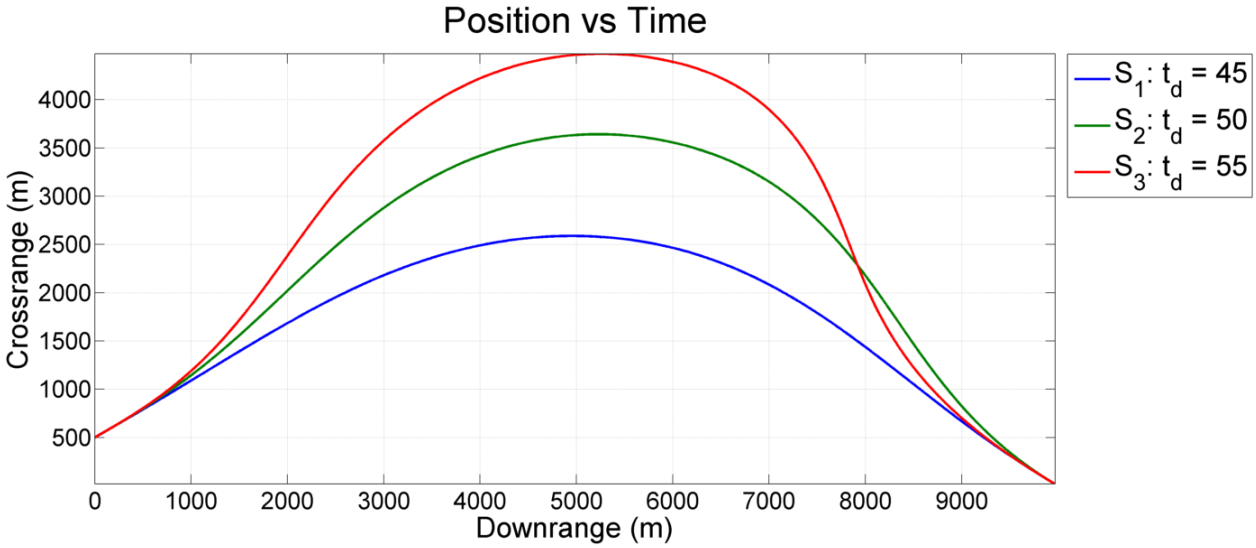

Figure 4.9: Results: ITCG Trajectory

Fig. 4.10 shows the time-to-go estimate for each case. The time-to-go estimator successfully converges to zero at each desired impact time. For each case, the estimator begins at the same estimate which is obviously shorter than the desired time-to-go for each case.

This estimation error is used by GENEX-ITACG to place the missile on a longer trajectory. Once this error is eliminated the ITCG portion of GENEX-ITACG is not used and the missile strictly flies on a trajectory using a combination of GENEX and IACG.

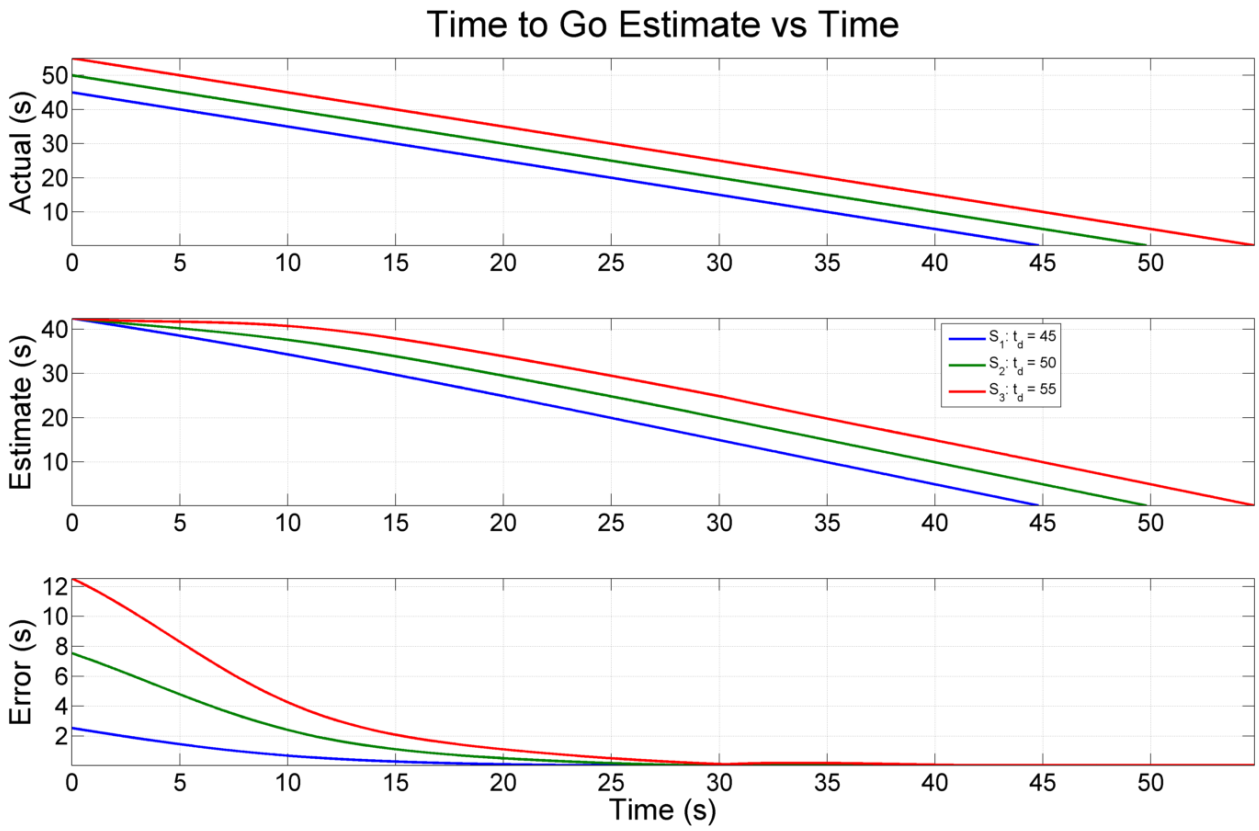

Figure 4.10: Results: ITCG Time to Go

As shown in Fig. 4.11 in each case the missile successfully achieved the desired impact angle at the desired impact time. The larger the desired impact time the larger the range of flight path angles achieved by the missile to waste energy.

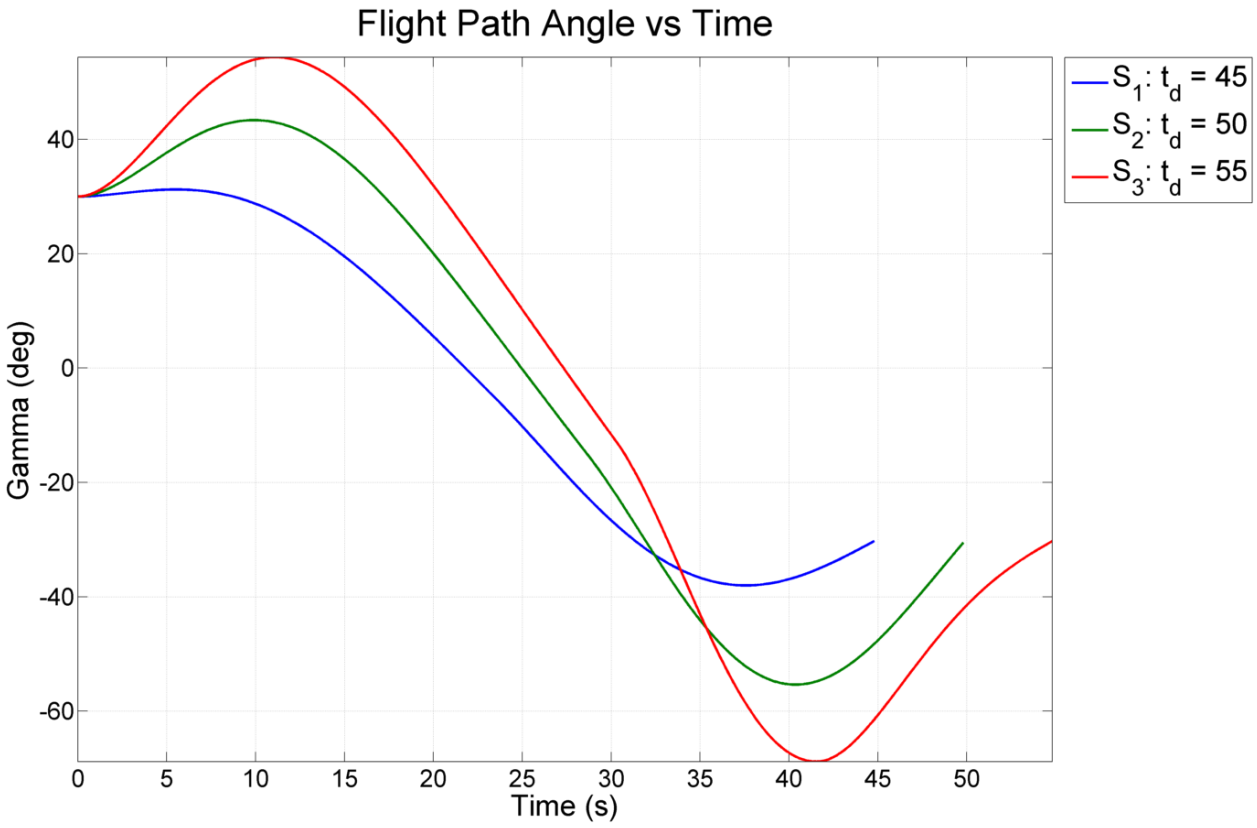

Figure 4.11: Results: ITCG Flight Path Angle

The ITCG command and commanded acceleration is shown below in Fig. 4.12 and Fig. 4.13. It is apparent that by increasing the desired impact time more acceleration is commanded throughout flight. This behavior agrees with the need to burn more energy to meet larger desired impact time.

The first nonlinearity in the jerk command occurs because the η_L term of the guidance law changes polarity. The second nonlinearity is due to implementation. As the missile approaches the target, the guidance laws sensitivity to time-to-go estimation error increases. Once estimation error dropped below 1 millisecond the impact time control was set to zero.

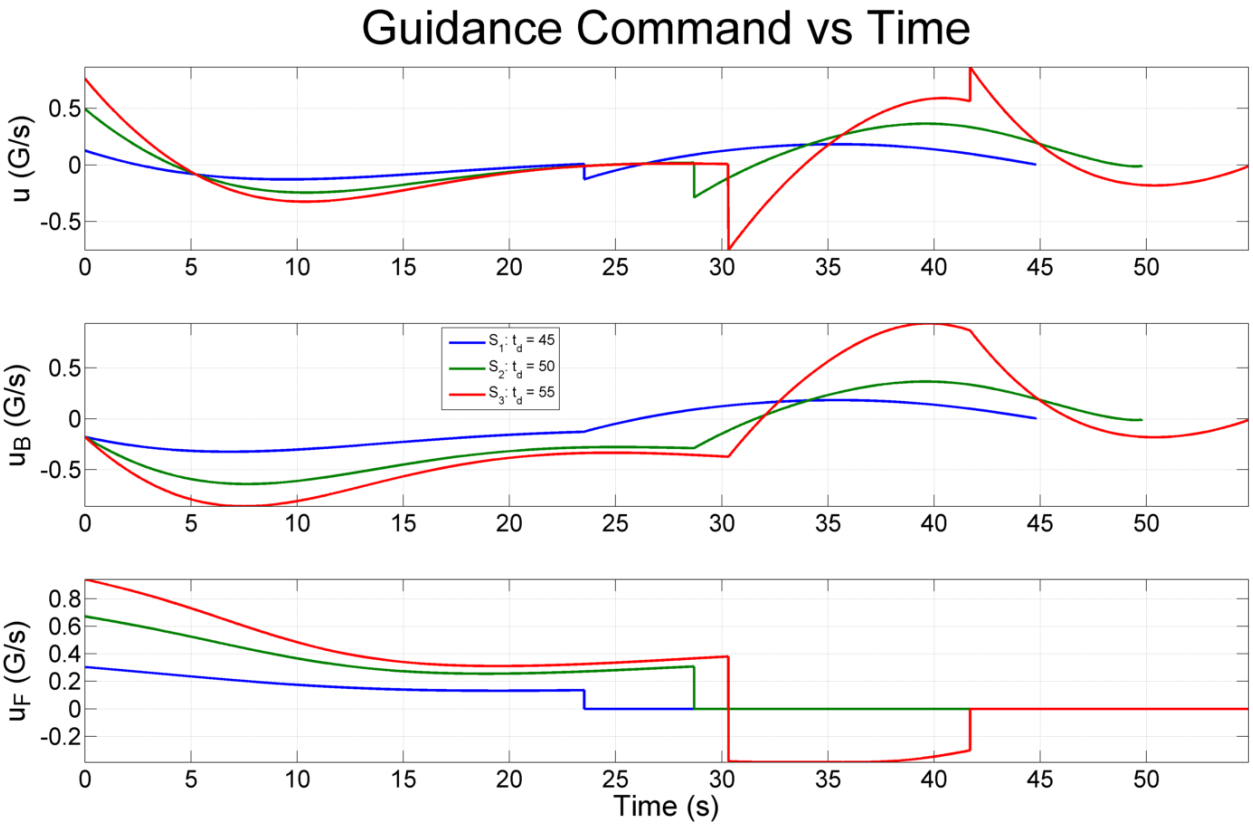

Figure 4.12: Results: ITCG Guidance Command

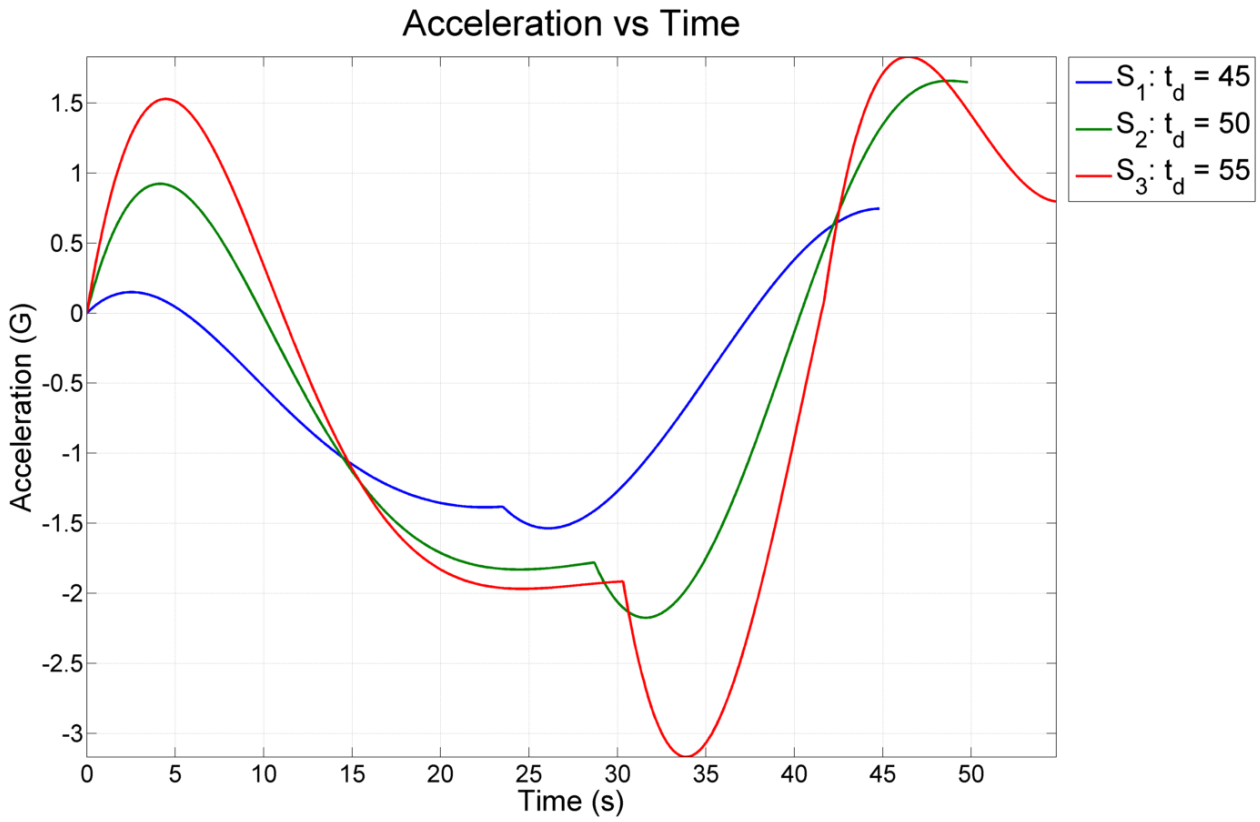

Figure 4.13: Results: ITCG Acceleration

4.5 Case 4: GENEX-ITACG Single Missile Flyout

Case 4 demonstrates the ability of GENEX-ITACG to hit a stationary target at an impact time of 50 seconds, with a impact angle of -30 degrees, using three different values of n. The trajectories for each subcase in shown below in Fig. 4.14. The blue, green and red traces represent n values of 0,0.1, and 0.2, respectively.

Similar to Case 2, during the initial phase of flight the trajectory of the missile changes more rapidly as n is increased. However, the missile's flight path differs during the terminal phase of flight. Contrary to GENEX, the missile's flight path behaves more aggressively during the terminal phase of flight. The reason for this difference is explained later.

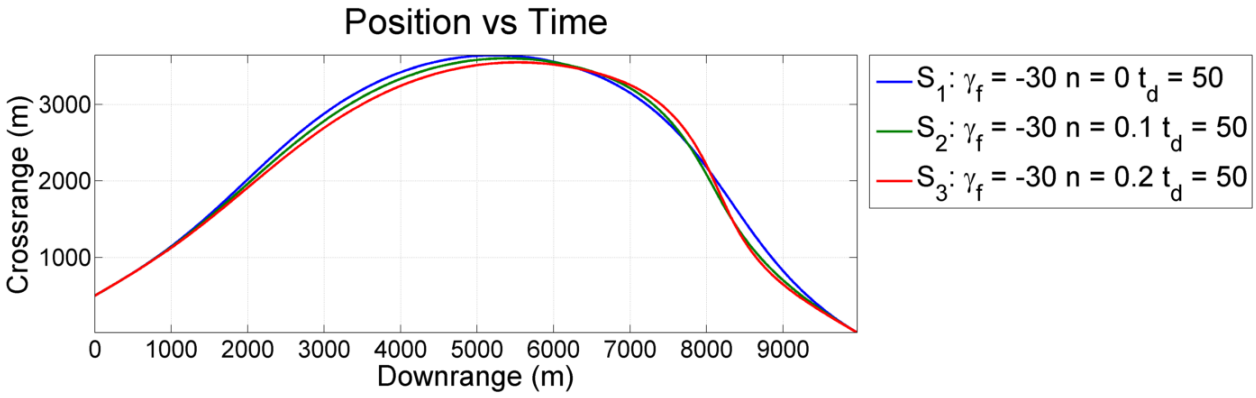

Figure 4.14: Results: GENEX-ITACG Trajectory

Fig. 4.15 shows the time-to-go estimate for each case. For each case the time-to-go estimator successfully converges to zero at the desired impact time of 50 seconds.

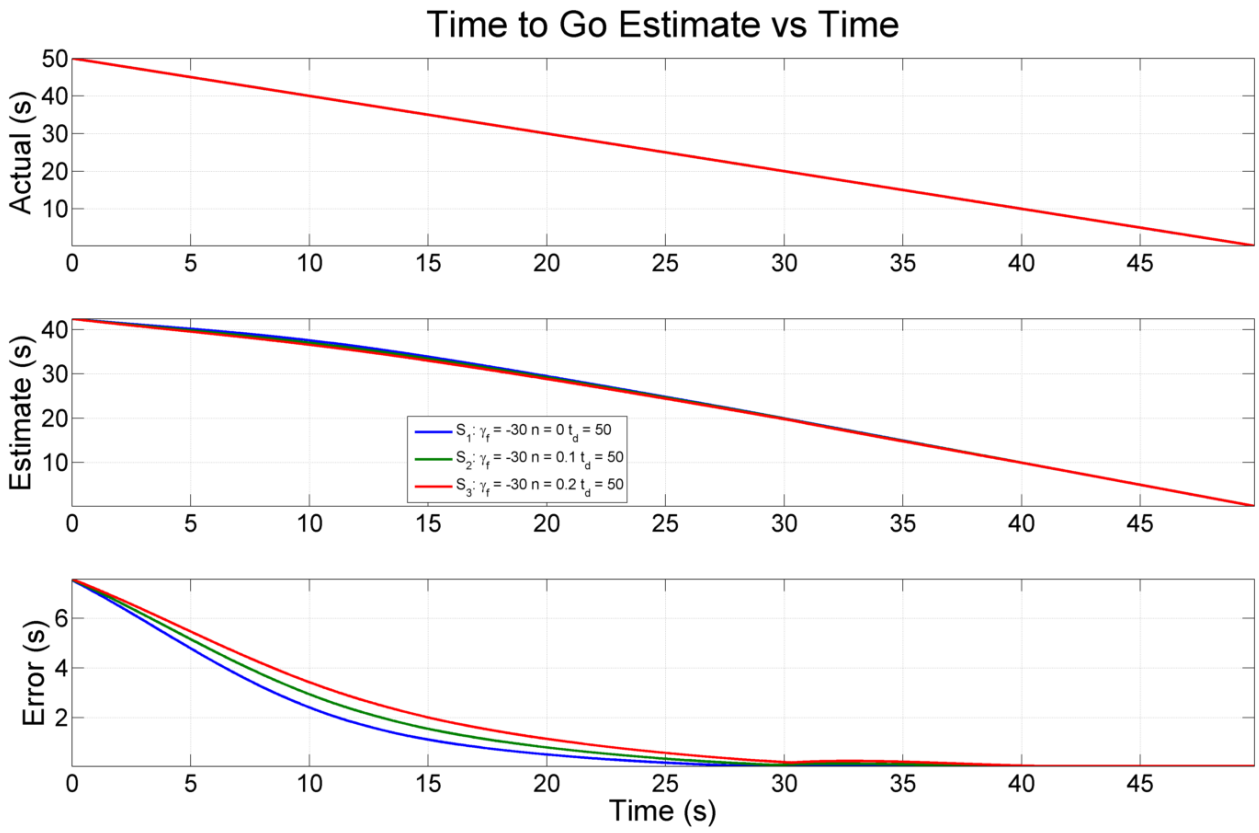

Figure 4.15: Results: GENEX-ITACG Time to Go

As shown in Fig. 4.16 in each case the missile successfully achieved the desired impact angle at the desired impact time. The flight path angle behavior during the initial phase of flight becomes less aggressive as n is increased. Whereas, the flight path angle behavior during the terminal phase of flight becomes more aggressive as n is increased.

Although this seems to contradict the goal of GENEX, this occurs because of the logic to turn off time correction when the time-to-go estimation error drops below 1 millisecond. This nonliearity causes the guidance law to jump to a different parameterized cost function and behave as if it is the initial phase of flight again.

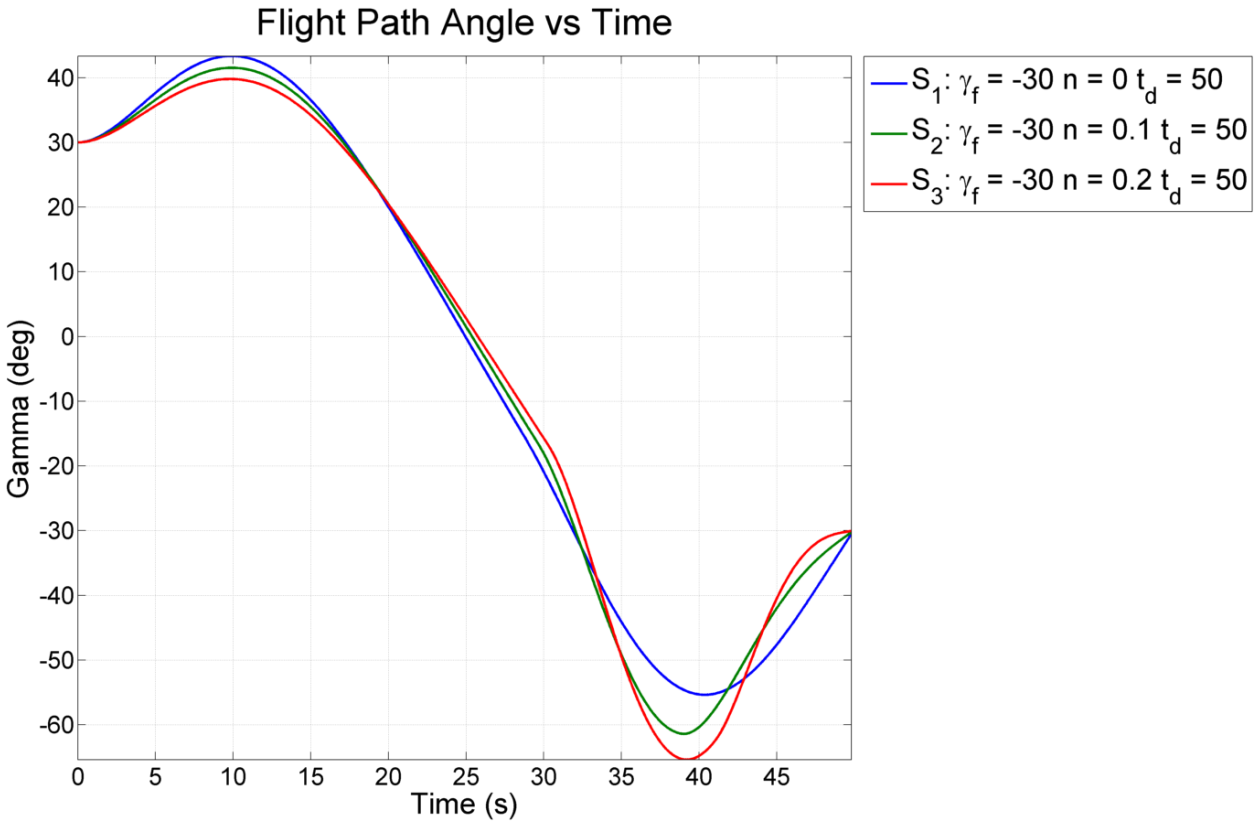

Figure 4.16: Results: GENEX-ITACG Flight Path Angle

The GENEX-ITACG command and commanded acceleration is shown below in Fig. 4.17 and Fig. 4.18. Unlike Case 2, it is apparent that with increasing value of n less acceleration is being commanded during the initial phase of flight and more acceleration is being commanded during the terminal phase of flight.

This due to the inclusion of the impact time correcting term. Once this term is zeroed out, the behavior of the acceleration agrees with that of Case 2.

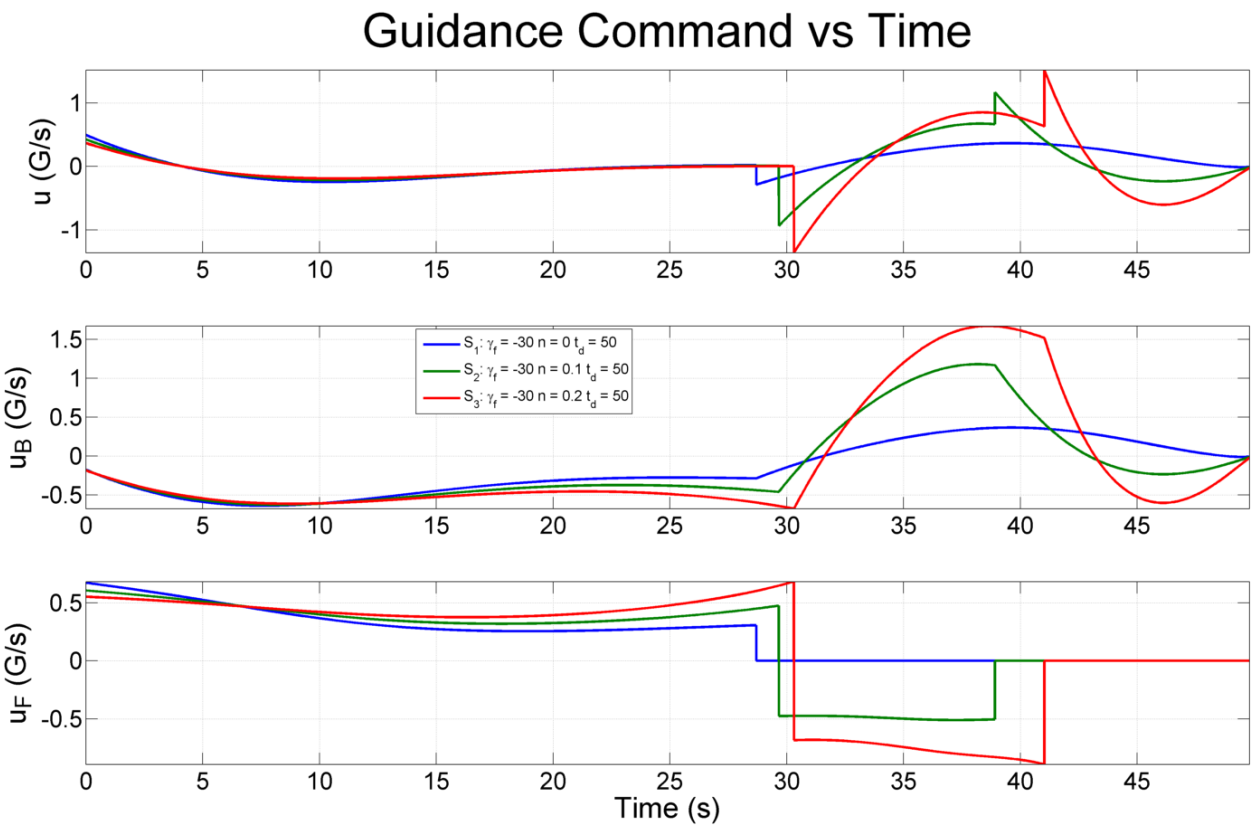

Figure 4.17: Results: GENEX-ITACG Guidance Command

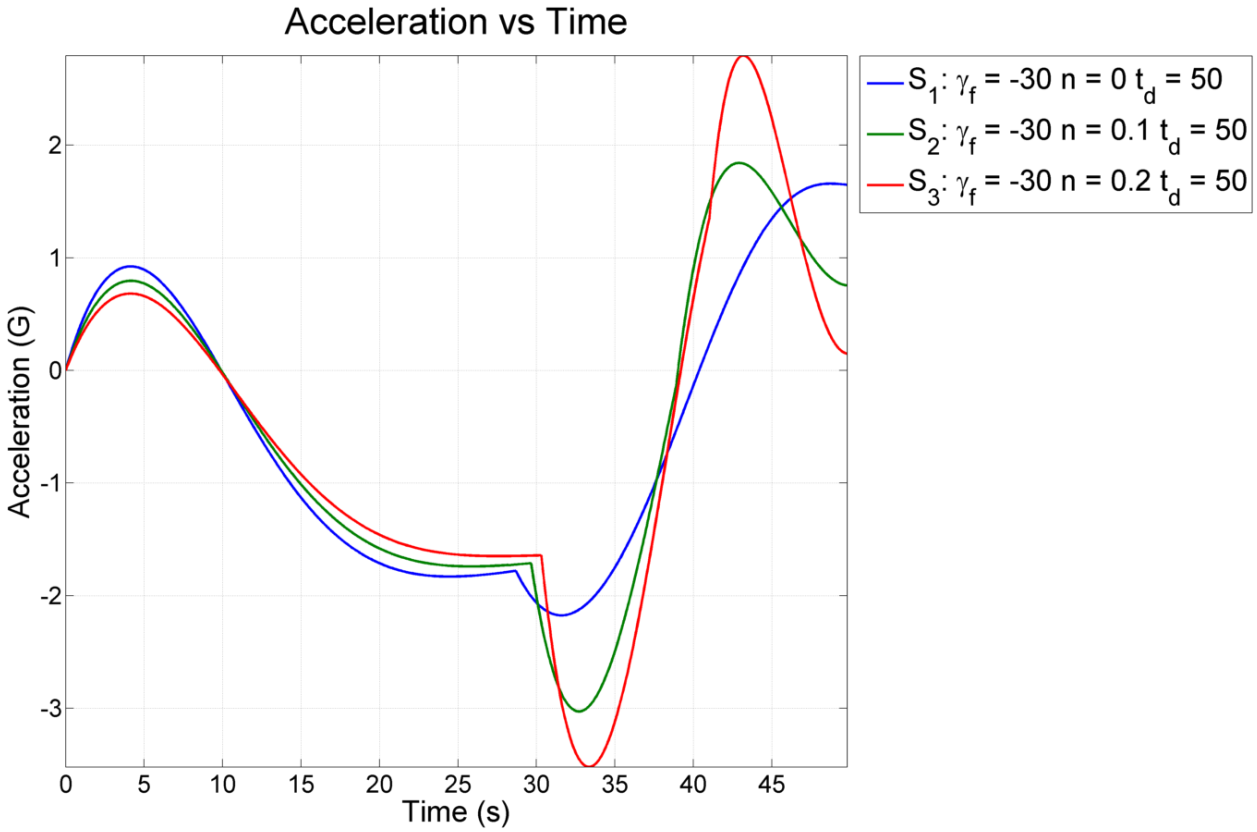

Figure 4.18: Results: GENEX-ITACG Acceleration

4.6 Case 5: GENEX-ITACG Salvo Attack Flyout

Case 5 demonstrates the ability of GENEX-ITACG to guide three missiles to hit a stationary target at an impact time of 50 seconds, with three different impact angle of -30 degrees, using three different values of n.

The trajectories for each subcase in shown below in Fig. 4.19. Each missile has the ability to hit the target with different trajectories.

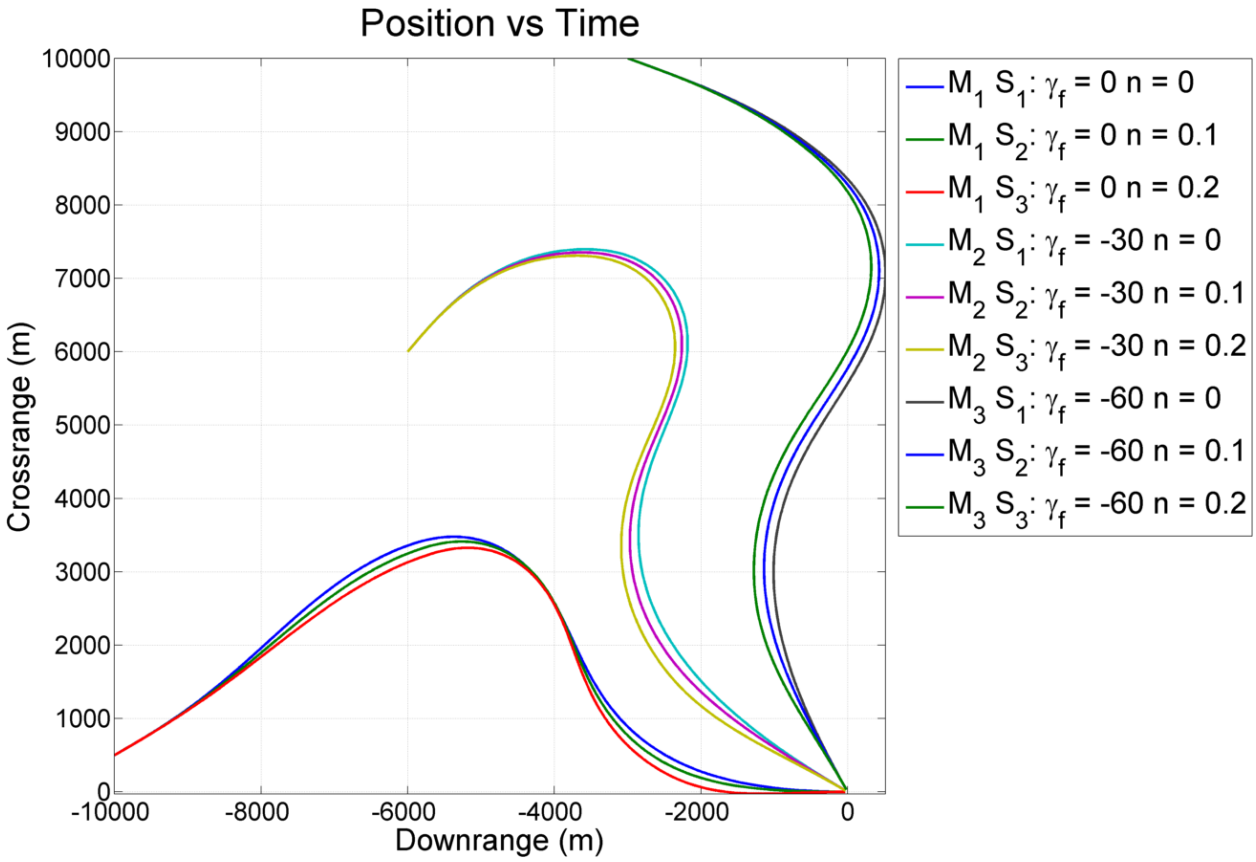

Figure 4.19: Results: GENEX-ITACG Salvo Trajectory

As shown in Fig. 4.20 the missiles successfully achieved the desired impact angle at the desired impact time with varying levels of impact angle aggressiveness.

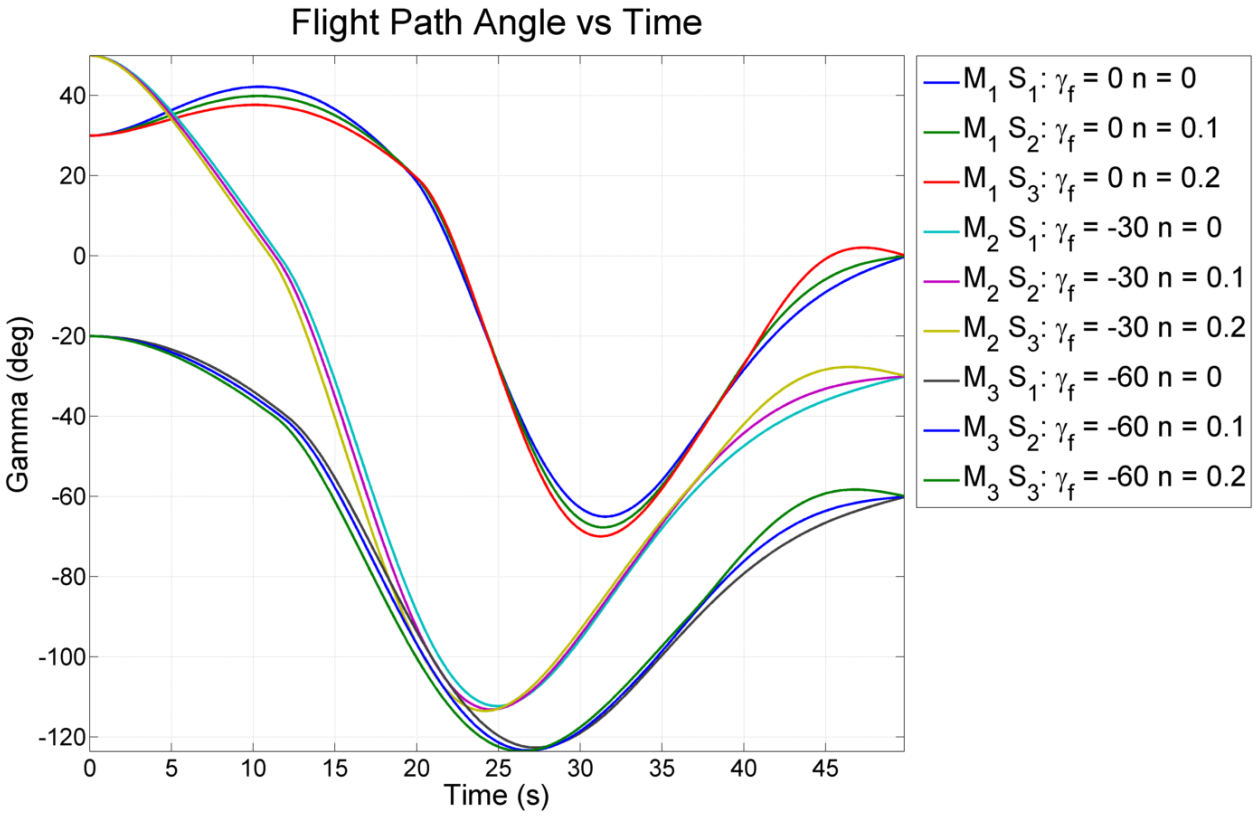

Figure 4.20: Results: GENEX-ITACG Salvo Flight Path Angle

CHAPTER 5: CONCLUSION

In conclusion, it has been proven that GENEX-ITACG allows a salvo of missile to simultaneously hit a stationary target at a prescribed impact time and impact angle, while adjusting the aggressiveness of the trajectory with a user design parameter. Although, the design parameter acts differently from GENEX during the terminal stage of flight, this is not an undesirable behavior. A family of different trajectories can still be flown through its use, with increasingly aggressive trajectories.

Future areas of research, include removing the need to specify a impact time to achieve the salvo attack. Instead of incorporating ITACG into GENEX, a cooperative function can be designed that penalizes terminal miss distances between each missile. Thus, the impact time would be negotiated between the missiles involved in the salvo attack and not specified by the end user.

Another area of future research is to add the ability to hit a maneuvering target. GENEX has the ability to do this. Adding these capabilities into GENEX-ITACG would have greatly increased the complexity of the derivation. Hopefully, GENEX-ITACG can serve as a stepping stone to accomplishing this feat.

APPENDIX A: DETAILED DERIVATION OF GENEX-ITACG

A.1 Equations of Motion

In this section, a detailed derivation of GENEX-ITACG law is presented. Lets first consider the equations of motion for a planar target missile engagement scenario. The nonlinear planar target missile engagement equations are

$$\dot{X}(t) = V\,\cos(\gamma(t))\,,\;\; \dot{Y}(t) = V\,\sin(\gamma(t))\,,\;\; \dot{\gamma}(t) = \frac{A(t)}{V},\;\; \dot{A}(t) = g(t) = g_B(t) + g_F(t) \quad \text{(A.1)}$$

where $X(t)$ is the missile's downrange position, $Y(t)$ is the missile's crossrange position, V is the missile's velocity, $A(t)$ is the missile's acceleration which is applied normal to the velocity vector, and $\gamma(t)$ is the missile's flight path angle.

The missile acceleration rate, jerk, is included to provide an additional degree of freedom for impact time control. The first jerk term, $g_B(t)$, is the command to eliminate the miss distance and the impact angle error. The second jerk term, g_F, is the additional command that corrects the trajectory to achieve impact at the desired impact time.

Without loss of generality, it is assumed that the flight path angle remains small for most of the flight. With this small angle assumption, the following linearizations can be made: $\sin(\gamma(t)) = \gamma(t)$ and $\cos(\gamma(t)) = 1$. Therefore, the state equations of A.1 are simplified to

$$\dot{X}(t) = V,\;\; \dot{Y}(t) = V\,\gamma(t),\;\; \dot{\gamma}(t) = A(t)/V,\;\; \dot{A}(t) = g(t) \quad \text{(A.2)}$$

These simplified dynamic equation are used to carry out the derivation of the proposed guidance law.

First, to further reduce the complexity of the derivation lets introduce nondimensional state variables. The state variables are nondimensionalized as follows

$$x(t) = \frac{X(t)}{V\,t_f}, y(t) = \frac{Y(t)}{V\,t_f},\;\; a = \frac{A(t)\,t_f}{V},\;\; \tau = \frac{t}{t_f},\;\; u(t) = \frac{{t_F}^2\,g(t)}{V} \tag{A.3}$$

Taking the derivative with respect to time on both sides of the dimensionless time relation yields

$$\frac{dt}{dt} = t_f\,\frac{d\tau}{dt} = 1 \;\text{ or }\; dt = d\tau\,t_f \tag{A.4}$$

Furthermore, by taking the derivative with respect to time of both sides of the rest of the dimensionless relations, substituting A.4 into the results and then equating to A.2 yields

$$\begin{aligned}
\frac{dX}{dt} &= Vt_f\frac{dx}{dt} = V\frac{dx}{d\tau} = V \\
\frac{dY}{dt} &= Vt_f\frac{dy}{dt} = V\frac{dy}{d\tau} = V\gamma \\
\frac{d\gamma}{dt} &= \frac{d\gamma}{dt} = \frac{1}{t_f}\frac{d\gamma}{d\tau} = \frac{A}{V} \\
\frac{dA}{dt} &= \frac{V}{t_f}\frac{da}{dt} = \frac{V}{t_f^2}\frac{da}{d\tau} = g(t) = g_B(t) + g_F(t)
\end{aligned} \tag{A.5}$$

Now from A.5 the nondimensional state equations are expressed as

$$\begin{aligned}
\frac{dx}{d\tau} &= 1 \\
\frac{dy}{d\tau} &= V\gamma(t) \\
\frac{d\gamma}{d\tau} &= \frac{A(t)\,t_f}{V} = a(t) \\
\frac{da}{d\tau} &= \frac{{t_F}^2\,g(t)}{V} = u(t) = u_B(t) + u_F(t)
\end{aligned} \tag{A.6}$$

To aid in the derivation of the impact time control term, u_F, the independent variable of A.6 is changed from dimensionless time, τ, to dimensionless downrange x such that

$$\begin{aligned} \frac{dx}{dx} &= 1 \\ \frac{dy}{dx} &= \gamma(x) \\ \frac{d\gamma}{dx} &= a(x) \\ \frac{da}{dx} &= u(x) = u_B(x) + u_F(x) \end{aligned} \tag{A.7}$$

By specifying the state variables as $\bar{X} = [y(x) \;\; \gamma(x) \;\; a(x)]^T$, these equations can be expressed in state space format as

$$\dot{\bar{X}} = A\,\bar{X} + B\,u = \begin{pmatrix} 0 & 1 & 0 \\ 0 & 0 & 1 \\ 0 & 0 & 0 \end{pmatrix} \bar{X} + \begin{pmatrix} 0 \\ 0 \\ 1 \end{pmatrix} (u_B(x) + u_F(x)) \tag{A.8}$$

A.2 Linear Quadratic Control Problem

Now that the state equations are defined the linear optimal control problem is formulated as a terminal controller problem with a quadratic performance index. The formal problem definition is stated as

$$\begin{aligned} \underset{u_B(t)}{\text{minimize}} \;\; & J = \frac{1}{2}\int_{x_0}^{x_f} u_B^2(x) R(x) dx \\ \text{subject to} \;\; & \dot{\bar{X}} = A\bar{X}(x) + B(u_B(x) + u_F) \\ & E = D\bar{X}(x_f) \end{aligned}$$

$R(x)$ is the control weighting function defined as

$$R(x) = \frac{1}{(x_f - x)^n} \tag{A.9}$$

that penalizes the control effort more severely as the missile approaches its final destination, the target.

This penalization not only limits excessive commanded maneuvering during the terminal phases of flights, but also allows the missile to command additional acceleration at handover. Handover is the transition between the midcourse phase of flight and the terminal phase of flight. At handover additional acceleration may be needed to eliminate large heading errors between the predicted location of the target and the actual location of the target at handover.

D is the terminal weighting cost matrix defined as

$$D = \begin{pmatrix} 1 & 0 & 0 \\ 0 & 1 & 0 \\ 0 & 0 & 0 \end{pmatrix} \tag{A.10}$$

that places constraints on terminal crossrange and terminal flight path angle, but places no constraint on terminal acceleration. No constraint is placed on terminal acceleration because there is no way of knowing this value beforehand.

E is the terminal state matrix defined as

$$E = \begin{pmatrix} y(x_f) \\ \gamma(x_f) \\ 0 \end{pmatrix} \tag{A.11}$$

that consists of two user defined parameters: the missile's terminal crossrange position and terminal flight path angle. Intuitively, the desired terminal crossrange position would be the targets crossrange position or some position close to it.

Now that the linear optimal control problem is clearly stated the Hamiltonian function may be expressed as

$$H(x) = \frac{{u_B}^2(x)}{2\,(x_f - x)^n} + a(x)\,\lambda_\gamma + \gamma(x)\,\lambda_y + \left[u_B(x) + u_F(x)\right]\,\lambda_a \tag{A.12}$$

and the terminal cost function may be expressed as

$$\phi(x_f) = v^\top [D\bar{x}(x_f)] = v_y y(x_f) + v_\gamma \gamma(x_f) \tag{A.13}$$

From linear optimal control theory the costate equations are obtained as

$$\frac{\partial H}{\partial x} = \begin{bmatrix} \frac{\partial H}{\partial y} \\ \frac{\partial H}{\partial \gamma} \\ \frac{\partial H}{\partial a} \end{bmatrix} = \begin{bmatrix} 0 \\ \lambda_y \\ \lambda_\gamma \end{bmatrix} = -\dot{\lambda} = - \begin{bmatrix} \dot{\lambda}_y \\ \dot{\lambda}_\gamma \\ \dot{\lambda}_a \end{bmatrix} \tag{A.14}$$

and the costate equations at terminal downrange are obtained as

$$\frac{\partial \phi(x_f)}{\partial x} = \begin{bmatrix} \frac{\partial \phi(x_f)}{\partial y} \\ \frac{\partial \phi(x_f)}{\partial \gamma} \\ \frac{\partial \phi(x_f)}{\partial a} \end{bmatrix} = \begin{bmatrix} v_y \\ v_\gamma \\ 0 \end{bmatrix} = \lambda(x_f) = \begin{bmatrix} \lambda_y(x_f) \\ \lambda_\gamma(x_f) \\ \lambda_a(x_f) \end{bmatrix} \tag{A.15}$$

The costate dynamic equations are solved by first integrating $\dot{\lambda}_y(x)$ from A.14 downrange to in the following manner

$$-\int_{x_f}^{x} \dot{\lambda}_y(s)ds = -\lambda_y(x) + \lambda_y(x_f) = \int_{x_f}^{x} 0ds = 0 \tag{A.16}$$

Substitution of Eq. A.15 yields

$$\lambda_y(x) = \lambda_y(x_f) = v_y \tag{A.17}$$

Then by integrating $\dot{\lambda}_\gamma(x)$ from A.14 backwards in downrange in the following manner

$$\begin{aligned} -\int_{x_f}^{x} \dot{\lambda}_\gamma(s)ds = -\lambda_\gamma(x) + \lambda_\gamma(x_f) = \\ \int_{x_f}^{x} \lambda_y(s)ds = \int_{x_f}^{x} v_y ds = v_y\left(x - x_f\right) \end{aligned} \tag{A.18}$$

Substitution of Eq. A.15 yields

$$\lambda_\gamma(x) = -v_y\left(x - x_f\right) + \lambda_\gamma(x_f) = v_y\left(x_f - x\right) + v_\gamma \tag{A.19}$$

Finally, by integrating $\dot{\lambda}_a(x)$ from A.14 backwards in downrange in the following manner

$$\begin{aligned} -\int_{x_f}^{x} \dot{\lambda}_a(s)ds = -\lambda_a(x) + \lambda_a(x_f) = \\ \int_{x_f}^{x} \lambda_\gamma(s)ds = \int_{x_f}^{x} \left[v_y\left(x_f - s\right) + v_\gamma\right] ds \\ = -\frac{1}{2}v_y\left(x_f - x\right)^2 + v_\gamma\left(x - x_f\right) \end{aligned} \tag{A.20}$$

Substitution of Eq. A.15 yields

$$\lambda_a(x) = \frac{1}{2}v_y\left(x_f - x\right)^2 - v_\gamma\left(x - x_f\right) + \lambda_a(x_f) = \frac{1}{2}v_y\left(x_f - x\right)^2 + v_\gamma\left(x_f - x\right) \tag{A.21}$$

In summary, the costate equations are

$$\begin{aligned} \lambda_y(x) &= v_y \\ \lambda_\gamma(x) &= v_\gamma + v_y\left(x_f - x\right) \\ \lambda_a(x) &= v_\gamma\left(x_f - x\right) + \frac{1}{2}v_y(x_f - x)^2 \end{aligned} \tag{A.22}$$

Furthermore, the optimal control to minimize the terminal miss distance and flight path angle error is obtained by applying the optimality condition and through the use of A.22 obtained as

$$\begin{aligned} \frac{\partial H}{\partial u_B} &= \frac{u_B}{\left(x_f - x\right)^n} + \lambda_a(x) = 0 \\ u_B &= -\left(x_f - x\right)^n \lambda_a(x) = -v_\gamma\left(x_f - x\right)^{n+1} - \frac{1}{2}v_y\left(x_f - x\right)^{n+2} \end{aligned} \tag{A.23}$$

The control term u_B is not completely defined because the terminal constant multipliers v_y and v_γ have not been defined. These terms are obtained by solving the state space equations of A.6 to obtain explicit equations for each state and then solving for these multipliers.

First, an explicit equation for acceleration is obtained by A.23 plugging into A.22 and integrating from x to some intermediate point in space $s \in [x, x_f]$ such that

$$\begin{gathered}\int_x^s \dot{a}(s)ds = a(s) - a(x) = a(s) - a_x = \\ \int_x^s \left[u_B(s) + u_F\right] ds = \int_x^s \left[-v_\gamma \left(x_f - s\right)^{n+1} - \frac{1}{2} v_y \left(x_f - s\right)^{n+2} + u_F\right] ds\end{gathered} \tag{A.24}$$

and solving for $a(s)$ yields

$$\begin{aligned}a(s) = a_x + u_F\ (s - x) - \frac{v_\gamma}{(n+2)}(x_f - x)^{n+2} - \frac{v_y}{2\,(n+3)}(x_f - x)^{n+3} \\ + \frac{v_\gamma}{(n+2)}(x_f - s)^{n+2} + \frac{v_y}{2\,(n+3)}(x_f - s)^{n+3}\end{aligned} \tag{A.25}$$

Second, an explicit equation for flight path angle is obtained by A.23 plugging into A.22 and integrating backwards in time from x_f such that

$$\begin{aligned}-\int_{x_f}^s \dot{\gamma}(s)ds = -\gamma(s) + \gamma(x_f) = -\gamma(s) + \gamma_f = \\ -\int_{x_f}^s a(s)ds = -\int_{x_f}^s [a_x + u_F\ (s - x) - \frac{v_\gamma}{(n+2)}(x_f - x)^{n+2} - \frac{v_y}{2\,(n+3)}(x_f - x)^{n+3} \\ + \frac{v_\gamma}{(n+2)}(x_f - s)^{n+2} + \frac{v_y}{2\,(n+3)}(x_f - s)^{n+3}\Big] ds\end{aligned} \tag{A.26}$$

and solving for $\gamma(s)$ yields

$$\begin{aligned}\gamma(s) = \gamma_f - a_x \left(x_f - s\right) + \left(\frac{1}{2}(x_f - s)^2 - \left(x_f - x\right)\left(x_f - s\right)\right) u_F \\ \left(\frac{1}{(n+2)}(x_f - x)^{n+2}\left(x_f - s\right) - \frac{1}{(n+2)\ (n+3)}(x_f - s)^{n+3}\right) v_\gamma \\ \left(\frac{1}{2\,(n+3)}(x_f - x)^{n+3}\left(x_f - s\right) - \frac{1}{2\ (n+3)\ (n+4)}(x_f - s)^{n+4}\right) v_y\end{aligned} \tag{A.27}$$

Last, an explicit equation for crossrange is obtained by A.23 plugging into A.22 and integrating backwards in time from x_f such that

$$\begin{aligned} -\int_{x_f}^{s} \dot{y}(s)ds = -y(s) + y(x_f) = -y(s) + y_f = \\ -\int_{x_f}^{s} \gamma(s)ds = -\int_{x_f}^{s} \left[\gamma_f - a_x \left(x_f - s\right) + \left(\frac{1}{2}(x_f - s)^2 - \left(x_f - x\right)\left(x_f - s\right) \right) u_F \right. \\ \left(\frac{1}{(n+2)}(x_f - x)^{n+2}\left(x_f - s\right) - \frac{1}{(n+2)\ (n+3)}(x_f - s)^{n+3} \right) v_\gamma \\ \left. \left(\frac{1}{2\,(n+3)}(x_f - x)^{n+3}\left(x_f - s\right) - \frac{1}{2\ (n+3)\ (n+4)}(x_f - s)^{n+4} \right) v_y \right] ds \end{aligned} \tag{A.28}$$

and solving for $y(s)$ yields

$$\begin{aligned} y(s) = y_f - \gamma_f\ (x_f - s) + \frac{1}{2}a_x(x_f - s)^2\ + \left(\frac{1}{2}\left(x_f - x\right)(x_f - s)^2 - \frac{1}{6}(x_f - s)^3 \right) u_F \\ \left(\frac{1}{(n+2)\ (n+3)\ (n+4)}(x_f - s)^{n+4} - \frac{1}{2\ (n+2)}(x_f - x)^{n+2}(x_f - s)^2 \right) v_\gamma \\ \left(\frac{1}{2\ (n+3)\ (n+4)\ (n+5)}(x_f - s)^{n+5} - \frac{1}{4\ (n+3)}(x_f - x)^{n+3}(x_f - s)^2 \right) v_y \end{aligned} \tag{A.29}$$

Now each state variable can be expressed as a function of x by substituting $s = x$. By means of this substitution A.25 becomes

$$\begin{aligned} a(x) = a_x + u_F\ (x - x) - \frac{v_\gamma}{(n+2)}(x_f - x)^{n+2}\ - \frac{v_y}{2\,(n+3)}(x_f - x)^{n+3} \\ + \frac{v_\gamma}{(n+2)}(x_f - x)^{n+2} + \frac{v_y}{2\,(n+3)}(x_f - x)^{n+3} \end{aligned} \tag{A.30}$$

A.27 becomes

$$\begin{aligned}\gamma(x) = \gamma_f - a_x\,(x_f - x) + \left(\frac{1}{2}(x_f - x)^2 - (x_f - x)^2\right) u_F \\ + \left(\frac{1}{(n+2)}(x_f - x)^{n+3} - \frac{1}{(n+2)\ (n+3)}(x_f - x)^{n+3}\right) v_\gamma \\ + \left(\frac{1}{2\,(\,n+3)}(x_f - x)^{n+4} - \frac{1}{2\ (n+3)\ (n+4)}(x_f - x)^{n+4}\right) v_y\end{aligned} \tag{A.31}$$

and A.29 becomes

$$\begin{aligned}y(x) = y_f - \gamma_f\ (x_f - x) + \frac{1}{2}\,a_x(x_f - x)^2 + \left(\frac{1}{2}(x_f - x)^3 - \frac{1}{6}(x_f - x)^3\right) u_F \\ + \left(\frac{1}{(n+2)\ (n+3)\ (n+4)}(x_f - x)^{n+4} - \frac{1}{2\ (n+2)}(x_f - x)^{n+4}\right) v_\gamma \\ + \left(\frac{1}{2\ (n+3)\ (n+4)\ (n+5)}(x_f - x)^{n+5} - \frac{1}{4\ (n+3)}(x_f - x)^{n+5}\right) v_y\end{aligned} \tag{A.32}$$

Furthermore, by making algebraic simplifications and denoting $x - x_f$ as downrange to go, x_{go}, A.30 becomes

$$a(x) = a_x \tag{A.33}$$

A.31 becomes

$$\gamma(x) = \gamma_f - a_x x_{go} - \frac{1}{2}u_F\,x_{go}^2 + \frac{1}{(n+3)}v_\gamma\,x_{go}^{n+3} + \frac{1}{2\ (n+4)}v_y\,x_{go}^{n+4} \tag{A.34}$$

and A.32 becomes

$$\begin{aligned}y(x) = y_f - \gamma_f\,x_{go} + \frac{1}{2}a_x\,x_{go}^2 + \frac{1}{3}u_F\,x_{go}^3 \\ - \frac{(n+5)}{2\ (n+3)\ (n+4)}v_\gamma\,x_{go}^{n+4} - \frac{(n+6)}{4\ (n+4)\ (n+5)}v_y\,x_{go}^{n+5}\end{aligned} \tag{A.35}$$

From A.34 the terminal time costate term v_y is solved for as

$$v_\gamma = \frac{(n+3)}{x_{go}^{n+3}} \left(\gamma_x - \gamma_f + a_x\, x_{go} + \frac{1}{2} u_F\, x_{go}^2 - \frac{1}{2\ (n+4)} v_y\, x_{go}^{n+4} \right) \tag{A.36}$$

and from A.35 the other terminal time costate term v_γ is solved for as

$$\begin{aligned} v_y = -\frac{4\ (n+4)\ (n+5)}{(n+6)\ x_{go}^{n+5}} \Bigg(& y_x - y_f + \gamma_f\, x_{go} - \frac{1}{2} a_x\, x_{go}^2 - \frac{1}{3} u_F\, x_{go}^3 \\ & + \frac{(n+5)}{2\ (n+3)\ (n+4)} v_\gamma\, x_{go}^{n+4} \Bigg) \end{aligned} \tag{A.37}$$

Substitution of A.36 into A.37 yields

$$\begin{aligned} v_y = -\frac{4\ (n+4)\ (n+5)}{(n+6)\ x_{go}^{n+5}} \Bigg[& y_x - y_f + \gamma_f\, x_{go} - \frac{1}{2} a_x\, x_{go}^2 - \frac{1}{3} u_F\, x_{go}^3 \\ & + \frac{(n+5)}{2\ (n+4)} x_{go} \left(\gamma_x - \gamma_f + a_x x_{go} + \frac{1}{2} u_F\, x_{go}^2 - \frac{1}{2\ (n+4)} v_y\, x_{go}^{n+4} \right) \Bigg] \end{aligned} \tag{A.38}$$

or equivalently

$$\begin{aligned} & v_y - \frac{(n+5)^2}{(n+4)\ (n+6)} v_y = \left(1 - \frac{(n+5)^2}{(n+4)\ (n+6)} \right) v_y = -\frac{1}{(n+4)\ (n+6)} v_y = \\ & -\frac{4\ (n+4)\ (n+5)}{(n+6)\ x_{go}^{n+5}} \left(y_x - y_f + \gamma_f\, x_{go} - \frac{1}{2} a_x\, x_{go}^2 - \frac{1}{3} u_F\, x_{go}^3 \right) \\ & -\frac{2\ (n+5)^2}{(n+6)\ x_{go}^{n+4}} \left(\gamma_x - \gamma_f + a_x\, x_{go} + \frac{1}{2} u_F\, x_{go}^2 \right) \end{aligned} \tag{A.39}$$

Therefore

$$\begin{aligned} v_y = & \frac{4\ (n+4)^2\ (n+5)}{x_{go}^{n+5}} \left(y_x - y_f + \gamma_f\, x_{go} - \frac{1}{2} a_x\, x_{go}^2 - \frac{1}{3} u_F\, x_{go}^3 \right) \\ & + \frac{(n+4)\ (n+5)^2}{x_{go}^{n+4}} \left(\gamma_x - \gamma_f + a_x\, x_{go} + \frac{1}{2} u_F\, x_{go}^2 \right) \end{aligned} \tag{A.40}$$

or by collection of variables

$$
\begin{aligned}
v_y \;=\; & \frac{4\,(n+4)^2\,(n+5)}{x_{go}^{n+5}}y_x + \frac{2\,(n+4)\,(n+5)^2}{x_{go}^{n+4}}\gamma_x + \frac{2\,(n+4)\,(n+5)}{x_{go}^{n+3}}a_x \\
& - \frac{4\,(n+4)^2\,(n+5)}{x_{go}^{n+5}}y_f + \frac{2\,(n+3)\,(n+4)\,(n+5)}{x_{go}^{n+4}}\gamma_f \\
& - \frac{(n+1)\,(n+4)\,(n+5)}{3\,x_{go}^{n+2}}u_F
\end{aligned}
\tag{A.41}
$$

Substitution of A.40 into A.36 yields

$$
\begin{aligned}
v_\gamma = \frac{(n+3)}{x_{go}^{n+3}} \Bigg[& \gamma_x - \gamma_f + a_x\,x_{go} + \frac{1}{2}u_F\,x_{go}^2 \\
& - \frac{2\,(n+4)\,(n+5)}{x_{go}} \left(y_x - y_f + \gamma_f\,x_{go} - \frac{1}{2}a_x\,x_{go}^2 - \frac{1}{3}u_F\,x_{go}^3 \right) \\
& - (n+5)^2 \left(\gamma_x - \gamma_f + a_x\,x_{go} + \frac{1}{2}u_F\,x_{go}^2 \right) \Bigg]
\end{aligned}
\tag{A.42}
$$

or by collection of variables

$$
\begin{aligned}
v_\gamma \;=\; & -\frac{2\,(n+3)\,(n+4)\,(n+5)}{x_{go}^{n+4}}y_x - \frac{(n+3)\,(n+4)\,(n+6)}{x_{go}^{n+3}}\gamma_x - \frac{(n+3)\,(n+4)}{x_{go}^{n+2}}a_x \\
& + \frac{2\,(n+3)\,(n+4)\,(n+5)}{x_{go}^{n+4}}y_f - \frac{(n+3)\,(n+4)^2}{x_{go}^{n+3}}\gamma_f \\
& + \frac{(n+2)\,(n+3)\,(n+4)}{6\,x_{go}^{n+1}}u_F
\end{aligned}
\tag{A.43}
$$

Now the control term u_B of A.23 is completely defined.

For simplicity A.40 and A.43 are combined in a compact format such that

$$\begin{bmatrix} v_y \\ v_\gamma \end{bmatrix} = \begin{bmatrix} \frac{4\,(n+4)^2\,(n+5)}{x_{go}^{n+5}} & \frac{2\,(n+4)\,(n+5)^2}{x_{go}^{n+4}} & \frac{2\,(n+4)\,(n+5)}{x_{go}^{n+3}} \\ -\frac{2\,(n+3)\,(n+4)\,(n+5)}{x_{go}^{n+4}} & -\frac{(n+3)\,(n+4)\,(n+6)}{x_{go}^{n+3}} & -\frac{(n+3)\,(n+4)}{x_{go}^{n+2}} \end{bmatrix} \begin{bmatrix} y_x \\ \gamma_x \\ a_x \end{bmatrix}$$
$$+ \begin{bmatrix} -\frac{4\,(n+4)^2\,(n+5)}{x_{go}^{n+5}} & \frac{2\,(n+3)\,(n+4)\,(n+5)}{x_{go}^{n+4}} \\ \frac{2\,(n+3)\,(n+4)\,(n+5)}{x_{go}^{n+4}} & -\frac{(n+3)\,(n+4)^2}{x_{go}^{n+3}} \end{bmatrix} \begin{bmatrix} y_f \\ \gamma_f \end{bmatrix} \tag{A.44}$$
$$+ \begin{bmatrix} -\frac{(n+1)\,(n+4)\,(n+5)}{3\,x_{go}^{n+2}} \\ \frac{(n+2)\,(n+3)\,(n+4)}{6\,x_{go}^{n+1}} \end{bmatrix} u_F$$

Furthermore, by making the following definitions

$$z = \begin{bmatrix} UPN \\ \gamma_{go} \\ a \end{bmatrix} \qquad UPN = \frac{\mathrm{y_{go}}\,(n+3)}{\mathrm{xgo}^2} - \frac{\gamma\,(n+3)}{\mathrm{xgo}} \qquad \gamma_{go} = \gamma_f - \gamma \tag{A.45}$$

Eq.A.44 is expressed in a simpler form as

$$\begin{bmatrix} v_y \\ v_\gamma \end{bmatrix} = \begin{bmatrix} -\frac{4\,\mathrm{UPN}\,(n+4)^2\,(n+5)}{{x_{\mathrm{go}}}^{n+3}\,(n+3)} & \frac{2\,\gamma_{\mathrm{go}}\,(n+3)\,(n+4)\,(n+5)}{{x_{\mathrm{go}}}^{n+4}} & \frac{2\,a\,(n+4)\,(n+5)}{{x_{\mathrm{go}}}^{n+3}} \\ \frac{2\,\mathrm{UPN}\,(n+4)\,(n+5)}{{x_{\mathrm{go}}}^{n+2}} & -\frac{\gamma_{\mathrm{go}}\,(n+3)\,(n+4)^2}{{x_{\mathrm{go}}}^{n+3}} & -\frac{a\,(n+3)\,(n+4)}{{x_{\mathrm{go}}}^{n+2}} \end{bmatrix} z + \begin{bmatrix} -\frac{u_F\,(n+1)\,(n+4)\,(n+5)}{3\,{x_{\mathrm{go}}}^{n+2}} \\ \frac{u_F\,(n+3)\left(n^2+6\,n+8\right)}{6\,{x_{\mathrm{go}}}^{n+1}} \end{bmatrix} u_F$$

Plugging A.44 into A.23 yields the completely defined GENEX-ITACG

$$u_B = K^\top z + \frac{(n-1)(n+4)}{6} u_F$$

where

$$K = \begin{pmatrix} \frac{2\,(n+4)\,(n+5)}{x_{\mathrm{go}}\,(n+3)} \\ -\frac{(n+3)\,(n+4)}{{x_{\mathrm{go}}}^2} \\ -\frac{2\,(n+4)}{x_{\mathrm{go}}} \end{pmatrix}$$

and the total control term becomes

$$u = u_B + u_F = K^\top z + \frac{(n+1)(n+2)}{6} u_F$$

A.3 Additional Impact Time Correction Command

Next, the additional command, u_F, is solved for. This command corrects the trajectory to ensure the missile impacts the target at the designated impact time. The remaining distance the missile will travel can be expressed as a function of the flight path angle such that

$$D = \int_x^{x_f} \sqrt{1 + \gamma^2(s, u_F) ds} \tag{A.46}$$

The missile's velocity is constant. Therefore, time to go is expressed as

$$\bar{t}_{go} = t_d - t = \frac{\int_x^{x_f} \sqrt{1 + \gamma^2(s) ds}}{V} \tag{A.47}$$

where t_d is the designated impact time. Introducing non-dimensional time,$\tau = \frac{t}{t_f}$, and nondimension distamce, $d = \frac{D}{t_f V}$, into Eq. A.47 yields

$$\bar{\tau}_{go} = \int_x^{x_f} \sqrt{1 + \gamma^2(s, u_F) ds} \tag{A.48}$$

The square root term can be approximated using a Taylor series expansion such that

$$\sqrt{1 + \gamma^2(s, u_F) ds} = 1 + \frac{1}{2}\gamma^2(s, u_F) - \frac{1}{8}\gamma^4(s, u_F) + \frac{1}{16}\gamma^5(s, u_F) - \frac{5}{258}\gamma^7(s, u_F) + h.o.t$$

The flight path angle is assumed to be small. Therefore, every term higher than the first two terms are very close to zero. Thus, the time to go is approximately

$$\bar{\tau}_{go} \simeq \int_x^{x_f} \left(1 + \frac{1}{2}\gamma^2(s, u_F)\right) ds \tag{A.49}$$

Furthermore, by letting $\zeta = x_f - s$ the time to go can be expressed as

$$\bar{\tau}_{go} = \int_0^{x_f - x} \left(1 + \frac{1}{2}\gamma^2(\zeta, u_F)\right) ds \tag{A.50}$$

where by substituting $\zeta = x_f - s$ into Eq. A.27 yields

$$\begin{aligned}\gamma(\zeta, u_F) = \gamma_f - a_x\zeta + \left(\frac{1}{2}\zeta^2 - (x_f - x)\,\zeta\right) u_F \\ \left(\frac{1}{(n+2)}(x_f - x)^{n+2}\zeta - \frac{1}{(n+2)\ (n+3)}\zeta^{n+3}\right) v_\gamma \\ \left(\frac{1}{2\,(\,n+3)}(x_f - x)^{n+3}\zeta - \frac{1}{2\ (n+3)\ (n+4)}\zeta^{n+4}\right) v_y\end{aligned} \tag{A.51}$$

If the additional control command is not applied, an estimation of time to go can be expressed as

$$\hat{\tau}_{go} = \int_0^{x_f - x} \sqrt{1 + \gamma^2(\zeta, u_F = 0) ds} \tag{A.52}$$

Substituting Eq. A.51 into Eq. A.52 yields

$$\begin{aligned}\hat{\tau}_{go} = &\left(\frac{3\,n + 13}{6\ (2\,n + 7)\ (2\,n + 9)\ (n + 5)\ (n + 6)}\right) {x_{\rm go}}^3\, a^2 \\ &- \left(\frac{4\,n + 19}{3\ (2\,n + 7)\ (2\,n + 9)\ (n + 3)\ (n + 6)}\right) {x_{\rm go}}^3\, a\,{\rm UPN} \\ &+ \left(\frac{2\ (4\,n + 19)\ (n + 4)\ (n + 5)}{3\ (2\,n + 7)\ (2\,n + 9)\ (n + 3)^2\ (n + 6)}\right) {x_{\rm go}}^3\,{\rm UPN}^2 \\ &- \left(\frac{(4\,n + 19)\ (n + 3)}{6\ (2\,n + 7)\ (2\,n + 9)\ (n + 5)\ (n + 6)}\right) {x_{\rm go}}^2\,\gamma_{\rm go}\,a \\ &- \left(\frac{(16\,n^3 + 206\,n^2 + 880\,n + 1245)}{3\,(2\,n + 7)\ (2\,n + 9)\ (n + 3)\ (n + 6)}\right) {x_{\rm go}}^2\,\gamma_{\rm go}\,{\rm UPN} \\ &- \left(\frac{\frac{17\,n^3}{6} + \frac{71\,n^2}{2} + 147\,n + 201}{(2\,n + 7)\ (2\,n + 9)\ (n + 5)\ (n + 6)} - \frac{2}{3}\right) x_{\rm go}\,{\gamma_{\rm go}}^2 \\ &+ \frac{1}{(n + 3)}\,{x_{\rm go}}^2\,\gamma_f\,{\rm UPN} - \gamma_f\,x_{\rm go}\,\gamma_{\rm go} + \left(\frac{{\gamma_f}^2}{2} + 1\right) x_{\rm go}\end{aligned} \tag{A.53}$$

By making the following definitions

$$C = x_{\mathrm{go}} \left(\frac{{\gamma_{\mathrm{f}}}^2}{2} + 1 \right)$$

$$L = \begin{pmatrix} \frac{\gamma_{\mathrm{f}} {x_{\mathrm{go}}}^2}{n+3} \\ -\gamma_{\mathrm{f}} x_{\mathrm{go}} \\ 0 \end{pmatrix}$$

$$Q = \begin{pmatrix} \frac{2 {x_{\mathrm{go}}}^3 (4n+19)(n+4)(n+5)}{3(2n+7)(2n+9)(n+3)^2(n+6)} & -\frac{x_{\mathrm{go}}^2 \left(16n^3+206n^2+880n+1245\right)}{6(2n+7)(2n+9)(n+3)(n+6)} & -\frac{x_{\mathrm{go}}^3 (4n+19)}{6(2n+7)(2n+9)(n+3)(n+6)} \\ -\frac{x_{\mathrm{go}}^2 \left(16n^3+206n^2+880n+1245\right)}{6(2n+7)(2n+9)(n+3)(n+6)} & -\frac{x_{\mathrm{go}} \left(\frac{17n^3}{6}+\frac{71n^2}{2}+147n+201\right)}{(2n+7)(2n+9)(n+5)(n+6)} + \frac{2x_{\mathrm{go}}}{3} & -\frac{x_{\mathrm{go}}^2 (4n+19)(n+3)}{12(2n+7)(2n+9)(n+5)(n+6)} \\ -\frac{x_{\mathrm{go}}^3 (4n+19)}{6(2n+7)(2n+9)(n+3)(n+6)} & -\frac{x_{\mathrm{go}}^2 (4n+19)(n+3)}{12(2n+7)(2n+9)(n+5)(n+6)} & \frac{x_{\mathrm{go}}^3 (3n+13)}{6(2n+7)(2n+9)(n+5)(n+6)} \end{pmatrix}$$

Eq. A.53 can be expressed in compact form as

$$\hat{\tau}_{go} = C + L^\top z + z^\top Q z \tag{A.54}$$

Now by substituting $\zeta = x_f - x$ in , time to go is expressed as

$$\bar{\tau}_{go} = \int_0^{x_f - x} \sqrt{1 + \gamma^2(\zeta, u_F) ds} \tag{A.55}$$

and evaluation of the integral yields

$$
\begin{aligned}
\bar{\tau}_{go} = & \left(\frac{(8\,n+35)\ (n+1)^2\,(n+2)^2}{(1080\ (2\,n+7)\ (2\,n+9)\ (n+5)\ (n+6)\ (n+7))} \right) {x_{\rm go}}^5\,u_F^2 \\
& + \left(\frac{(8\,n+35)\ (n+1)\ (n+2)}{(36\ (2\,n+7)\ (2\,n+9)\ (n+5)\ (n+6)\ (n+7))} \right) {x_{\rm go}}^4\,u_F\,a \\
& + \left(\frac{((n+1)\ (n+2)\ (4\,n^2+20\,n+7))}{((2\,n+7)\ (2\,n+9)\ (n+3)\ (n+6)\ (n+7)\ 36)} \right) {x_{\rm go}}^4\,u_F\,{\rm UPN} \\
& - \left(\frac{u_F\ (n+1)\ (n+2)\ (n+3)\ (4\,n^2+38\,n+91)}{(2\,n+7)\ (2\,n+9)\ (n+5)\ (n+6)\ (n+7)\ 36} \right) {x_{\rm go}}^3\,u_F\,\gamma_{\rm go} \\
& + \left(\frac{3\,n+13}{6\ (2\,n+7)\ (2\,n+9)\ (n+5)\ (n+6)} \right) {x_{\rm go}}^3\,a^2 \\
& - \left(\frac{4\,n+19}{3\ (2\,n+7)\ (2\,n+9)\ (n+3)\ (n+6)} \right) {x_{\rm go}}^3\,a\,{\rm UPN} \\
& + \left(\frac{2\ (4\,n+19)\ (n+4)\ (n+5)}{3\ (2\,n+7)\ (2\,n+9)\ (n+3)^2\ (n+6)} \right) {x_{\rm go}}^3\,{\rm UPN}^2 \\
& - \left(\frac{(4\,n+19)\ (n+3)}{6\ (2\,n+7)\ (2\,n+9)\ (n+5)\ (n+6)} \right) {x_{\rm go}}^2\,\gamma_{\rm go}\,a \\
& - \left(\frac{16\,n^3+206\,n^2+880\,n+1245}{3\,(2\,n+7)\ (2\,n+9)\ (n+3)\ (n+6)} \right) {x_{\rm go}}^2\,\gamma_{\rm go}\,{\rm UPN} \\
& - \left(\frac{\frac{17\,n^3}{6}+\frac{71\,n^2}{2}+147\,n+201}{(2\,n+7)\ (2\,n+9)\ (n+5)\ (n+6)} - \frac{2}{3} \right) x_{\rm go}\,{\gamma_{\rm go}}^2 \\
& + \frac{1}{(n+3)}\,{x_{\rm go}}^2\,\gamma_f\,{\rm UPN} - \gamma_f\,x_{\rm go}\,\gamma_{\rm go} + \left(\frac{{\gamma_f}^2}{2}+1 \right) x_{\rm go}
\end{aligned}
\tag{A.56}
$$

Through the use of Eq. A.53, Eq. A.56 is simplified to

$$
\begin{aligned}
\bar{\tau}_{go} &= \int_x^{x_f} \sqrt{1+\gamma^2(s,u_F)ds} \\
&= \alpha u_F^2 + \beta u_F + \hat{\tau}_{go}
\end{aligned}
$$

where

$$
\alpha = \frac{x_{\rm go}^5\ (8\,n+35)\ (n+1)^2\,(n+2)^2}{1080\ (2\,n+7)\ (2\,n+9)\ (n+5)\ (n+6)\ (n+7)}
$$

$$\beta = \begin{bmatrix} \frac{x_{\mathrm{go}}^4\,(n+1)\,(n+2)\left(4\,n^2+20\,n+7\right)}{36\,(2\,n+7)\,(2\,n+9)\,(n+3)\,(n+6)\,(n+7)} \\ -\frac{{x_{\mathrm{go}}}^3\,(n+1)\,(n+2)\,(n+3)\left(4\,n^2+38\,n+91\right)}{36\,(2\,n+7)\,(2\,n+9)\,(n+5)\,(n+6)\,(n+7)} \\ \frac{x_{\mathrm{go}}^4\,(8\,n+35)\,(n+1)\,(n+2)}{36\,(2\,n+7)\,(2\,n+9)\,(n+5)\,(n+6)\,(n+7)} \end{bmatrix} z$$

Furthermore, by defining the difference between the actual time-to-go and the estimate of time to go without the additional control command as

$$\epsilon_t = \bar{\tau}_{go} - \hat{\tau}_{go}$$

the following relation can be made

$$u_F^2 + \frac{\beta}{\alpha} u_F - \frac{\epsilon_t}{\alpha} = 0$$

Solving for u_F yields

$$\begin{aligned} u_F = &-\frac{1}{2}\eta_L \pm \frac{1}{2}\sqrt{\eta_L^2 + \eta_E} \\ &-\frac{1}{2}\eta_L \pm \frac{1}{2}\eta_L\sqrt{1 + \frac{\eta_E}{\eta_L^2}} \end{aligned} \tag{A.57}$$

where

$$\eta_L = \frac{\alpha}{\beta} = M^\top z$$

$$M = \begin{pmatrix} \frac{(n+5)\left(4\,n^2+20\,n+7\right)30}{x_{\mathrm{go}}\,(8\,n+35)\,(n+1)\,(n+2)\,(n+3)} \\ -\frac{(n+3)\left(4\,n^2+38\,n+91\right)30}{x_{\mathrm{go}}^2\,(8\,n+35)\,(n+1)\,(n+2)} \\ \frac{30}{x_{\mathrm{go}}\,(n+1)\,(n+2)} \end{pmatrix}$$

$$\eta_E = \frac{4}{\alpha}\epsilon_t = N\epsilon_t$$

$$N = \frac{4320\ (2\,n+7)\ (2\,n+9)\ (n+5)\ (n+6)\ (n+7)}{x_{\mathrm{go}}^5\ (8\,n+35)\ (n+1)^2\,(n+2)^2}$$

When the impact error goes to zero the additional control command should equal zero. Therefore, the positive sign solution of Eq. A.57 should be used. Furthermore, $\frac{\eta_E}{\eta_L^2} << 1$ and approaches zero as $\epsilon_t \to 0$.

Therefore, Eq. A.57 can be approximated as

$$u_F \simeq -\frac{1}{2}\eta_L + \frac{1}{2}\eta_L \left(1 + \frac{\eta_E}{2\eta_L^2}\right) \simeq \frac{\eta_E}{4\eta_L}$$

A.4 GENEX-ITACG With Dimensional State Variables

Finally, by reversing the relations of Eq. A.3, GENEX-ITACG with dimensional state variables can be expressed as

$$G = g_B + \frac{(n+1)(n+2)}{6} g_F$$

The first jerk term ,g_B, which eliminates the miss distance and the impact angle error can be expressed as

$$g_B = K^\top z$$

where

$$z = \begin{pmatrix} APN \\ \gamma_{\mathrm{go}} \\ A \end{pmatrix}$$

$$K = \begin{pmatrix} \frac{2\,V\,(n+4)\,(n+5)}{\mathrm{Xgo}\,(n+3)} \\ -\frac{V^3\,(n+3)\,(n+4)}{\mathrm{Xgo}^2} \\ -\frac{2\,V\,(n+4)}{\mathrm{Xgo}} \end{pmatrix}$$

$$APN = \frac{V^2\,\mathrm{Ygo}\;(n+3)}{\mathrm{Xgo}^2} - \frac{V^2\,\gamma\;(n+3)}{\mathrm{Xgo}}$$

The time to go estimate can be expressed as

$$\hat{t}_{go} = C + L^\top z + z^\top Q z$$

$$C = \frac{\mathrm{Xgo}\;\left(\frac{\gamma \mathrm{f}^2}{2} + 1\right)}{V}$$

$$L = \begin{pmatrix} \frac{\mathrm{Xgo}^2\,\gamma_\mathrm{f}}{V^3\,(n+3)} \\ -\frac{\mathrm{Xgo}\,\gamma_\mathrm{f}}{V} \\ 0 \end{pmatrix}$$

$$Q = \begin{pmatrix} \frac{2\,\mathrm{Xgo}^3\,(4\,n+19)\,(n+4)\,(n+5)}{3\,V^5\,(2\,n+7)\,(2\,n+9)\,(n+3)^2\,(n+6)} & -\frac{\mathrm{Xgo}^2\left(16\,n^3+206\,n^2+880\,n+1245\right)}{V^3\,(2\,n+7)\,(2\,n+9)\,(n+3)\,(n+6)\,6} & -\frac{\mathrm{Xgo}^3\,(4\,n+19)}{6\,V^5\,(2\,n+7)\,(2\,n+9)\,(n+3)\,(n+6)} \\ -\frac{\mathrm{Xgo}^2\left(16\,n^3+206\,n^2+880\,n+1245\right)}{V^3\,(2\,n+7)\,(2\,n+9)\,(n+3)\,(n+6)\,6} & -\frac{\mathrm{Xgo}\left(\frac{\left(\frac{17\,n^3}{6}+\frac{71\,n^2}{2}+147\,n+201\right)}{(2\,n+7)\,(2\,n+9)\,(n+5)\,(n+6)}-\frac{2}{3}\right)}{V} & -\frac{\mathrm{Xgo}^2\,(4\,n+19)\,(n+3)}{12\,V^3\,(2\,n+7)\,(2\,n+9)\,(n+5)\,(n+6)} \\ -\frac{\mathrm{Xgo}^3\,(4\,n+19)}{6\,V^5\,(2\,n+7)\,(2\,n+9)\,(n+3)\,(n+6)} & -\frac{\mathrm{Xgo}^2\,(4\,n+19)\,(n+3)}{12\,V^3\,(2\,n+7)\,(2\,n+9)\,(n+5)\,(n+6)} & \frac{\mathrm{Xgo}^3\,(3\,n+13)}{6\,V^5\,(2\,n+7)\,(2\,n+9)\,(n+5)\,(n+6)} \end{pmatrix}$$

The time to go estimation error can be expressed as

$$\epsilon_t = \bar{t}_{go} - \hat{t}_{go} = (t_d - t) - \hat{t}_{go}$$

The second jerk term, g_F, which corrects the trajectory to achieve a desired impact time, can be expressed as

$$g_F = \frac{\eta_E}{4\eta_L}$$

$$\eta_E = M^\top z$$

$$M = \begin{pmatrix} \frac{V\,(n+5)\left(4\,n^2+20\,n+7\right)30}{\mathrm{Xgo}\,(8\,n+35)\,(n+1)\,(n+2)\,(n+3)} \\ -\frac{V^3\,(n+3)\left(4\,n^2+38\,n+91\right)30}{\mathrm{Xgo}^2\,(8\,n+35)\,(n+1)\,(n+2)} \\ \frac{30\,V}{\mathrm{Xgo}\,(n+1)\,(n+2)} \end{pmatrix}$$

$$\eta_L = N\epsilon_t$$

$$N = \frac{4320\,V^7\;(2\,n+7)\;(2\,n+9)\;(n+5)\;(n+6)\;(n+7)}{\mathrm{Xgo}^5\;(8\,n+35)\;(n+1)^2\,(n+2)^2}$$

APPENDIX B: SIMULINK MODEL

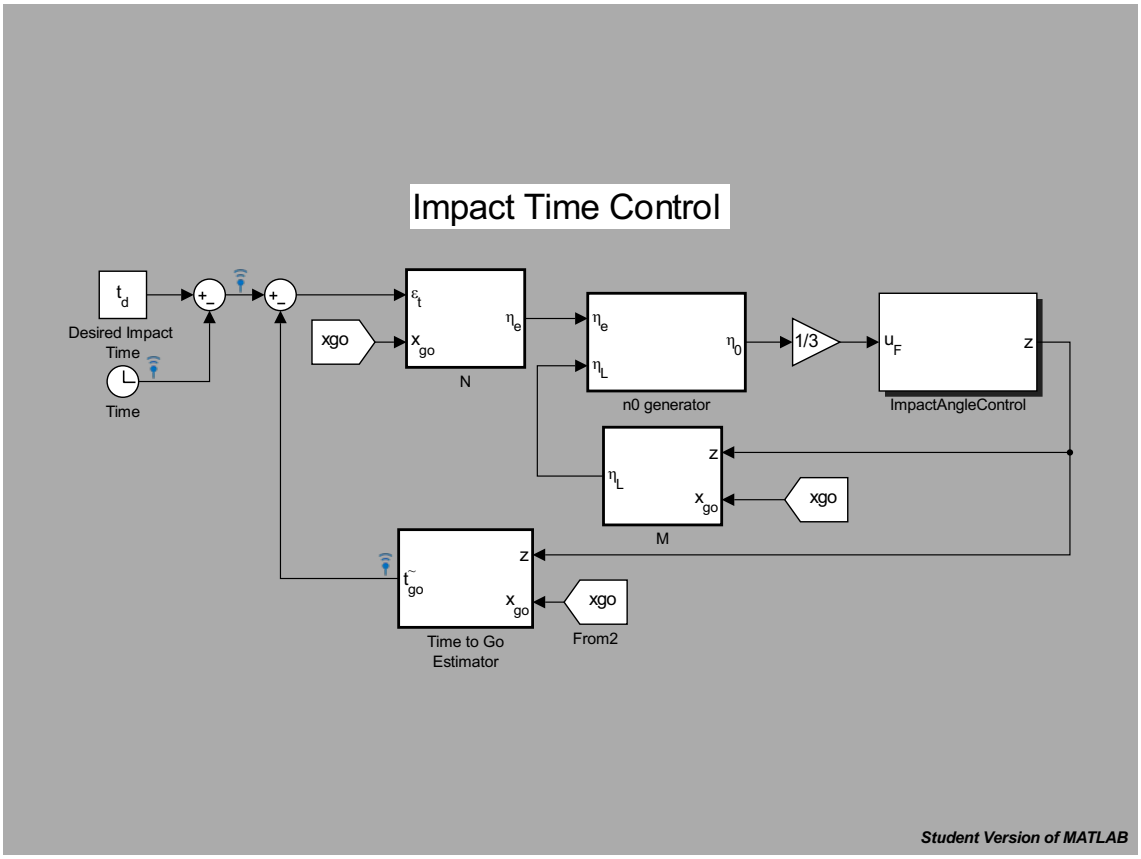

Figure B.1: Simulink Model: Time Control

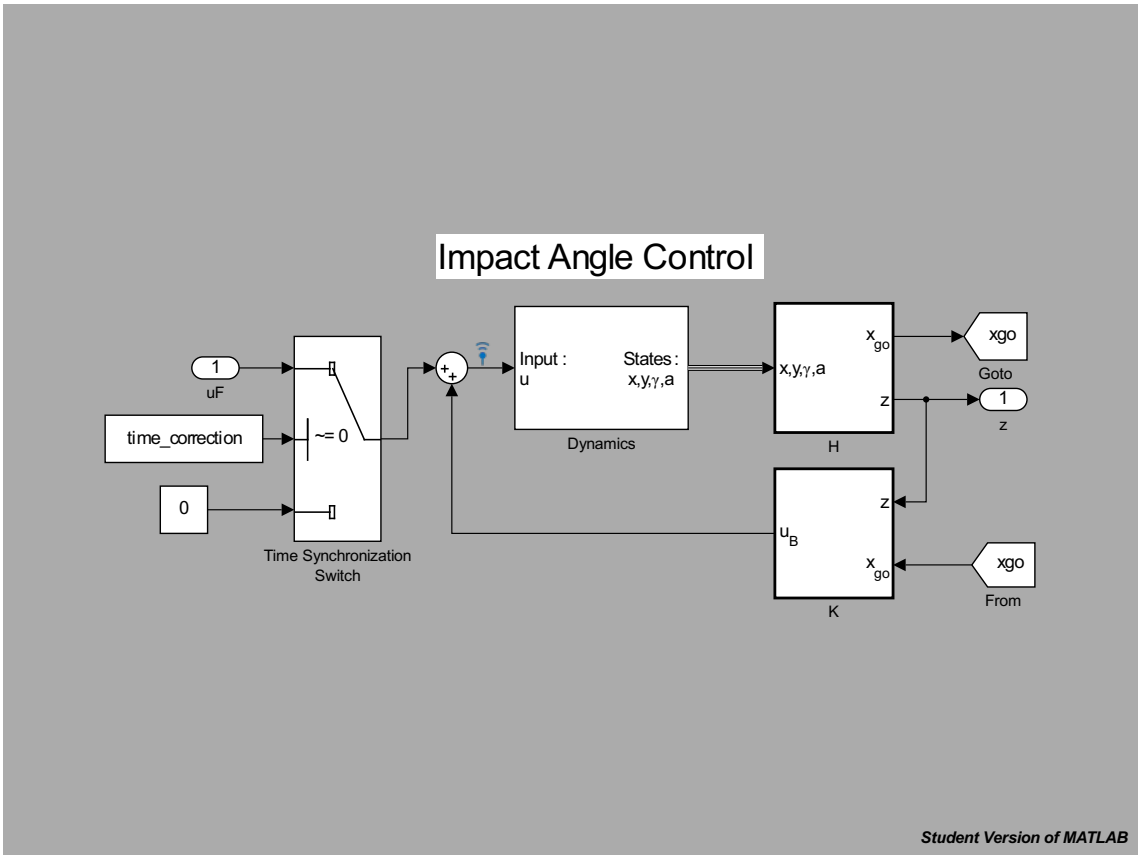
Impact Angle Control
1
uF
time_correction
~= 0
0
Time Synchronization
Switch
Input :
u
States :
x,y,γ,a
Dynamics
x,y,γ,a
x
go
z
H
xgo
Goto
1
z
z
u
B
x
go
K
xgo
From
Student Version of MATLAB

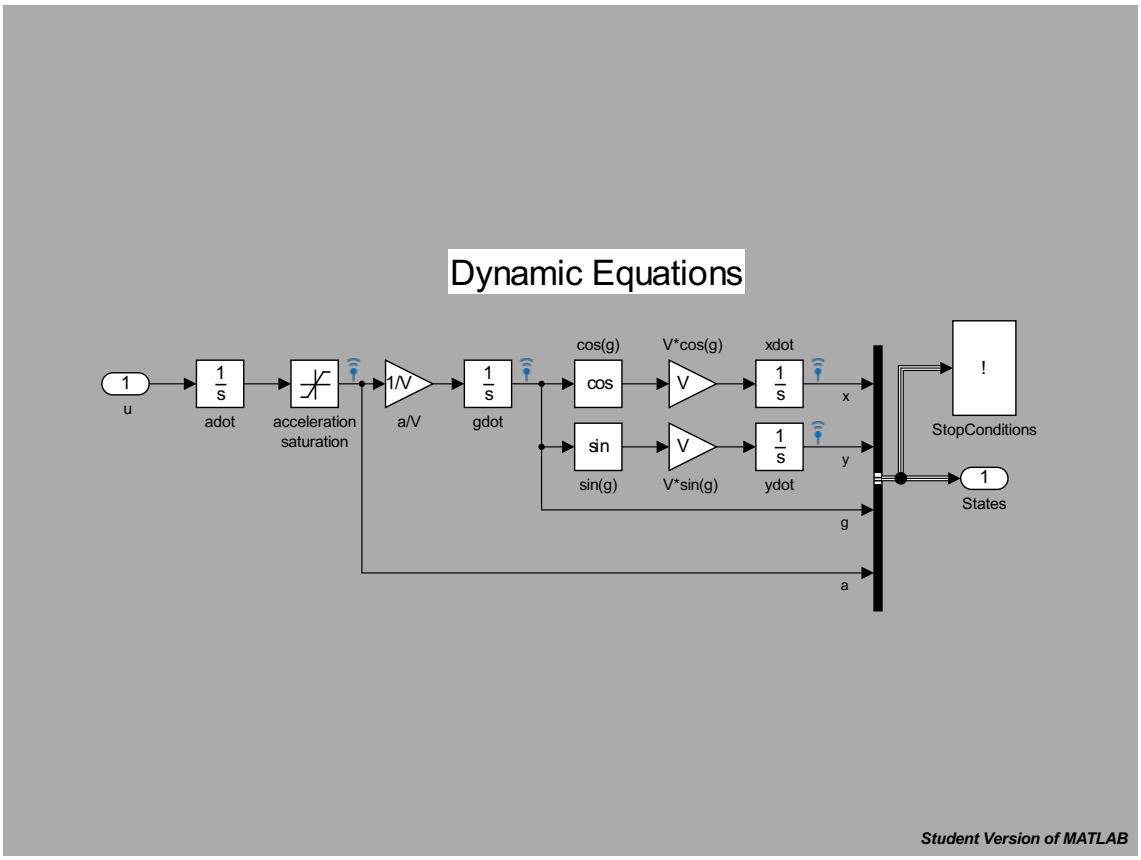

Figure B.2: Simulink Model: Nonlinear Dynamic Equations

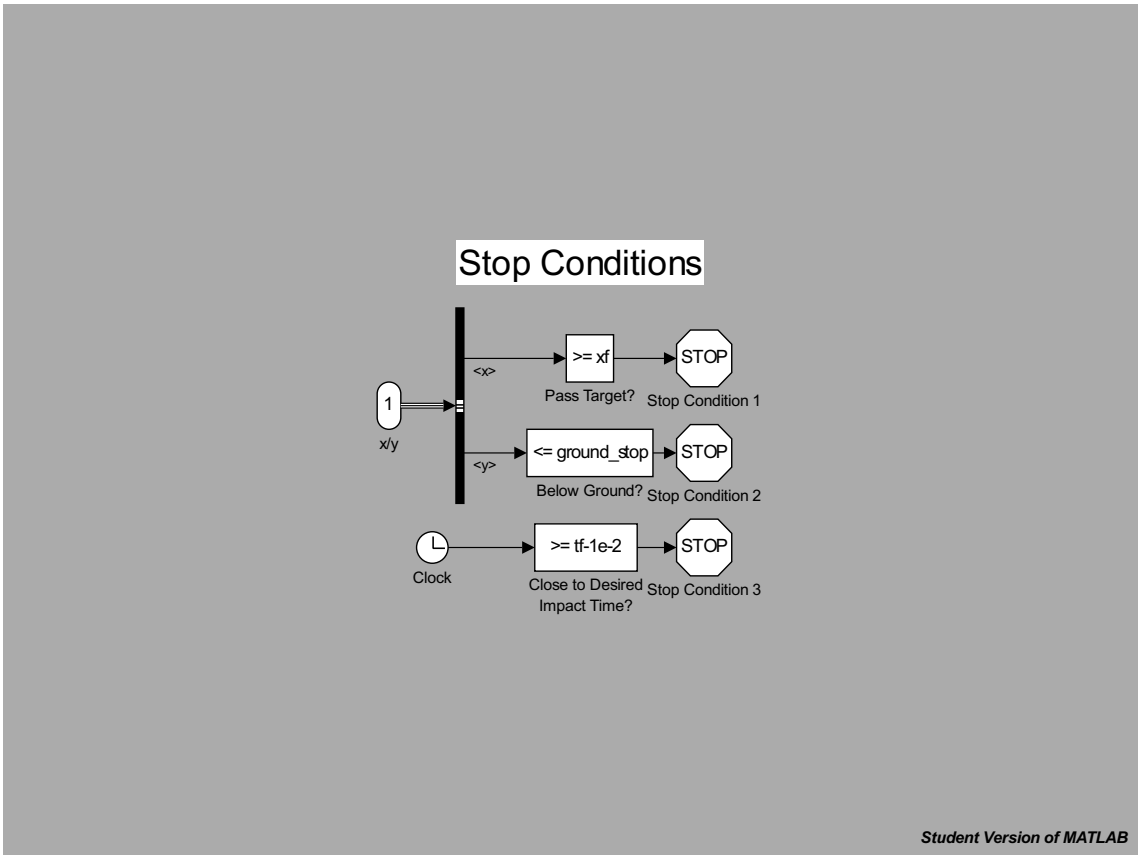

Figure B.3: Simulink Model: Stop Conditions

APPENDIX C: FIGURE REPRODUCTION PERMISSIONS

UNIVERSITY OF CENTRAL FLORIDA

10/24/2014

Loren Robinson, 4000 Central Florida Blvd, Orlando, FL 32816

Dear Linda L. Maier Tyler:

This letter will confirm our recent email conversation. I am completing a doctoral dissertation/master's degree at the University of Central Florida entitled "Cooperative General Vector Explicit Guidance." I would like your permission to reprint in my thesis figures from the following:

Neil F. Palumbo. Guest's editor's introduction: Homing missile guidance and control. *John Hopkins APL Technical Digest*, 29(1):2–8, 2010.

The figures to be reproduced are: Figure 2 and Figure 3.

Figure 2 illustrates the three phases of flight for a multi-mode missile. I would like to use this figure in the introduction of my thesis when I talk about the different guidance objectives of the three phases of flight. Figure 3 illustrates the traditional missile GNC topology. I would like to use this figure in the introduction of my thesis to inform the reader of where my thesis focuses on in this topology (guidance).

The requested permission extends to any future revisions and editions of my thesis/dissertation, including non-exclusive world rights in all languages. These rights will in no way restrict republication of the material in any other form by you or by others authorized by you. Your signing of this letter will also confirm that you own or your company owns the copyright to the above-described material.

If these arrangements meet with your approval, please sign this letter where indicated below and return it to me in the enclosed return envelope. Thank you for your attention in this matter.

Sincerely,

Loren Robinson

PERMISSION GRANTED FOR THE USE REQUESTED ABOVE:

By: Michelle N Swanter on behalf of Linda L. Maier-Tyler

Linda L. Maier Tyler

Date: 10/28/14

UNIVERSITY OF CENTRAL FLORIDA

10/24/2014

Loren Robinson, 4000 Central Florida Blvd, Orlando, FL 32816

Dear Linda L. Maier Tyler:

This letter will confirm our recent email conversation. I am completing a doctoral dissertation/master's degree at the University of Central Florida entitled "Cooperative General Vector Explicit Guidance." I would like your permission to reprint in my thesis figures from the following:

Neil F. Palumbo, Paul B. Jackson, and Ross A. Blauwkamp. Basic principles of homing guidance. *John Hopkins APL Technical Digest*, 29(1):25–41, 2010.

The figure to be reproduced is: Figure 1.

Figure 1 illustrates the errors in predicted target position and actual target position between the mid-course and terminal phases of flight (handover analysis). I would like to use this figure to also illustrate how the actual position of the target at the end of the mid-course phase may differ from the predicted point of intercept in my presentation of existing terminal phase guidance laws.

The requested permission extends to any future revisions and editions of my thesis/dissertation, including non-exclusive world rights in all languages. These rights will in no way restrict republication of the material in any other form by you or by others authorized by you. Your signing of this letter will also confirm that you own or your company owns the copyright to the above-described material.

If these arrangements meet with your approval, please sign this letter where indicated below and return it to me in the enclosed return envelope. Thank you for your attention in this matter.

Sincerely,

Loren Robinson

PERMISSION GRANTED FOR THE USE REQUESTED ABOVE:

By: Michele A Trowter on behalf of Linda L Maier-Tyler

Linda L. Maier Tyler

Date: 10/28/14

UNIVERSITY OF CENTRAL FLORIDA

10/24/2014

Loren Robinson, 4000 Central Florida Blvd, Orlando, FL 32816

Dear Linda L. Maier Tyler:

This letter will confirm our recent email conversation. I am completing a doctoral dissertation/master's degree at the University of Central Florida entitled "Cooperative General Vector Explicit Guidance." I would like your permission to reprint in my thesis figures from the following:

Neil F. Palumbo, Paul B. Jackson, and Ross A. Blauwkamp. Modern homing missile guidance theory and technique. *John Hopkins APL Technical Digest*, 29(1):42–59, 2010.

The figure to be reproduced is: Figure 2.

Figure 2 illustrates a planar engagement geometry between a missile and its target. I would like to use this figure to aid in the development of linear kinematic equations which are used in the development of my cooperative guidance law.

The requested permission extends to any future revisions and editions of my thesis/dissertation, including non-exclusive world rights in all languages. These rights will in no way restrict republication of the material in any other form by you or by others authorized by you. Your signing of this letter will also confirm that you own or your company owns the copyright to the above-described material.

If these arrangements meet with your approval, please sign this letter where indicated below and return it to me in the enclosed return envelope. Thank you for your attention in this matter.

Sincerely,

Loren Robinson

PERMISSION GRANTED FOR THE USE REQUESTED ABOVE:

By: Michele L. Swanter on behalf of Linda L. Maier-Tyler

Linda L. Maier Tyler

Date: 10/28/14

UNIVERSITY OF CENTRAL FLORIDA

10/24/2014

Loren Robinson, 4000 Central Florida Blvd, Orlando, FL 32816

Dear Radhakant Padhi:

This letter will confirm our recent email conversation. I am completing a doctoral dissertation/master's degree at the University of Central Florida entitled "Cooperative General Vector Explicit Guidance." I would like your permission to reprint in my thesis figures from the following:

Generalized model predictive static programming and angle-constrained guidance of air-to-ground missiles. *AIAA Journal of Guidance, Control and Dynamics*, 0(0):1–17, April 2014.

The figure to be reproduced is: Figure 4.

Figure 2 illustrates three dimensional engagement geometry between a missile and its target. I would like to use this figure to aid in the development of dynamic equations which are used in the simulation of my cooperative guidance law.

The requested permission extends to any future revisions and editions of my thesis/dissertation, including non-exclusive world rights in all languages. These rights will in no way restrict republication of the material in any other form by you or by others authorized by you. Your signing of this letter will also confirm that you own or your company owns the copyright to the above-described material.

If these arrangements meet with your approval, please sign this letter where indicated below and return it to me in the enclosed return envelope. Thank you for your attention in this matter.

Sincerely,

Loren Robinson

PERMISSION GRANTED FOR THE USE REQUESTED ABOVE:

By: _____

Radhakant Padhi

Date: _____

REFERENCES

[1] Michael Athans and Peter L. Falb. *Optimal control;An Introduction to the Theory and Its Applications*. McGraw-Hill, New York, 1966.

[2] D. Ghose. True proportional navigation with maneuvering target. *Aerospace and Electronic Systems, IEEE Transactions on*, 30(1):229–237, Jan 1994.

[3] M. Guelman. A qualitative study of proportional navigation. *Aerospace and Electronic Systems, IEEE Transactions on*, AES-7(4):637–643, July 1971.

[4] M. Guelman. Proportional navigation with a maneuvering target. *Aerospace and Electronic Systems, IEEE Transactions on*, AES-8(3):364–371, May 1972.

[5] M. Guelman. The closed-form solution of true proportional navigation. *Aerospace and Electronic Systems, IEEE Transactions on*, AES-12(4):472–482, July 1976.

[6] In-Soo Jeon, Jin-Ik Lee, and Min-Jea Tahk. Impact-time-control guidance law for anti-ship missiles. *Control Systems Technology, IEEE Transactions on*, 14(2):260–266, March 2006.

[7] IV John A. Lukacs and Oleg A. Yakimenko. Trajectory-shape-varying missile guidance for interception of ballistic missiles during the boost phase. In *AIAA Gudiance, Navigation, and Control Conference and Exhibit*, number 6538, pages 1–21. American Institute of Aeronautics and Astronautics, American Institute of Aeronautics and Astronautics, 2007.

[8] Byung S. Kim, Jang G. Lee, and Hyung S. Han. Biased png law for impact with angular constraint. *IEEE Transactions on Aerospace and Electronics Systems*, 34(1):277–288, January 1998.

[9] M. Kim and K.V. Grider. Terminal guidance for impact attitude angle constrained flight trajectories. *Aerospace and Electronic Systems, IEEE Transactions on*, AES-9(6):852–859, Nov 1973.

[10] Jin-Ik Lee, In-Soo Jeon, and Min-Jea Tahk. Guidance law to control impact time and angle. *Aerospace and Electronic Systems, IEEE Transactions on*, 43(1):301–310, January 2007.

[11] Ernest J. Ohlmeyer and Craig A. Phillips. Generalized vector explicit guidance. *AIAA Journal of Guidance, Control and Dynamics*, 29(2):261–268, mar-apr 2006.

[12] Neil F. Palumbo. Guest's editor's introduction: Homing missile guidance and control. *John Hopkins APL Technical Digest*, 29(1):2–8, 2010.

[13] Neil F. Palumbo, Paul B. Jackson, and Ross A. Blauwkamp. Modern homing missile guidance theory and technique. *John Hopkins APL Technical Digest*, 29(1):42–59, 2010.

[14] G. Richey. Guided missiles: A review of their history and design features. *Students' Quarterly Journal*, 38(151):139–145, March 1968.

[15] U.S. Shukla and P.R. Mahapatra. The proportional navigation dilemma-pure or true? *Aerospace and Electronic Systems, IEEE Transactions on*, 26(2):382–392, Mar 1990.

[16] Paul Zarchan. *Tactical and Strategic Missile Guidance*, volume 239 of *Progress in Astronautics and Aeronautics*. American Institute of Aeronatics and Astronautics, Inc., Reston, VA, sixth edition, 2013.

[17] Peter Zipfel. *Modeling and Simulation of Aerospace Vehicle Dynamics*. American Institute of Aeronatics and Astronautics, Inc., Reston, VA, second edition, 2007.